

Investigating 14-3-3 Protein Subcellular Localization, Colocalization with Subcellular Markers,  
and Interaction with Rac1

by

Daniel Brandwein

A thesis submitted in partial fulfillment of the requirements for the degree of

Master of Science

Medical Sciences - Medical Genetics  
University of Alberta

© Daniel Brandwein, 2019

## Abstract

14-3-3 proteins are a group of widely expressed, highly conserved homo/heterodimeric acidic proteins. They usually bind to serine/threonine phosphorylated proteins, but also bind to proteins in a phosphorylation-independent manner. 14-3-3 proteins have over 200 binding partners. 14-3-3 proteins are involved in multiple cellular processes acting mainly as a scaffold protein. Mammals have seven 14-3-3 isoforms ( $\alpha/\beta$ ,  $\epsilon$ ,  $\eta$ ,  $\gamma$ ,  $\sigma$ ,  $\tau/\theta$ , and  $\delta/\zeta$ ), which are encoded by separate genes and are expressed on different chromosomes. While the existence of multiple isoforms may represent one more level of regulation in 14-3-3 signaling, knowledge regarding the isoform-specific functions of 14-3-3 proteins is very limited. Determination of the subcellular localization of the different 14-3-3 isoforms could give important clues into their specific functions. Most of the subcellular localization studies have been done in yeast, flies and plants and little isoform-specific subcellular localization studies have been done in mammals. By using immunocytochemistry, subcellular fractionation, and immunoblotting, I studied the subcellular localization of the total 14-3-3 protein and each of the seven 14-3-3 isoforms, their redistribution throughout the cell cycle and their translocation in response to EGF. In this thesis, I showed that 14-3-3 proteins are broadly distributed throughout the cell and associated with many subcellular organelles/structures including the plasma membrane, endosomes, mitochondria, endoplasmic reticulum, nucleus, centrosomes, microtubules, and actin fibers. I conclude that different isoforms of 14-3-3 have distinct subcellular localizations, which suggest their distinct cellular functions.

I then focused my research to identify the novel binding partners of 14-3-3 proteins. Rac1, a member of the Rho GTPases, promotes the reorganization of actin filament polymerization in lamellipodia and membrane ruffles. It is interesting to notice that both 14-3-3

proteins and Rho GTPases regulate cytoskeleton remodeling and cell migration, which suggests a possible interaction between the signaling pathways. Indeed, previous research has only shown indirect interactions between 14-3-3 proteins and various Rac1 regulators and effectors. However, it is not clear if 14-3-3 proteins bind to Rac1 directly. Using co-immunoprecipitation, I show in this thesis that 14-3-3 proteins bind to Rac1 through serine 71 in a phosphorylation-dependent manner.

## Preface

This thesis is an original work by Daniel Brandwein. All the experimental work in this thesis was designed and conceived by myself under the guidance and mentorship of my supervisor Dr. Zhixiang Wang.

Sections of the thesis are based partly on my previous works. Part of Chapter 1 of this thesis has been published as a literature review: Brandwein, D., & Wang, Z. (2017). Interaction between Rho GTPases and 14-3-3 Proteins. *International Journal of Molecular Sciences*, 18(10), 2148. doi: 10.3390/ijms18102148. Part of Chapter 4 of this thesis has also been published as an original article: Abdrabou, A. M., Brandwein, D., Liu, C., & Wang, Z. (2019). Rac1 S71 mediates the interaction between Rac1 and 14-3-3 proteins. *Cells*, 8(9), 1006. doi: 10.3390/cells8091006.

Chapter 3 of this thesis is currently under revision with me as a co-first author: Abdrabou, A., Brandwein, D., & Wang, Z. (2019). Differential subcellular distribution and translocation of seven 14-3-3 isoforms in response to EGF and during cell cycle.

I was responsible for the data collection and analysis as well as the manuscript composition. A. Abdrabou assisted with the data collection and contributed to manuscript edits. Z. Wang was the supervisory author and also contributed to manuscript edits.

## Acknowledgments

I would first like to thank my mentor and supervisor Dr. Zhixiang Wang for giving me the chance to pursue graduate studies in his lab. Thank you for your patience, guidance and dedication to my project. I would like to thank the current lab members: Xinmei Chen, Babak Nami Mallalou, Hamid Maadi and Abdalla M. Abdrabou. Thank you for your technical expertise, guidance, encouragement, and wisdom throughout my project. I will forever remember our late-night lab discussions, lab meetings, and hangouts. I would also like to thank the past lab members: Dr. Ping Wee, Dr. Jorge Gutierrez, Sichun Xu, Alex Liu, Ezra Ketema and Evan Maloney for all their help. I would like to give my extended thanks to my committee members Dr. Michael Walter and Dr. Barbara Ballermann for their excellent suggestions, guidance and encouragement. I would also like to thank Dr. David Brindley for giving his time to be my external examiner. I also want to thank Dr. Mark R. Phillips (NYU School of Medicine) for providing GFP-Rac1. This project could not have been done without the financial support of the Canadian Institutes of Health Research (CIHR) and the Natural Sciences and Engineering Research Council (NSERC). I would also like to thank Dr. Sarah Hughes for letting me use her lab equipment and for giving advice, expertise and wisdom throughout my degree. I also want to thank Dr. Rachel Wevrick for making sure I fulfill all my graduate requirements and providing guidance throughout my degree. Finally, I want to thank the Department of Medical Genetics office for their endless support in making sure I completed all my requirements. Finally, I want to thank my family and friends for all their support over the years.

## Table of Contents

Abstract	ii
Preface	iv
Acknowledgments	v
Table of Contents	vi
List of Tables	ix
List of Figures	x
Abbreviations	xii
<b>Chapter 1: Introduction</b>	<b>1</b>
1.1 Overview	1
1.2 14-3-3 protein isoforms	2
1.2.1 14-3-3 structure	3
1.2.2 14-3-3 function and subcellular localization	6
1.2.3 14-3-3 and cancer	7
1.2.4 14-3-3 and neurological disease	8
1.3 Rho GTPases	9
1.3.1 Rac1 regulation and phosphorylation	11
1.4 Interactions between 14-3-3 proteins and Rho GTPases	14
1.5 Thesis rationales, hypotheses, and objectives	19
<b>Chapter 2: Materials and Methods</b>	<b>20</b>
2.1 Materials	20
2.1.1 Chemicals and reagents	20
2.1.2 Enzymes	22

2.1.3	Experimental kits	23
2.1.4	Plasmids	23
2.1.5	Antibodies	23
2.1.5.1	Primary Antibodies	23
2.1.5.2	Secondary Antibodies	24
2.1.6	Molecular size markers	24
2.1.7	Buffers and other solutions	24
2.1.8	Other materials	24
2.2	Methods	26
2.2.1	Cell lines	26
2.2.2	Cell culture, transfection and treatment	26
2.2.3	Culture and purification of GFP-Rac1 plasmids	28
2.2.4	Preparation of total cell lysates	29
2.2.5	SDS-PAGE and immunoblotting	30
2.2.6	Subcellular fractionation	32
2.2.7	Co-immunoprecipitation	32
2.2.8	Fluorescence microscopy	33
<b>Chapter 3:</b>	<b>Results I - Subcellular Localization of 14-3-3 Proteins</b>	<b>36</b>
3.1	Total 14-3-3 protein and 14-3-3 isoforms have different expressions and subcellular localizations in COS-7 cells	36
3.2	Pan 14-3-3 localizes to the actin fibers in COS-7 cells	41
3.3	14-3-3 $\beta$ localizes to the microtubules in COS-7 cells	44
3.4	14-3-3 $\epsilon$ localizes to the microtubules in COS-7 cells	47

3.5	14-3-3 $\eta$ localizes to the mitochondria in COS-7 cells	47
3.6	14-3-3 $\gamma$ localizes to the nucleus and forms smaller particles in response to EGF in COS-7 cells	47
3.7	14-3-3 $\sigma$ localizes to the centrosomes and to the microtubules during mitosis in COS-7 cells	54
3.8	14-3-3 $\tau/\theta$ localizes to the endoplasmic reticulum in COS-7 cells	54
3.9	14-3-3 $\zeta$ localizes to the actin fibers, microtubules, endoplasmic reticulum, plasma membrane and endosomes in response to EGF in COS-7 cells	59
3.10	Summary of total 14-3-3 protein and 14-3-3 isoform subcellular localizations and colocalizations with different subcellular markers in COS-7 cells	59
3.11	Total 14-3-3 protein and 14-3-3 isoforms in HEK293T, MDA-MB-231 and MCF-7 cells have similar subcellular localizations to COS-7 cells	64
3.12	Antibody specificity was established using blocking peptides to several 14-3-3 isoforms in COS-7 cells	68
<b>Chapter 4: Results II - Interaction Between Rac1 and 14-3-3 proteins</b>		<b>71</b>
4.1	Rac1 and 14-3-3 proteins interact in response to EGF-induced Akt phosphorylation in COS-7 cells	71
4.2	Total 14-3-3 protein and some 14-3-3 isoforms co-immunoprecipitate with Rac1 in GFP-Rac1 WT but not in GFP-Rac1 S71A COS-7 cells	74
<b>Chapter 5: Discussion</b>		<b>77</b>
<b>References</b>		<b>92</b>

## **List of Tables**

Table 2.1 Buffers and other solutions used in this thesis	25
Table 2.2 Antibodies and their dilutions used for Western blotting	31
Table 2.3 Antibodies and their concentrations used for co-immunoprecipitation	33
Table 2.4 Antibodies and their dilutions used for immunofluorescence	34
Table 3.1 Summary of total 14-3-3 protein and 14-3-3 isoform subcellular localizations	63

## List of Figures

Figure 1.1 Phylogenetic tree depicting homology of the primary structure of the seven 14-3-3 isoforms using ClustalOmega	4
Figure 1.2 Rac1 amino acid sequence depicting motifs and phosphorylation sites	13
Figure 1.3 Reported interactions between 14-3-3 proteins and Rho GTPases	15
Figure 3.1 The expression levels and subcellular localizations of pan 14-3-3 and 14-3-3 isoforms in COS-7 cells	37
Figure 3.2 Pan 14-3-3 localizes to the actin fibers in COS-7 cells	42
Figure 3.3 14-3-3 $\beta$ localizes to the microtubules in COS-7 cells	45
Figure 3.4 14-3-3 $\epsilon$ localizes to the microtubules in COS-7 cells	48
Figure 3.5 14-3-3 $\eta$ localizes to the mitochondria in COS-7 cells	50
Figure 3.6 14-3-3 $\gamma$ localizes to the nucleus and forms smaller particles in response to EGF in COS-7 cells	52
Figure 3.7 14-3-3 $\sigma$ localizes to the centrosomes and to the microtubules during mitosis in COS-7 cells	55
Figure 3.8 14-3-3 $\tau/\theta$ localizes to the endoplasmic reticulum in COS-7 cells	57
Figure 3.9 14-3-3 $\zeta$ localizes to the actin fibers, microtubules, endoplasmic reticulum, plasma membrane and endosomes in response to EGF in COS-7 cells	60
Figure 3.10 Total 14-3-3 protein and 14-3-3 isoforms in HEK293T cells have similar subcellular localizations to COS-7 cells	65
Figure 3.11 Total 14-3-3 protein and 14-3-3 isoforms in MDA-MB-231 cells have similar subcellular localizations to COS-7 cells	66
Figure 3.12 Total 14-3-3 protein and 14-3-3 isoforms in MCF-7 cells have similar	

subcellular localizations to COS-7 cells	67
Figure 3.13 14-3-3 isoforms have different subcellular localizations after adding the blocking peptides in a dose-dependent manner in COS-7 cells	69
Figure 4.1 Rac1 and 14-3-3 proteins interact in response to EGF-induced Akt phosphorylation in COS-7 cells	72
Figure 4.2 Total 14-3-3 protein and some 14-3-3 isoforms co-immunoprecipitate with Rac1 in GFP-Rac1 WT but not in GFP-Rac1 S71A COS-7 cells	75

## Abbreviations

14-3-3 protein	Tyrosine 3-monooxygenase/tryptophan 5-monooxygenase activation protein
$\alpha/\beta, \epsilon, \gamma, \eta, \sigma, \tau/\theta, \delta/\zeta$	Alpha/beta, epsilon, gamma, eta, sigma, tau/theta, delta/zeta
AD	Alzheimer's disease
AEBSF	4-(2-aminoethyl)-benzenesulfonyl fluoride
AICD	amyloid $\beta$ -protein precursor intracellular domain fragment
AKAP-Lbc	A kinase anchoring protein-lymphoid blast crisis oncogene
Akt	Protein kinase B
APS	Ammonium persulfate
ARHGEF2	Rho guanine nucleotide exchange factor 2
ARP2/3	Actin-related protein 2/3
ATCC	American type culture collection
$\beta$ 1PIX	P21-activated kinase-interacting exchange factor beta
BAD	Bcl-2-associated death promoter
BES	<i>N,N</i> -bis(2-hydroxyethyl)-2-aminoethanesulfonic acid
BSA	Bovine serum albumin
BSE	Bovine spongiform encephalopathy
BV02	2-(2,3-Dihydro-1,5-dimethyl-3-oxo-2-phenyl-1H-pyrazol-4-yl)-2,3-dihydro-1,3-dioxo-1H-isoindole-5-carboxylic acid
c-Abl	Human Abelson murine leukemia virus
CDC25B	Cell division cycle 25B
Cdc42	Cell division cycle 42

CJD	Creutzfeldt–Jakob disease
CLL	Chronic lymphocytic leukemia
COS-7	CV-1 (simian) in origin, and carrying the SV40 genetic material-7
DAPI	4',6-diamidino-2-phenylindole
DLC1	Deleted in liver cancer 1
DMEM	Dulbecco's modified eagle medium
ECM	Extracellular matrix
EDTA	Ethylenediaminetetracetic acid
EGF	Epidermal growth factor
EGTA	Ethylene glycol-bis( $\beta$ -aminoethyl ether)-N,N,N',N'-tetraacetic acid
ER	Endoplasmic reticulum
ERK	Extracellular regulated kinase
FAK	Focal adhesion kinase
FAM65B	Family with sequence similarity 65, member B
FBS	Fetal bovine serum
FITC	Fluorescein isothiocyanate
G2/M	Second gap phase to mitosis DNA damage checkpoint
GAP	GTPase-activating protein
GDI	Guanine nucleotide dissociation inhibitor
GDP	Guanosine diphosphate
GEF	Guanine nucleotide exchange factor
GFP	Green fluorescent protein
gRNA	Guide RNA

GTP	Guanosine triphosphate
HEK293T	Human embryonic kidney 293T
HLB	Histone locus bodies
HSP60	Heat shock protein 60
hTERT	Human telomerase reverse transcriptase
IRDyes	Infrared fluorescent dyes
JAK/STAT	Janus kinase/signal transducer and activator of transcription
KANK1	KN motif-and ankyrin repeat domains 1
kDa	Kilodalton
LB broth base	Luria Bertani broth base medium
LIMK	LIM domain kinase
LKB1	Liver kinase B1
MAPT	Microtubule associated protein tau
MCF-7	Michigan cancer foundation-7
MDA-MB-231	MD Anderson metastasis breast cancer
MDD	Major depressive disorder
MgCl <sub>2</sub>	Magnesium chloride
MOC	Manders' overlap coefficient
M-PER	Mammalian protein extraction reagent
MS	Multiple sclerosis
NaCl	Sodium chloride
NADPH	Nicotinamide adenine dinucleotide phosphate (reduced form)
NaF	Sodium fluoride

Na <sub>2</sub> HPO <sub>4</sub>	Sodium phosphate dibasic
NaN <sub>3</sub>	Sodium azide
Na <sub>3</sub> VO <sub>4</sub>	Sodium orthovanadate
NEAAs	Non-essential amino acids
NFTs	Neurofibrillary tangles
NLS	Nuclear localization signal
NP-40	Nonidet P40
NtCDPK1	<i>Nicotiana tabacum</i> Ca <sup>2+</sup> -dependent protein kinase 1
Opti-MEM	Reduced-serum minimal essential medium
p21Waf1/Cip1	Cyclin-dependent kinase inhibitor 1/CDK-interacting protein 1
PAK1	P21 activated kinase 1
Pan 14-3-3	Total 14-3-3
Par3	Partitioning-defective protein 3
PBR	Polybasic region
PBS	Phosphate buffered saline
PC3	Human prostate cancer
PCC	Pearson's correlation coefficient
PD	Parkinson's disease
pEGFR	Phospho-epidermal growth factor receptor
PI3K	Phosphoinositide 3-kinase
PM	Plasma membrane
PML	Promyelocytic leukemia protein
PP1 $\alpha$	Protein phosphatase 1 alpha

PPI	Protein-protein interaction
PrP <sup>C</sup>	Cellular prion protein
pSX1-2-COOH	14-3-3 consensus binding motif extreme C-terminus (mode III)
Q61L	Glutamine to leucine substitution at position 61
Rac1	Ras-related C3 botulinum toxin substrate 1
Rac2	Ras-related C3 botulinum toxin substrate 2
Rac3	Ras-related C3 botulinum toxin substrate 3
RGS14	Regulator of G Protein Signaling 14
RhoA	Ras homolog gene family, member A
RhoGDI $\alpha$	Rho guanine dissociation inhibitor alpha
Rnd3	Rho family GTPase 3
ROCK	Rho-associated coiled coil containing protein kinase
ROR1	Receptor tyrosine kinase-like orphan receptor 1
RSXpSXP	14-3-3 consensus binding motif mode I
RXY/FXpSXP	14-3-3 consensus binding motif mode II
S71A	Mutation of serine 71 to alanine
S71E	Mutation of serine 71 to glutamic acid
SDS	Sodium dodecyl sulfate
SDS-PAGE	Sodium dodecyl sulfate-polyacrylamide gel electrophoresis
SGK1	Serum- and glucocorticoid-induced protein kinase 1
siRNA	Small interfering ribonucleic acid
SRC	Sarcoma viral oncogene
T108A	Mutation of threonine 108 to alanine

T108E	Mutation of threonine 108 to glutamic acid
T17N	Mutation of threonine 17 to asparagine
TBS	Tris-buffered saline
TBS-T	Tris-buffered saline-Tween 20
TcdA	Clostridium difficile toxin A
TCL	Total cell lysate
TCR	T-cell receptor
TEMED	Tetramethylethylenediamine
TGF- $\beta$ 1	Transforming growth factor-beta 1
Tiam1	T-cell lymphoma invasion and metastasis-inducing protein 1
Tir	Translocated intimin receptor
TM	Trabecular meshwork
Tris-HCl	Tris (hydroxymethyl) aminomethane hydrochloride
TRITC	Tetramethylrhodamine isothiocyanate
UTKO1	Cell migration inhibitor
WAVE	WASP-family verprolin-homologous
WT	Wild-type
Y64F/D	Mutation of tyrosine 64 to phenylalanine/aspartic acid

## Chapter 1: Introduction

### 1.1 Overview

The family of 14-3-3 proteins (tyrosine 3-monooxygenase/tryptophan 5-monooxygenase activation protein) comprise seven isoforms in mammals and exist as homo/heterodimers in cells. 14-3-3 proteins play important roles in many signaling networks as they specifically bind to serine/threonine phosphorylated proteins by altering the conformation, activity, and subcellular localization of their binding partners (Thomas et al., 2005; Freeman and Morrison 2011; Gardino and Yaffe, 2011; Zhu et al., 2015). 14-3-3 proteins interact with many proteins involved in cytoskeleton remodelling, DNA repair, and transcriptional regulation and regulate cell cycle development, cell proliferation, cell motility and apoptosis. The Rho GTPase family mediates a plethora of cellular processes including the regulation of cell size, proliferation, apoptosis/survival, cytoarchitecture, cell polarity, cell adhesion, cell motility and membrane trafficking (Benitah et al., 2004). The Rho GTPase family accounts for as many as 20 members. Among them, the Ras homolog gene family, member A (RhoA), ras-related C3 botulinum toxin substrate 1 (Rac1), and cell division cycle 42 (Cdc42) have been the most well-characterized (van Aelst and D'Souza-Schorey, 1997; Aznar and Lacal, 2001). Like all members of the small GTPases superfamily, Rho proteins act as molecular switches to control cellular processes by cycling between active, GTP-bound states and inactive, GDP-bound states.

Both 14-3-3 proteins and Rho GTPases regulate similar processes such as cytoskeleton remodeling and cell migration, which may suggest a possible interaction between the signaling pathways regulated by these two groups of proteins. My thesis provides novel insights and answers previously unknown questions about 14-3-3 protein subcellular localization and 14-3-3 protein interaction with Rac1.

## 1.2 14-3-3 protein isoforms

14-3-3 proteins were first identified in 1967 during a systematic classification of a family of abundant acidic brain proteins found in vertebrates and invertebrates. The name 14-3-3 was given based on their elution pattern at the 14<sup>th</sup> fraction number on diethylaminoethyl (DEAE)-cellulose chromatography, and their position at fraction 3.3 after subsequent purification using starch gel-electrophoresis (Moore and Perez, 1967). 14-3-3 proteins were then considered activators of enzymes for dopamine and neurotransmitter biosynthesis (Ichimura et al., 1988). 14-3-3 proteins were later shown to regulate protein kinase C activity (Aitken et al., 1990; Toker et al., 1990) and act as substrates for c-Bcr serine/threonine kinases (Reuther et al., 1994). 14-3-3 isoforms were then shown to interact with many protein kinases such as Raf (Fantl et al., 1994; Freed et al., 1994; Fu et al., 1994; Liu et al., 1996; Honda et al., 1997; Franger et al., 1998).

Various types and numbers of 14-3-3 proteins exist in different species (Thomas et al., 2005). 12 isoforms have been identified in *Arabidopsis* plants, 2 in *Drosophila* flies, and 2 in *Saccharomyces* yeast (Wang and Shakes, 1996; Rosenquist et al., 2000; Rosenquist et al., 2001). In mammalian cells, there are seven 14-3-3 isoforms, including alpha/beta, epsilon, gamma, eta, sigma, tau/theta, delta/zeta ( $\alpha/\beta$ ,  $\epsilon$ ,  $\gamma$ ,  $\eta$ ,  $\sigma$ ,  $\tau/\theta$ , and  $\delta/\zeta$ ), with  $\alpha$  and  $\delta$  representing the phosphorylated versions of  $\beta$  and  $\zeta$ , respectively (Ichimura et al., 1988; Toker et al., 1992; Gardino and Yaffe, 2011; Aghazadeh and Papadopoulos, 2016; Sluchanko and Gusev, 2017). Each isoform is encoded by a separate gene (*YWHAB*, *YWHAE*, *YWHAG*, *YWHAH*, *YWHAS/SFN*, *YWHAQ*, *YWHAZ*) and the genes are located on different chromosomes (Aitken, 2002; Thomas et al., 2005). In mammals, despite their highest expression in the central nervous system, 14-3-3 proteins are ubiquitously expressed in almost all other tissues, especially in the

intestines and testes (Boston et al., 1982a). Different 14-3-3 isoforms display tissue specificity and are present at different tissue concentrations (Perego and Berruti, 1997).

### 1.2.1 14-3-3 structure

X-ray crystallography data shows that the 14-3-3 subunits form a dimer that resembles a cup or horseshoe conformation. Each monomer contains a highly conserved amphipathic groove that acts as a ligand-binding channel for target binding (Liu et al., 1995; Xiao et al., 1995; Rittinger et al., 1999). Therefore, each dimer contains two binding pockets and can interact with two phosphoserine and/or two phosphothreonine motifs simultaneously. This dimeric structure is important for proper functioning of 14-3-3 and destabilization of the dimer results in decreased interaction with various target proteins (Shen et al., 2003; Gu et al., 2005). Each monomer of 14-3-3 consists of nine  $\alpha$ -helices and non-conserved carboxyl-terminal and amino-terminal regions (Aitken, 2006). The rigid helix of 14-3-3 may provide a functional basis for target protein binding (Bridges and Moorhead, 2004). The amino-terminal region is important for dimerization, which determines the specific combinations of isoforms (Bridges and Moorhead, 2004; Aitken, 2006). Also, certain pairs of 14-3-3 isoforms are more similar to each other based on their primary structure (Figure 1.1). This is consistent with previous research that used different software packages to phylogenetically group the isoforms based on shared regions of homology in their primary sequence (Aitken, 2002; Sluchanko and Gusev, 2010). The isoforms share about 50% amino acid identity and, consequently, highly similar protein conformations form either homodimers or heterodimers that serve as the functional protein units. Most 14-3-3 isoforms form homodimers and heterodimers *in vitro* and *in vivo*. 14-3-3 $\epsilon$  and  $\zeta$  were shown to form heterodimers *in vivo* (Jones et al., 1995). 14-3-3 $\gamma$  and  $\sigma$  prefer to homodimerize while 14-3-3 $\epsilon$

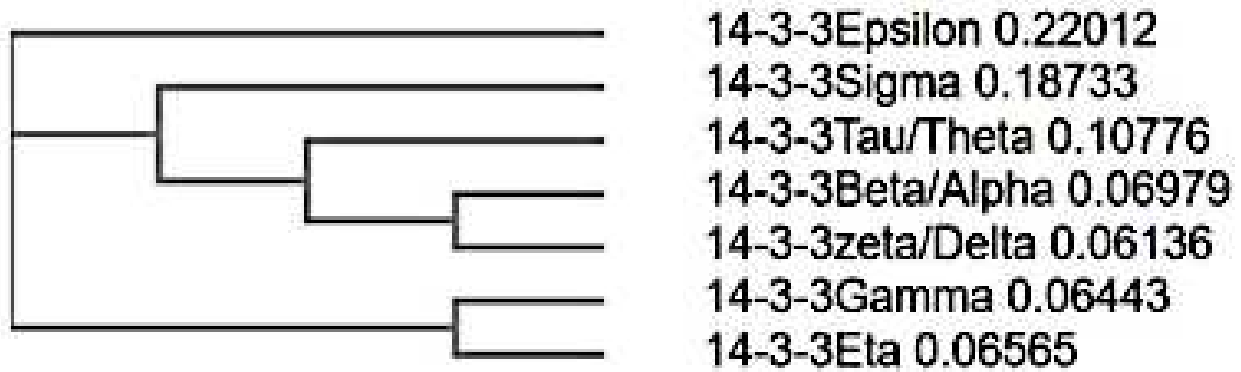


**Figure 1.1 Phylogenetic tree depicting homology of the primary structure of the seven 14-3-3 isoforms using ClustalOmega.** The primary structure of certain pairs of 14-3-3 isoforms, namely  $\eta$  and  $\gamma$ ,  $\beta$  and  $\zeta$ , as well as  $\sigma$  and  $\tau/\theta$  are quite similar to each other. However, the  $\epsilon$  isoform is significantly different from the other six 14-3-3 isoforms (unpublished figure created by A. Abdrabou).

prefers to heterodimerize in PC12 and COS-7 cells (Chaudhri et al., 2003). 14-3-3 $\gamma$  prefers to heterodimerize mainly with 14-3-3 $\epsilon$ . 14-3-3 $\epsilon$  heterodimerizes with 14-3-3 $\beta$ ,  $\eta$ ,  $\gamma$  and  $\zeta$  but do not homodimerize.

14-3-3 proteins are 28 kilodaltons (kDa) to 33 kDa and are regarded as a class of evolutionarily conserved, widely expressed homo/heterodimeric acidic proteins that bind vast numbers of intracellular proteins in normal cells and cancer cells (Mhawech, 2005; Cheng et al., 2012). There are many mammalian 14-3-3 isoforms, yet the protein binding partners interact on the same sites at specific recognition motifs (Wang et al., 1999). 14-3-3 proteins have been shown initially to bind to two phosphorylation-dependent high affinity binding motifs: 14-3-3 consensus binding motif mode I (RSXpSXP) and 14-3-3 consensus binding motif mode II (RXY/FXpSXP) (Yaffe et al., 1997; Rittinger et al., 1999). However, 14-3-3 proteins also bind to variations on the canonical motifs, for example, the +2 proline is present in only around half of validated 14-3-3-binding sites (Madeira et al., 2015). In addition to the two binding motifs, it was shown later that 14-3-3 proteins exhibit binding to the extreme C-terminus (pSX1–2–COOH) of numerous proteins, lately defined as mode III (Shikano et al., 2005; Coblitz et al., 2006; Sluchanko and Gusev, 2017). 14-3-3 proteins can also bind target proteins in a phosphorylation-independent manner. These proteins include phosphatase cell division cycle 25B (CDC25B) (Mils et al., 2000), human telomerase reverse transcriptase (hTERT) (Seimiya et al., 2000), serum- and glucocorticoid-activated protein kinase 1 (SGK1) and tau, a microtubule associated protein (MAPT) (Chun et al., 2004), amyloid  $\beta$ -protein precursor intracellular domain fragment (AICD) (Sumioka et al., 2005), heat shock protein 60 (HSP60) and cellular prion protein (PrP<sup>C</sup>) (Sato et al., 2005), enteropathogenic *Escherichia coli* translocated intimin receptor (Tir) protein (Patel et al., 2006), exoenzyme S (Ottmann et al., 2007), *Nicotiana*

*tabacum* Ca<sup>2+</sup>-dependent protein kinase 1 (NtCDPK1) (Ito et al., 2014), liver kinase B1 (LKB1) (Lu et al., 2017), regulator of G protein signaling 14 (RGS14) (Gerber et al., 2018) and non-muscle myosin II (West-Foyle et al., 2018). Among these proteins, SGK1, LKB1, NtCDPK1, and RGS14 interact with 14-3-3 in both phosphorylation-dependent and phosphorylation-independent manners.

### 1.2.2 14-3-3 function and subcellular localization

As mentioned above, 14-3-3 proteins are involved in many dynamic cellular processes, such as mitogenesis, cell cycle control, DNA damage checkpoints, and apoptosis (Moores et al., 2000; Aghazadeh and Papadopoulos, 2016; Sluchanko and Gusev, 2017). Recently, a growing number of proteins involved in actin remodeling have been identified as 14-3-3 binding partners. 14-3-3 proteins have been shown to play important roles in signal transduction pathways and cancer progression; however, the mechanisms have not been elucidated (Freeman and Morrison, 2011). Determining 14-3-3 isoform subcellular localization could provide new insights into their specific functions. However, most studies on 14-3-3 protein subcellular localization have been done in yeast, flies and plants (Su et al., 2001; Paul et al., 2005). It was previously reported that Rad24, a yeast 14-3-3 protein, acts as an attachable nuclear export signal to enhance the nuclear export of Cdc25 in response to DNA damage (Lopez-Girona et al., 1999). However, it was later shown that 14-3-3 mostly localized to the nucleus without binding to the ligand, but translocated to the cytoplasm following ligand-binding (Brunet et al., 2002). There have also been some studies done in mammals showing that both 14-3-3 $\gamma$  and  $\epsilon$  isoforms associate with the centrosome in tissues such as the human spleen (Pietromonaco et al., 1996). It has also been shown that 14-3-3 $\gamma$  localized to the centrosome and that loss of 14-3-3 $\gamma$  leads to centrosome

amplification (Mukhopadhyay et al., 2016). As mentioned above, 14-3-3 was initially discovered in brain extracts and it was later shown that 14-3-3 proteins were detected in cytoplasmic compartments of the rat hippocampus, while 14-3-3 $\gamma$  and  $\zeta$  were also present in mitochondrial and microsome-enriched fractions (Schindler et al., 2006). Specifically, 14-3-3 $\gamma$  and  $\zeta$  colocalize and interact with HSP60 in the mitochondria of human neuronal progenitor cells in culture (Satoh et al., 2005). 14-3-3 $\zeta$  was initially shown to localize in the glial cell progenitor cytoplasm, but later translocated into the nucleus when the progenitor differentiated (Lamba et al., 2009). 14-3-3 $\zeta$  was also reported to regulate nuclear trafficking of protein phosphatase 1 $\alpha$  (PP1 $\alpha$ ) (Jerome and Paudel, 2014). 14-3-3 $\zeta$  was also shown to regulate actin dynamics by binding to phosphocofilin to depolymerize actin (Gohla and Bokoch, 2002; Birkenfeld et al., 2003). 14-3-3 $\eta$  has been shown to localize and regulate cell apoptosis and oxidation in the mitochondria (Sreedhar et al., 2015; Liu et al., 2018). 14-3-3 $\tau/\theta$  also was shown to localize to both the nuclear and cytoplasmic compartments and also form a ternary protein complex with SGK1 and tau (Chun et al., 2004). Many more tissue and cell-specific expression of 14-3-3 isoforms have been reported in the literature (Lamba et al., 2009; Inamdar et al., 2018).

### 1.2.3 14-3-3 and cancer

Global downregulation of 14-3-3 expression causes tumor suppression, while overexpression of 14-3-3 proteins is often seen in many cancerous phenotypes (Nakanishi et al., 1997; Masters et al., 2002; Cao et al., 2006; Radhakrishnan and Martinez, 2010; Wang et al., 2011; Lee et al. 2012). 14-3-3 $\beta$ ,  $\epsilon$ ,  $\gamma$ ,  $\tau/\theta$  and  $\zeta$  isoforms have been shown to produce oncogenic effects in solid tumours (Nakanishi et al., 1997; Takihara et al., 2000). Specifically,  $\beta$ ,  $\epsilon$ ,  $\gamma$ ,  $\tau/\theta$  and  $\zeta$  14-3-3 gene expressions have been shown to be higher in lung cancer (Qi and Martinez,

2003). High levels of 14-3-3 $\beta$  have been found in glioblastoma cells, while 14-3-3 $\epsilon$ ,  $\tau/\theta$  and  $\zeta$  have been linked to human meningioma malignancy. 14-3-3 $\tau/\theta$  binds to the cyclin-dependent kinase inhibitor 1 or CDK-interacting protein 1 (p21Waf1/Cip1) and induces ubiquitin-independent proteasomal degradation of p21, promoting cell growth (Wang et al., 2010). Overexpression of 14-3-3 $\tau/\theta$  is frequently observed in human breast cancer cells and is associated with lower patient survival, possibly by increasing invasion and metastasis by inhibiting Rho guanine dissociation inhibitor alpha (RhoGDI $\alpha$ ) (Xiao et al., 2014). However, there has yet to be a direct link between 14-3-3 $\tau/\theta$  overexpression in breast cancer and breast cancer metastasis. Of all the 14-3-3 gene isoforms, 14-3-3 $\sigma$  (stratifin) and  $\zeta$  have been most directly linked to cancer. 14-3-3 $\sigma$  and  $\zeta$  isoforms produce opposite effects in mammary epithelial cells (Hong et al., 2010). 14-3-3 $\sigma$  is shown to have tumor suppressor effects by inducing cell cycle arrest at the second gap phase to mitosis DNA damage checkpoint (G2/M) transition. (Hermeking et al., 1997). 14-3-3 $\sigma$  expression is downregulated in bladder (Moreira et al., 2004), prostate (Cheng et al., 2004), and ovarian cancers (Ravi et al., 2011). By contrast, 14-3-3 $\sigma$  has also been shown to have tumorigenic effects by binding with pro-apoptotic signaling factors such as the human homologue of the v-Abl Abelson murine leukemia virus (c-Abl) and the Bcl-2-associated death promoter (BAD) (Donovan et al., 2002; Yoshida et al., 2005). In contrast, increased expression of 14-3-3 $\zeta$  has been linked to enhanced tumor growth in glioma, cervical carcinoma, leukemia, lung cancer, prostate cancer and breast cancer. 14-3-3 $\zeta$  has been shown to be a potential marker for cancer prognosis and 14-3-3 $\zeta$  inhibition may be used as a targeted therapeutic strategy in the treatment of prostate cancer (Neal and Yu, 2010; Goc et al., 2012).

#### 1.2.4 14-3-3 and neurological disease

14-3-3 isoforms are involved in a wide range of neurological disorders including many neurodegenerative disorders such as Creutzfeldt–Jakob disease (CJD) (Wiltfang et al., 1999; Baxter et al., 2002; Mackie and Aitken, 2005), Alzheimer's disease (AD) (Layfield et al., 1996), Parkinson's disease (PD) (Ostrerova et al., 1999) and polyglutamine repeat diseases (Waelter et al., 2001; Chen et al., 2003; Mackie and Aitken, 2005). 14-3-3 $\gamma$  is considered a marker of different neurodegenerative diseases since 14-3-3 $\gamma$  is found to be elevated in certain prion diseases such as CJD in humans, scrapie in sheep, and bovine spongiform encephalopathy (BSE) in cattle (Xiao et al., 2005; Pennington et al., 2009). For instance, high concentrations of 14-3-3 $\beta$ ,  $\epsilon$  and  $\eta$  were detected in cerebrospinal fluid of patients with CJD (Green et al., 2001; Berg et al., 2003). In addition, PrP<sup>C</sup> co-immunoprecipitated and formed a complex with 14-3-3 in the human CNS and this complex might disassociate in prion diseases (Sato et al. 2005). The levels of 14-3-3 proteins were also increased in patients with tuberculous meningitis and multiple sclerosis (MS) (Boston et al., 1982b). Also 14-3-3 $\zeta$  has been shown to interact with tau proteins to stimulate tau phosphorylation by several protein kinases. This leads to aggregation in neurofibrillary tangles (NFTs) which affect neuronal function (Layfield et al., 1996; Sluchanko and Gusev, 2011). 14-3-3 $\eta$  has also been associated with and is a potential biomarker candidate for neuropsychiatric disorders such as schizophrenia, bipolar disorder, and depression (Toyo-Oka et al., 1999; Jia et al., 2004). However, the underlying molecular mechanisms have yet to be elucidated.

### **1.3 Rho GTPases**

Rho GTPases are a large subfamily of monomeric, small guanosine triphosphate (GTP)-binding proteins belonging to the Ras superfamily. The Rho family of GTPases accounts for as

many as 20 candidate members. RhoA, Rac1, and Cdc42 have been the most extensively characterized proteins within the Rho GTPase family (van Aelst and D'Souza-Schorey, 1997; Aznar and Lacal, 2001; Burridge and Wennerberg, 2004). Rho GTPases play pivotal roles in many biological processes such as regulating cell size, cell proliferation, cell polarity, cell adhesion, cell motility, membrane trafficking and apoptosis (Nobes and Hall, 1995; Zhu et al., 2015). Like all other small GTP-binding proteins, the regulatory cycle of Rho GTPases is exerted by three distinct families of proteins. Guanine nucleotide exchange factors (GEFs) activate Rho GTPases by promoting the exchange of guanosine diphosphate (GDP) by GTP. GTPase-activating proteins (GAPs) negatively regulate Rho GTPases by stimulating its intrinsic GTPase activity leading to an inactive GDP-bound state. Guanine nucleotide dissociation inhibitors (GDIs) inhibit the dissociation of GDP from Rho GTPases and prevent the binding of GDP-Rho GTPases to cell membranes. Rho GEFs, GAPs, and GDIs thus have been established as the mainstream regulators of Rho GTPases (Aznar and Lacal, 2001; Dvorsky and Ahmadian, 2004). It has become evident, however, that a simple GTPase cycle cannot solely explain the variety of functions and signaling initiated by Rho proteins.

Rac family members stimulate the formation of lamellipodia and membrane ruffles in cultured fibroblasts (Ridley and Hall, 1992; Ridley et al., 1992; Ridley, 2001a; Ridley, 2001b; Burridge and Wennerberg, 2004). The Rac subfamily of Rho GTPases includes Rac1 (and its splice variant Rac1b), Rac2 and Rac3, which share high sequence similarity (88%) (Boureux et al., 2007; Bosco et al., 2009). They diverge primarily by 15 residues in their C-termini. Rac1 is ubiquitously expressed, Rac2 is expressed in hematopoietic cells and also regulates superoxide generation via nicotinamide adenine dinucleotide phosphate (reduced form) (NADPH) oxidase in phagocytes (Didsbury et al., 1989; Shirsat et al., 1990) and Rac3 mRNA is expressed in the brain

(Haataja et al., 1997; Bolis et al., 2003; Corbetta et al., 2005). Rac1 has a molecular weight of 21.4 kDa and is mainly present at the plasma membrane (PM). It contains a common G-domain fold, which consists of a six-stranded  $\beta$ -sheet surrounded by  $\alpha$ -helices (Vetter and Wittinghofer, 2001). The differences between the GDP-bound and the GTP-bound forms are confined primarily to two segments, referred to as the switch I and the switch II regions (Milburn and Jeffrey, 1990). The amino acid sequence for Rac1 is shown in Figure 1.2. Rac1 is activated at the leading edge of motile cells and induces actin-rich lamellipodia formation, which drive cell movement (Nobes and Hall, 1999; Kraynov et al., 2000; Small et al., 2002). The major downstream proteins that mediate actin polymerization in lamellipodia protrusions are the WASP-family verprolin-homologous (WAVE) proteins, which are the activators of the actin-related protein 2/3 (Arp2/3) complex (Miki et al., 1998; Yamazaki et al., 2003). The activated Arp2/3 complex induces the rapid polymerization of actin and the formation of the branched actin filaments in lamellipodia (Welch and Mullins, 2002; Pollard and Borisy, 2003). However, the precise mechanisms that lead to Rac1 activation during cell migration are not fully understood.

### 1.3.1 Rac1 regulation and phosphorylation

Rho GTPases are best known for their role in regulating the cytoskeleton and in regulating gene expression. Rac1 also regulates important cellular processes relevant to cancer and transduces signals in many oncogenic pathways. Recent findings suggest that additional regulatory mechanisms such as post-transcriptional and post-translational regulation might further contribute to the tight regulation of Rho GTPases (Abdalla and Wang, 2018). These modifications include microRNAs (Liu et al., 2012), ubiquitination (Mettouchi and Lemichez,

2012), palmitoylation (Navarro-Lerida et al., 2012), and phosphorylation (Loirand et al. 2006). Prenylation also plays a role in the regulation of Rac1 by targeting Rac1 to the PM and Rac1 interaction with GEFs (Samuel and Hynds, 2010). RhoA was the first Rho protein shown to be phosphorylated (Lang et al., 1996; Sauzeau et al., 2000; Forget et al., 2002; Ellerbroeck et al., 2003). Subsequently, the other members of the Rho family, including Cdc42, RhoE, and Rac1 have been shown to be regulated by serine or tyrosine phosphorylation (Kwon et al., 2000; Riento et al., 2003; Tu et al., 2003; Chang et al., 2011). Rac1 was shown to be phosphorylated on serine 71 (S71) by protein kinase B (Akt) (Kwon et al., 2000). This phosphorylation of S71 on Rac1 inhibits its GTP binding activity without any significant change in GTPase activity. Both the GTP binding and the GTPase activities of the Rac1 mutation of serine 71 to alanine (S71A) are abolished regardless of Akt activity. In addition, Rac1 S71 phosphorylation decreases the pathogenic effect of *Clostridium difficile* toxin A (TcdA) (Schoentaube et al., 2009). Moreover, Rac1 S71 phosphorylation represents a reversible mechanism to determine the binding specificity of Rac1/Cdc42 to their downstream substrates (Schwarz et al., 2012). Rac1 is also phosphorylated on Y64 by focal adhesion kinase (FAK) and sarcoma viral oncogene (SRC) (Figure 1.2). Y64 phosphorylation targets Rac1 to focal adhesions and the mutation of tyrosine 64 to phenylalanine (Y64F) displayed increased GTP-binding, increased association with p21-activated kinase (PAK)-interacting exchange factor  $\beta$  ( $\beta$ 1PIX), and reduced binding to RhoGDI compared to Rac1 WT. Mutating Rac1 tyrosine to aspartic acid (Y64D) showed less binding to PAK than Rac1 WT or Rac1 Y64F. PAKs are serine/threonine kinases that bind activated Rac or Cdc42 (Manser et al., 1994). *In vitro* assays demonstrated that Rac1 Y64 is a target for FAK and SRC (Chang et al., 2011). Finally, extracellular regulated kinase (ERK) phosphorylates threonine 108 (T108) of Rac1 in response to epidermal growth factor (EGF) stimulation (Tong et al.,

1 mqaikcvvvg dgavgktcll isyttnafpg eyiptvfdny  
41 sanvmvdgkp vnlglwdtag qedydrlrpl sypqtdvfli  
81 cfslvspasf envrakwype vrhhcpntpi ilvgtkldlr  
121 ddkdtieklk ekkltptyp qglamakeig avkylecsal  
161 tqrglktvfd eairavlcpp pvkkkrkrkcl //

**pntp**: PLC- $\gamma$ 1 SH3 binding sites and Erk phosphorylation site

**kkkrkrkcl II**: PBR (polybasic region) and Erk docking site (D-site)

**kkkrkrk**: NLS (nuclear localization signal)

**k147 and k166**: Ubiquitination sites

**S71, T108 and Y64**: Phosphorylation sites

**cIII**: CAAX box

Figure 1.2 Rac1 amino acid sequence depicting motifs and phosphorylation sites

(Brandwein and Wang, 2017).

2013). This phosphorylation alters Rac1 activity, subcellular localization and cell migration. The subcellular localization of Rac1 is also regulated by its C-terminal polybasic region (PBR) (Figure 1.2). It was shown that the PBR of Rac1 has a functional nuclear localization signal (NLS) sequence, which acts as an NLS for protein complexes containing Rac1 (Lanning et al., 2003) (Figure 1.2). Rac1 is phosphorylated at multiple sites; however, the function and the significance of these phosphorylations are not clear.

#### **1.4 Interactions between 14-3-3 proteins and Rho GTPases**

Accumulating evidence suggests that the interaction between the signaling pathways of 14-3-3 proteins and Rho proteins play important roles in the regulation of cytoskeleton remodeling and cell migration (Figure 1.3). Most findings support the role of 14-3-3 proteins regulating Rho GTPases. Research indicates that 14-3-3 proteins regulate RhoA through interactions with Rho GEFs and Rho GAPs. Previous research using a yeast two-hybrid screen shows 14-3-3 $\eta$  and  $\epsilon$  as p190RhoGEF binding partners. Deleting the p190RhoGEF 14-3-3 binding site abolishes their interaction *in vitro* as well as the ability of 14-3-3 $\eta$  to alter the cytoplasmic aggregation of p190RhoGEF in cotransfected cells (Zhai et al., 2001). The findings suggest a potential role for 14-3-3 in modulating p190RhoGEF activity. Other research shows a phospho-dependent 14-3-3 binding site on the A kinase anchoring protein (AKAP-Lbc). AKAP-Lbc is a GEF for Rho GTPases. Protein kinase A (PKA) induces 14-3-3 protein binding to AKAP-Lbc, which suppresses Rho activation *in vivo* (Jin et al., 2004). 14-3-3 $\beta$  negatively regulates the GEF activity of dimeric  $\beta$ 1Pix only, which suggests a role of  $\beta$ 1Pix GEF activity modulation by 14-3-3 $\beta$  (Chahdi and Sorokin, 2008). KN Motif and Ankyrin Repeat Domains 1 (KANK1) is shown to be a candidate tumor suppressor gene for renal cell carcinoma (Mettouchi

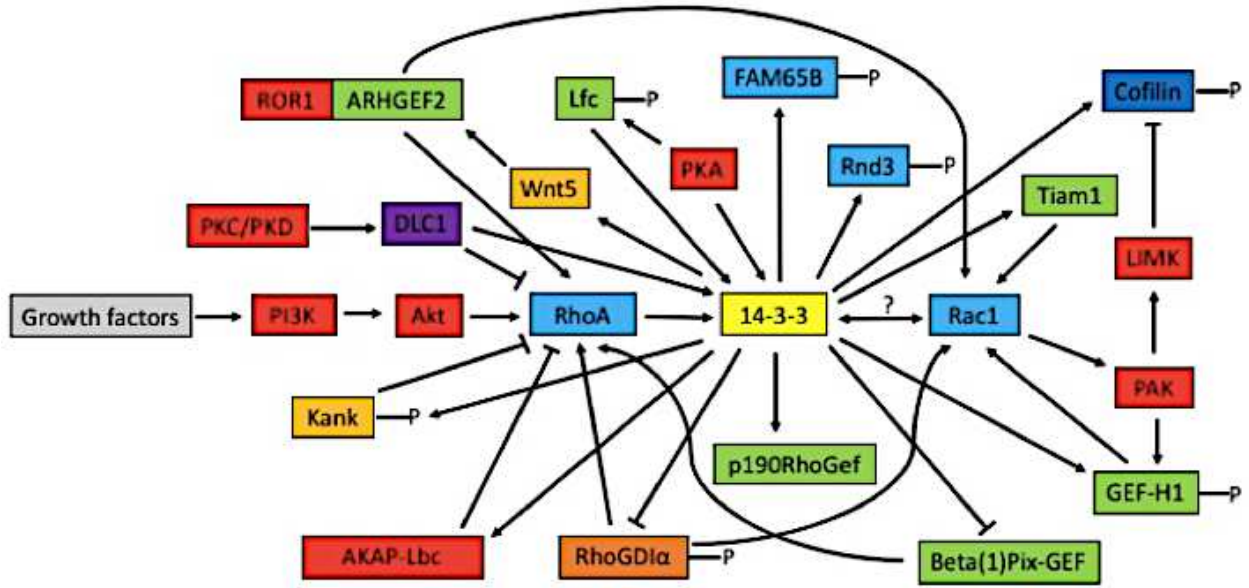


**Figure 1.3 Reported interactions between 14-3-3 proteins and Rho GTPases.** 14-3-3 proteins interact indirectly or directly with many Rho regulators, eventually affecting multiple functions of Rho GTPases including cytoskeletal remodeling and cell migration. Arrows represent activation and T-bars represent inhibition (Brandwein and Wang, 2017).

and Lemichez, 2012). KANK1 negatively regulates the formation of actin stress fibers and regulates cell migration through inhibiting RhoA activity, which is controlled by KANK1 binding to 14-3-3 in the phosphoinositide 3-kinase-Akt (PI3K-Akt) signaling pathway (Kakinuma et al., 2008). Deleted in liver cancer 1 (DLC1) is a Rho GAP that is downregulated in various tumor types. *In vitro*, DLC1 inactivates the small GTPases RhoA, RhoB and RhoC through its GAP domain and this contributes to its tumor suppressor function *in vivo*. DLC1 associates with 14-3-3 upon protein kinase C and protein kinase D activation, which inhibits DLC1 GAP activity and facilitates active Rho signaling (Scholz et al., 2009). 14-3-3 protein interacts directly, in a phosphorylation-dependent manner with Lfc, which suppresses the Lfc WT exchange activity on RhoA (Meiri et al., 2009). Studies also support the role of 14-3-3 in regulating Rac1. EGF induces biphasic Rac1 activation during cell migration. UTKO1, a cell migration inhibitor, only inhibits the second EGF-induced wave of Rac1 activation, not the first wave. UTKO1 functions to abrogate 14-3-3 $\zeta$  binding to T-cell lymphoma invasion and metastasis-inducing protein 1 (Tiam1) that is responsible for the second wave of Rac1 activation. This suggests that the interaction between 14-3-3 $\zeta$  and Tiam1 is involved in Rac1 activation (Kobayashi et al., 2001). Previous studies show that 14-3-3 $\zeta$  mediates the integrin-induced activation of Cdc42 and Rac1 (Bialkowska et al., 2003). For instance, 14-3-3 $\zeta$  recruits Tiam1 to  $\beta$ 1-integrin complexes where it mediates integrin-induced Rac1 activation and motility (O'Toole et al., 2011). 14-3-3 $\zeta$  WT expression significantly enhances Rac activity in human prostate cancer (PC3) cells, which enhances prostate cancer cell–matrix interactions, motility and ultimately transendothelial migration (Goc et al., 2012). In contrast, 14-3-3 $\zeta$  repression inhibits Rac1 activation and decreases lamellipodia formation (Deakin et al., 2009; Sluchano and Gusev, 2010; Goc et al., 2012). Human T cell activation through the T-cell receptor (TCR) leads to

many downstream effects including the binding and interaction between Tiam1 and 14-3-3 protein, which activates Rac1 (Gronholm et al., 2011). The Tiam1-14-3-3 protein complex subsequently leads to downstream cytoskeleton remodeling, cell adhesion and cell migration. One study shows that 14-3-3 $\zeta$  binds to Tiam1 upon loss of the partitioning-defective protein 3 (Par3), which triggers the high levels of Rac-GTP (Tong et al. 2016). Partitioning-defective proteins are responsible for establishing cell polarity. Rac1 activation then triggers Janus kinase/signal transducer and activator of transcription (JAK-STAT) pathway activation, which results in lung adenocarcinoma tumor growth, cell proliferation, angiogenesis and metastasis. 14-3-3 protein binds to the phosphorylated Rho family GTPase 3 (Rnd3), an atypical constitutively GTP-bound Rho protein, which inhibits cell rounding and apoptosis by translocating it to the cytosol from the PM (Riou et al., 2013).

Lfc is a Rho GEF that also associates with microtubules and is phosphorylated in an AKAP-dependent manner by PKA. 14-3-3 $\tau/\theta$  promotes breast cancer metastasis by binding and inhibiting RhoGDI $\alpha$ , which is a negative regulator of Rho GTPases and a metastasis suppressor. Specifically, 14-3-3 $\tau/\theta$  binds phosphorylated RhoGDI $\alpha$  and blocks its association with Rho GTPases, thereby promoting EGF-induced RhoA, Rac1, and Cdc42 activation (Xiao et al., 2014). 14-3-3 proteins also bind to the phosphorylated family with sequence similarity 65, member B (FAM65B), an atypical RhoA inhibitor, which regulates myoblast and hair cell differentiation, lymphocyte T proliferation and neutrophil polarization. Splice site mutations lead to hearing loss in patients since it is a component of hair cell stereocilia (Gao et al., 2015). 14-3-3 $\zeta$  regulates cytoskeletal structures, extracellular matrix (ECM) homeostasis, and transforming growth factor-beta 1 (TGF- $\beta$ 1)-induced contraction in trabecular meshwork (TM) cells using the RhoA signaling pathway (Ye et al., 2016). 14-3-3 $\zeta$  also plays a critical role in Wnt5a-induced

recruitment of Rho guanine nucleotide exchange factor 2 (ARHGEF2) to receptor tyrosine kinase-like orphan receptor 1 (ROR1), thereby activating ARHGEF2, RhoA and Rac1 in chronic lymphocytic leukemia (CLL) cells (Yu et al., 2017).

14-3-3 protein also acts downstream of Rho GTPases including RacE, which associates with the myosin II heavy chain needed for myosin II bipolar thick filament remodeling (Zhou et al., 2010). Rho GTPases also act through p21 activated kinase 1 (PAK1) and Rho kinase to inhibit cofilin activity by the LIM domain kinase (LIMK)-mediated phosphorylation of cofilin (Gohla and Bokoch, 2002). 14-3-3 $\zeta$  binds to phosphocofilin, and 14-3-3 $\zeta$  with LIMK further elevate phosphocofilin levels, affecting the actin cytoskeleton. Bound 14-3-3 $\zeta$  somehow protects phosphocofilin from phosphatase-mediated dephosphorylation. Rho GTPases regulate 14-3-3 $\zeta$  binding to phosphocofilin through PAK1, which regulates actin fibers through maintaining phosphocofilin levels. Rho and 14-3-3 proteins are also regulated through GEF-H1, which is a phosphorylation target of PAK1. GEF-H1 phosphorylation by PAK1 regulates 14-3-3 docking to GEF-H1 and its recruitment to microtubules. This suggests that PAK1 and 14-3-3 are involved in regulating GEF-H1 activity, which may affect downstream Rac/Cdc42- and Rho-dependent signaling pathways (Zenke et al., 2004). 14-3-3 proteins also assist in the localization of activated Rac1 to membrane ruffles (Somanath and Byzova, 2009). Rnd3 directly interacts with 14-3-3 protein through its C-terminal site, which consists of a Rho-associated coiled coil-containing protein kinase (ROCK)-dependent Ser240 phosphorylation site (Riou et al., 2013). However, as Rac1 is geranylgeranylated, rather than farnesylated at the C-terminal, and S71 is far away from the C-terminal, the mechanisms underlying its interaction with 14-3-3 protein may differ. The interactions mentioned above between 14-3-3 proteins and Rac1 are indirect and no data has shown a direct interaction.

## 1.5 Thesis rationales, hypotheses, and objectives

While the existence of multiple isoforms may represent one more level of regulation in 14-3-3 signaling, knowledge regarding the isoform-specific functions of 14-3-3 proteins is limited. Determination of the subcellular localization of the different 14-3-3 isoforms could give important clues into their specific functions. However, most subcellular localization studies have been done on yeast, flies, and plants. There have yet to be studies done on the subcellular localization of the mammalian 14-3-3 isoforms, their specific redistribution throughout the cell cycle and translocation in response to growth factors in the same cell/tissue. In this thesis, by using immunocytochemistry, subcellular fractionation, and immunoblotting, I studied the subcellular localization of the total 14-3-3 protein and each 14-3-3 isoform, their redistribution throughout the cell cycle and translocation in response to EGF in COS-7 cells. **I hypothesize that the 14-3-3 isoforms have different subcellular localizations, which underlines the diverse functions of 14-3-3 proteins.** So far, all the data regarding the interaction between Rho GTPases and 14-3-3 proteins are indirect. However, it is possible that Rac1 could interact with 14-3-3 proteins directly. Rac1 is phosphorylated on S71 by Akt (Kwon et al., 2000). Examination of the Rac1 amino acid sequence shows that the <sup>68</sup>RPLpSYP<sup>73</sup> motif is close to the mode I 14-3-3 consensus binding RSXpSXP motif following the phosphorylation of S71 by Akt (Umahara et al., 2012; Obsilova et al., 2014). This suggests that S71 phosphorylation could regulate Rac1 interaction with 14-3-3 proteins. **I hypothesize that Rac1 S71 phosphorylation mediates the interaction between Rac1 and 14-3-3 proteins.**

## Chapter 2: Materials and Methods

### 2.1 Materials

All chemicals, enzymes, and kits were used according to the manufacturer specifications and in accordance with protocols set out by the Environmental Health and Safety (EHS) at the University of Alberta and the Workplace Hazardous Materials Information System (WHMIS).

#### 2.1.1 Chemicals and reagents

Acrylamide/bis	BioRad
4-(2-aminoethyl)-benzenesulfonyl fluoride (AEBSF)	Sigma
Agarose	Gibco
Ammonium persulfate (APS)	BDH
Ampicillin	Sigma
Aprotinin	Sigma
$\beta$ -mercaptoethanol	Sigma
N,N-bis(2-hydroxyethyl)-2-aminoethanesulfonic acid (BES)	Sigma
Bromophenol blue	BioRad
Calcium chloride (CaCl <sub>2</sub> )	Sigma
4',6-diamidino-2-phenylindole (DAPI)	Sigma
Dulbecco's modified eagle's medium (DMEM)	Gibco
Dimethyl sulfoxide (DMSO)	Fisher
Dithiothreitol (DTT)	Sigma
Ethylenediaminetetraacetic acid (EDTA)	Sigma
Epidermal growth factor (EGF)	Upstate

Ethylene glycol-bis( $\beta$ -aminoethyl ether)-	
N,N,N',N'-tetraacetic acid (EGTA)	Sigma
Ethanol, 95%	Fisher
Fetal bovine serum (FBS), 10%	Sigma
Glucose	EM science
Glycerol	BDH
Glycine	BioRad
Goat anti-mouse IgG agarose beads	Sigma
Goat anti-mouse protein G agarose beads	Sigma
Hydrochloric acid (HCl)	Fisher
Isopropanol	Fisher
Kanamycin	Sigma
Lipofectamine 2000	Life technologies
Luria-Bertani (LB) broth base	Invitrogen
Magnesium chloride ( $MgCl_2$ )	BDH
Mammalian protein extraction reagent (M-PER)	Pierce
Methanol	Sigma
Mouse anti-14-3-3 $\beta$ blocking peptide	Santa Cruz
Mouse anti-14-3-3 $\epsilon$ blocking peptide	Santa Cruz
Mouse anti-14-3-3 $\gamma$ blocking peptide	Santa Cruz
Mouse anti-14-3-3 $\sigma$ blocking peptide	Santa Cruz
Non-essential amino acids (NEAA)	Gibco
Nonidet P40 (NP-40)	BDH

Reduced-serum minimal essential media (Opti-MEM)	Gibco
Penicillin/streptomycin (100U)	Gibco
Pepstatin A	Sigma
Phosphate buffered saline (PBS)	OmniPur
Potassium chloride (KCl)	BDH
Rabbit protein A agarose beads	Millipore sigma
Sodium azide ( $\text{NaN}_3$ )	Sigma
Sodium chloride (NaCl)	Sigma
Sodium dodecyl sulfate (SDS)	BioRad
Sodium fluoride (NaF)	Sigma
Sodium orthovanadate ( $\text{Na}_3\text{VO}_4$ )	Sigma
Sucrose	BioBasic
Tetramethylethylenediamine (TEMED)	Sigma
Tris-buffered saline (TBS)/Odyssey blocking buffer	Li-Cor
Tris (hydroxymethyl) aminomethane	Invitrogen
Triton X-100	BDH
Tween 20	Sigma
Wortmannin	Sigma
Yeast extract, select	Gibco

### 2.1.2 Enzymes

RNase A	Qiagen
---------	--------

### 2.1.3 Experimental kits

EZ-Spin column plasmid DNA kit	BioBasic
Qiaprep Spin Midiprep kit	Qiagen
Qiaprep Spin Maxiprep kit	Qiagen

### 2.1.4 Plasmids

pEGFP-C3	Clontech
pGEX-3X	Clontech

### 2.1.5 Antibodies

#### 2.1.5.1 Primary Antibodies

Goat anti- $\alpha$ -actin antibody	Sigma
Goat anti-pEGFR1086 antibody	Santa Cruz
Mouse anti-14-3-3 $\beta$ antibody (A-6) (sc-25276)	Santa Cruz
Mouse anti-14-3-3 $\epsilon$ antibody (F-3) (sc-393177)	Santa Cruz
Mouse anti-14-3-3 $\eta$ antibody (6A12) (sc-293464)	Santa Cruz
Mouse anti-14-3-3 $\eta$ antibody (10847-MM06)	Sino Biological
Mouse anti-14-3-3 $\gamma$ antibody (D-6) (sc-398423)	Santa Cruz
Mouse anti-14-3-3 $\sigma$ antibody (E-11) (sc-166473)	Santa Cruz
Mouse anti-14-3-3 $\tau/\theta$ antibody (1A1) (NBP1-21301)	Novus Biologicals
Mouse anti-14-3-3 $\theta$ antibody (5J20) (sc-69720)	Santa Cruz
Mouse anti-14-3-3 $\zeta$ antibody (1B3) (sc-293415)	Santa Cruz
Mouse anti-14-3-3 $\zeta$ antibody (G-2) (sc-518031)	Santa Cruz

Mouse anti- $\alpha$ -tubulin antibody	Abcam
Mouse anti-pRac1 (S71) antibody	Abcam
Mouse anti-pan 14-3-3 antibody (H-8) (sc-1657)	Santa Cruz
Mouse anti-Rac1 antibody	Cytoskeleton
Rabbit anti-calnexin antibody	Santa Cruz
Rabbit anti-GFP antibody	Clontech
Rabbit anti-HSP60 antibody	Novus Biologicals
Rabbit anti-lamin A/C antibody	Santa Cruz
Rabbit anti-pAkt S473 antibody	Santa Cruz

#### 2.1.5.2 Secondary Antibodies

FITC-conjugated donkey anti-mouse IgG antibody	Jackson ImmunoRes
IRDye 680RD donkey anti-goat IgG antibody	Li-Cor
IRDye 800CW donkey anti-goat IgG antibody	Li-Cor
TRITC-conjugated donkey anti-rabbit IgG antibody	Jackson ImmunoRes

#### 2.1.6 Molecular size markers

Prestained marker for SDS-PAGE (BLUelf)	FroggaBio
---	-----------

#### 2.1.7 Buffers and other solutions

A list of all buffers and solutions used in this study is provided in Table 2.1.

#### 2.1.8 Other materials

Odyssey Infrared Scanner CLx Imaging System	Li-Cor
GE Healthcare DeltaVision Deconvolution Microscopy system	GE Healthcare
NanoVue Plus Spectrophotometer	GE Healthcare
Nitrocellulose membrane	BioRad
Whatman chromatography paper	Fisher

**Table 2.1 Buffers and other solutions used in this thesis**

Solution	Composition
BES buffer	140 mM NaCl, 0.75 mM Na <sub>2</sub> HPO <sub>4</sub> , 25 mM BES, pH 6.95
Homogenization buffer	0.25 M sucrose, 20 mM Tris-HCl pH 7.0, 1 mM MgCl <sub>2</sub> , 4 mM NaF, 0.5 mM Na <sub>3</sub> VO <sub>4</sub> , 0.1 mM AEBSF, 10 µg/ml aprotinin, 1 µM pepstatin A
Mammalian protein extraction reagent	0.5 mM Na <sub>3</sub> VO <sub>4</sub> , 0.02% NaN <sub>3</sub> , 0.1 mM AESBF, 10 µg/ml aprotinin, 1 µM pepstatin A
Phosphate buffered saline (PBS)	137 mM NaCl, 2.7 mM KCl, 10 mM phosphate buffer
Protease inhibitor cocktail	0.5 mM Na <sub>3</sub> VO <sub>4</sub> , 0.1 mM AEBSF, 10 µg/ml aprotinin, 1 µM pepstatin A

SDS-loading buffer	250 mM Tris-HCl, 40% glycerol, 8% SDS, 20% $\beta$ -mercaptoethanol, 2% bromophenol blue
Transfer buffer	48 mM Tris, 39 mM glycine, 20% methanol, 10% SDS, ddH <sub>2</sub> O
Tris-buffered saline-Tween 20 (TBS-T)	1 M Tris-HCl, pH 7.5, 150 mM NaCl, ddH <sub>2</sub> O, 0.05% Tween 20
Triton X-100 lysis buffer	0.4% Triton X-100, 140 mM NaCl, 50 mM Tris-HCl, pH 7.2, 1 mM EGTA

---

## 2.2 Methods

### 2.2.1 Cell lines

The following cell lines were used in this thesis: CV-1 (simian) in origin, and carrying the SV40 genetic material-7 (COS-7) [African green monkey kidney fibroblast cells transiently expressing green fluorescent protein (GFP)-tagged Rac1 wild-type (GFP-Rac1 WT)] (gift from Mark R. Philips, New York University) or GFP-tagged Rac1 S71A (GFP-Rac1 S71A); human embryonic kidney 293T (HEK293T) [human embryonic kidney cells, American type culture collection (ATCC) CRL-11268]; MD Anderson metastasis breast cancer (MDA-MB-231) and Michigan Cancer Foundation-7 (MCF-7) (human breast cancer cells, ATCC HTB-26 and ATCC HTB-22). These cell lines endogenously express 14-3-3 proteins to detectable levels.

### 2.2.2 Cell culture, transfection and treatment

COS-7, HEK293T, MDA-MB-231, and MCF-7 cells were grown at 37°C and maintained in a 5% CO<sub>2</sub> atmosphere in Dulbecco's modified Eagle's medium (DMEM) (Gibco) supplemented with 10% fetal bovine serum (FBS), penicillin (100 IU/ml), streptomycin (100 µg/ml) and non-essential amino acids (NEAA). Prior to transfection, cells were seeded into 100 mm plates and incubated until cells were 60-70% confluent.

COS-7 cells were transiently transfected with GFP-Rac1 WT and GFP-Rac1 S71A constructs by calcium phosphate precipitation or Lipofectamine 2000 reagent (Life technologies) according to the manufacturers' instructions. Plasmid DNA (~8 µg) was dissolved in distilled water (dH<sub>2</sub>O) with CaCl<sub>2</sub> at a concentration of 250 mM to a final volume of 500 µl. This mixture was then added dropwise to 500 µl of 50 mM *N,N*-bis(2-hydroxyethyl)-2-aminoethanesulfonic acid (BES) buffer containing 140 mM sodium chloride (NaCl), 0.75 mM sodium phosphate dibasic (Na<sub>2</sub>HPO<sub>4</sub>), 25 mM BES pH 6.95 to a final volume of 1000 µl. The mixture was then incubated at room temperature for 40 min, where it was then added dropwise to cell cultures at 70-80% confluency in 100 mm plates while shaking the plates gently. The medium was changed 24 h later and visualized with fluorescence microscope to detect the GFP constructs and make sure the transfection was successful. Twenty-four to forty-eight hours after transfection, the cells were used for all of the assays.

At 60-70% confluency, cells were transfected with purified plasmid DNA using the Lipofectamine 2000 (Life technologies) protocol. Reduced-serum Minimal Essential Medium (Opti-MEM) was incubated with Lipofectamine 2000 reagent for 5 min at room temperature and DNA was also incubated with Opti-MEM (Gibco, ThermoFisher Scientific). Then the complexes were added together in a 1:1 ratio and incubated for 20 min at room temperature. Then the mixture was added dropwise to the 100 mm plates with gentle shaking. 4-6 h after transfection,

the media was replaced with complete DMEM supplemented with 10% FBS. Cells were left to incubate overnight for 18-24 h and checked for GFP expression with fluorescence microscopy. Then, proteins were extracted from cells 48-60 h after transfection. The cells were then washed with room temperature or cold phosphate buffered saline (PBS) (137 mM NaCl, 2.7 mM KCl, 10 mM phosphate buffer) and harvested for protein extraction. The transfection efficiency of the cells for all of the experiments using Lipofectamine 2000 reagent was 60-70%. For the EGF treatments, cells were serum starved for 12 h, and EGF (50 ng/ml stock concentration) was added to a final concentration of 100 ng/ml for 5, 15 and 30 min. For wortmannin treatment, cells were incubated with wortmannin at 100 nM for 30 min prior to EGF treatment.

### 2.2.3 Culture and purification of GFP-Rac1 plasmids

GFP-Rac1 WT was a gift from Mark R. Philips (School of Medicine, New York University). The mutant GFP-Rac1 S71A with the point mutation was created with the QuikChange multiple site-directed mutagenesis kit (Stratagene, La Jolla, CA) with GFP-Rac1 WT as a template. The GFP-tagged mutant Rac1 has a mutation of serine 71 to alanine (termed S71A). The plasmid was sequenced to confirm the presence of the desired mutation.

To purify the plasmid DNA, the pEGFP-C3 plasmid containing GFP-Rac1 WT and GFP-Rac1 S71A were transformed into *Escherichia coli* (*E. coli*) DH5 $\alpha$ . Bacteria were grown to an optical density (OD)<sub>600</sub> of 0.3 to 0.4 in autoclaved Luria Bertani (LB) medium [1% (w/v) tryptone, 0.5% (w/v) yeast extract and 1% (w/v) NaCl] and kanamycin (50 mg/ml stock concentration) was added to a final concentration of 30 mg/ml. Then, the tubes were incubated on a shaker at 250 rpm for 12-16 h at 37°C. After the overnight incubation, plasmids for transient transfection were purified using the EZ-10 Spin Column Plasmid DNA miniprep kit (BioBasic)

or the Qiagen mini/midi-prep kits (Qiagen) according to the manufacturers' instructions. Before transfection, the plasmid DNA concentration was measured using NanoVue Plus Spectrophotometer (GE Healthcare) in Dr. Sarah Hughes' lab.

#### 2.2.4 Preparation of total cell lysates

To obtain total cell lysates, the cells were collected, lysed and homogenized in ice-cold Mammalian Protein Extraction Reagent (M-PER) [0.5 mM sodium orthovanadate ( $\text{Na}_3\text{VO}_4$ ), 0.02% sodium azide ( $\text{NaN}_3$ ), 0.1 mM 4-(2-aminoethyl)-benzenesulfonyl fluoride (AEBSF), 10  $\mu\text{g}/\text{ml}$  aprotinin, 1  $\mu\text{M}$  pepstatin A] (Pierce, Rockford, Illinois) containing a phosphatase and protease inhibitor cocktail [0.5 mM  $\text{Na}_3\text{VO}_4$ , 0.1 mM AEBSF, 10  $\mu\text{g}/\text{ml}$  aprotinin, 1  $\mu\text{M}$  pepstatin A]. The lysates were then centrifuged at 21,000 x g at 4°C for 15 min. The supernatant was collected, the protein concentration was quantified, and the sample was boiled in sodium dodecyl sulfate (SDS)-loading buffer (250 mM Tris (hydroxymethyl) aminomethane hydrochloride (Tris-HCl), 40% glycerol, 8% SDS, 20%  $\beta$ -mercaptoethanol, 2% bromophenol blue) for 5 min.

For co-immunoprecipitation experiments, proteins were extracted with M-PER and the protein inhibitor cocktail and then vortexed. The media was removed and then PBS was added to the side of the plates. M-PER and the protease inhibitor cocktail was subsequently added to the plates for 3 min on ice. Cells were then scraped into Eppendorf tubes with a cell scraper and pipette and centrifuged for 3000 rpm for 5 min at 4°C. The supernatant was removed completely and the proteins in the pellet were kept on ice. Proteins were then washed once with PBS and centrifuged for 5 min at 3000 rpm at 4°C. M-PER was added and a 26 Gauge (G) needle was used to sonicate the mixture after adding 70% ethanol and PBS to neutralize the solution. The 26

G needle was used to sonicate the cell membrane to disturb the pellet on a 3 continues setting for 10 seconds on ice to disrupt every membrane in the cell. Then M-PER was added to the tube for 30 min and then submerged in ice horizontally. Proteins were then centrifuged for 14,000 rpm for 15 min at 4°C and the supernatant was later transferred to new microcentrifuge tubes for co-immunoprecipitation. Proteins were quantitated using the Bradford protein dye assay, according to the method of Bradford (1976). Absorbance at  $\lambda = 595$  nm was measured by a Beckman DU 640 spectrophotometer (Beckman Instruments, Fullerton, CA). Bovine serum albumin (BSA) was used as a standard.

#### 2.2.5 SDS-PAGE and immunoblotting

Aliquots of protein from each sample were used for sodium dodecyl sulfate-polyacrylamide gel electrophoresis (SDS-PAGE). For the staining of total cell lysates, aliquots containing 20  $\mu$ g of protein from each cell lysate were used. For the detection of co-immunoprecipitation products, one-tenth of the immunoprecipitated from each lysate was used. To detect each subcellular fraction, aliquots containing one-tenth of the total protein from each fraction were used. Protein samples were separated by electrophoresis through 12% SDS-PAGE gels for approximately 100 min at 100 V equilibrated in running buffer. Prestained protein markers (FroggaBio) were used for molecular weight standards. Proteins were electrophoretically transferred onto nitrocellulose membranes (BioRad, Hercules, CA). The transfer was done using a semi-dry blotting apparatus (Model SD transfer cell, BioRad) for 90 min at 15 V equilibrated in transfer buffer (48 mM Tris-HCl, 39 mM glycine, 20% methanol, 10% SDS, ddH<sub>2</sub>O). The membranes were blocked with Odyssey blocking buffer (TBS) for 1 h at room temperature (Li-Cor Biosciences, Lincoln, NE) to reduce non-specific background

staining. The membranes were then incubated overnight at 4°C on a shaker with rotation with the respective primary antibodies in blocking buffer (Table 2.2). Membranes were then washed 3 times with 0.05% Tris-buffered saline-Tween 20 (TBS-T) (1 M Tris-HCl, pH 7.5, 150 mM NaCl, ddH<sub>2</sub>O, 0.05% Tween 20) for 5 min at room temperature. Membranes were then incubated on a shaker with rotation for 1 h at room temperature after adding the secondary antibodies conjugated with infrared fluorescent dyes (IRDyes) in Odyssey blocking buffer (Li-Cor) (Table 2.2). Membranes were then washed again 3 times with TBS-T for 5 min at room temperature. Secondary antibodies were detected using the Odyssey Infrared Scanner CLx Imaging System in Dr. Sarah Hughes' lab (Li-Cor Biosciences, Lincoln, NE). All antibodies are listed in Table 2.2 with their respective dilutions. I employed a dose response method to find the optimal concentrations for my primary and secondary antibodies.

**Table 2.2 Antibodies and their dilutions used for Western blotting.**

<b>Antibody</b>	<b>Dilution</b>	<b>Manufacturer</b>
IRDye 680RD donkey anti-mouse IgG	1:500	Li-Cor
IRDye 800CW donkey anti-rabbit IgG	1:500	Li-Cor
Mouse anti-14-3-3 $\beta$ antibody (A-6) (sc-25276)	1:500	Santa Cruz
Mouse anti-14-3-3 $\epsilon$ antibody (F-3) (sc-393177)	1:500	Santa Cruz
Mouse anti-14-3-3 $\eta$ antibody (6A12) (sc-293464)	1:500	Santa Cruz
Mouse anti-14-3-3 $\gamma$ antibody (D-6) (sc-398423)	1:500	Santa Cruz
Mouse anti-14-3-3 $\sigma$ antibody (E-11) (sc-166473)	1:500	Santa Cruz
Mouse anti-14-3-3 $\tau/\theta$ antibody (1A1) (NBP1-21301)	1:500	Novus Biologicals
Mouse anti-14-3-3 $\zeta$ antibody (1B3) (sc-293415)	1:500	Santa Cruz

Mouse anti- $\alpha$ -tubulin antibody	1:500	Abcam
Mouse anti-pan 14-3-3 antibody (H-8) (Sc-1657)	1:500	Santa Cruz
Mouse anti-Rac1 antibody	1:500	Cytoskeleton
Rabbit anti-lamin A/C antibody	1:500	Santa Cruz
Rabbit anti-GFP antibody	1:500	Clontech

---

### 2.2.7 Subcellular Fractionation

COS-7 cells in 100 mm plates were scraped into homogenization buffer [0.25 M sucrose, 20 mM Tris-HCl, pH 7.0, 1 mM MgCl<sub>2</sub>, 4 mM NaF, 0.5 mM Na<sub>3</sub>VO<sub>4</sub>, 0.1 mM AEBSF, 10  $\mu$ g/ml aprotinin, and 1  $\mu$ M pepstatin A]. The cells were then lysed using a 26 G syringe 15 times and were left on ice for 30 min. Afterwards, the cell homogenates were centrifuged at 3000 rpm for 6 min. The resulting supernatant contained the cytoplasmic fraction and the pellet contained the nuclei. The supernatant was transferred into another tube and the pellet was washed with 500  $\mu$ l homogenization buffer 3 times. The pellet was then dispersed using a micropipette and a 26 G syringe 10 times. Following the centrifugation of the pellet at 3000 rpm for 15 min, the supernatant was discarded. The pellet was re-suspended in TBS in 0.1% SDS and sonicated briefly on a 2 continues setting for 3 seconds to shear genomic material and homogenize the lysate.

### 2.2.8 Co-immunoprecipitation

80  $\mu$ g of mouse IgG agarose beads (Sigma) were first pre-cleared with ice-cold PBS and then centrifuged 2 times at 7500 rpm for 1 min each and then washed with M-PER for the last time. After washing the beads, the mouse IgG agarose beads were mixed with the cell lysates and

were incubated on a shaker for 1 h at 4°C. The mouse IgG agarose beads-lysate mixture were then centrifuged for 1 min at 7500 rpm at 4°C. The respective primary antibody to be IPed was mixed with the M-PER. Next, the mouse IgG agarose beads-lysate mixture were then added to the antibody-M-PER mixture and incubated for 1 h with shaking at 4°C. To activate the protein G agarose beads (Sigma), the beads were scraped into a tube containing ice-cold PBS and then centrifuged at 7500 rpm for 30-45 seconds. This step was repeated again before adding the M-PER. Then, the protein G beads were added to the mouse IgG agarose beads-lysate-antibody-M-PER mixture for 1 h with shaking at 4°C. For the controls, mouse or rabbit non-specific IgG were used instead of specific primary antibodies. Then, the mixture was washed and centrifuged 3 times with M-PER for 1 min at 7500 rpm at 4°C. Then, the samples were mixed with SDS-loading buffer and boiled for 5 min to elute the complex from the beads before loading 15-20 µg onto 12% SDS-PAGE gels or stored at -80°C for future use. Antibodies and their concentrations for co-immunoprecipitation are listed in Table 2.3.

**Table 2.3 Antibodies and their concentrations used for co-immunoprecipitation.**

<b>Antibody</b>	<b>Concentration (ng/ml)</b>	<b>Manufacturer</b>
Mouse anti-Rac1 antibody	50	Cytoskeleton, Inc
Rabbit anti-GFP antibody	100	Clontech

### 2.2.9 Fluorescence microscopy

Indirect immunofluorescence was carried out as described previously (Wang et al. 1999). Cells were grown on glass coverslips to 70-80% confluency and serum starved for 48 h before EGF treatment. For the cell cycle treatments, I did not synchronize the cells in mitosis since I can

differentiate interphase from the different mitotic stages. After treatment, the slides were rinsed in PBS and the cells were fixed by -20°C methanol for 5 min and then washed again with PBS. The cells were then permeabilized with 0.2% PBS-Triton X-100 for 15 min at room temperature. The slides were then incubated in 1 µg/ml solution of the indicated primary antibody in 0.1% Triton X-100 on a shaker for 1 h at room temperature or overnight at 4°C. 1 µg/ml solution of the indicated primary antibody in 0.1% Triton X-100 was incubated with blocking peptides of the indicated concentration for 1 h prior to incubating the cells. Afterwards, the slides were rinsed in PBS three times each and then incubated in 1 µg/ml solution of fluorescein isothiocyanate (FITC)-conjugated donkey anti-mouse IgG and/or tetramethylrhodamine isothiocyanate (TRITC)-conjugated donkey anti-rabbit IgG secondary antibodies in 0.1% Triton X-100 on a shaker for 1 h at room temperature (JacksonImmunoResearch Laboratories, Inc., West Grove, PA). Thereafter, the slides were washed completely in PBS three times each and then incubated in 1 µg/ml of 4',6-diamidino-2-phenylindole (DAPI) solution (in PBS) for 10 min at room temperature in the dark. The slides were rinsed in PBS to remove the DAPI. 1 µl of mounting medium was added under each coverslip and then a drop of immersion oil was added before inverting the slides to be observed using the GE Healthcare DeltaVision Deconvolution Microscopy system (GE Healthcare Life Science, Mississauga, ON, Canada). All the images were deconvolved. Antibodies and their concentrations are listed in Table 2.4. I employed a dose response method to find the optimal concentrations for my primary and secondary antibodies.

**Table 2.4 Antibodies and their dilutions used for immunofluorescence.**

<b>Antibody</b>	<b>Dilution</b>	<b>Manufacturer</b>
FITC-conjugated donkey anti-mouse IgG antibody	1:100	Jackson ImmunoRes

Goat anti- $\alpha$ -actin antibody	1:50	Sigma
Mouse anti-14-3-3 $\beta$ antibody (A-6) (sc-25276)	1:50	Santa Cruz
Mouse anti-14-3-3 $\epsilon$ antibody (F-3) (sc-393177)	1:50	Santa Cruz
Mouse anti-14-3-3 $\eta$ antibody (6A12) (sc-293464)	1:50	Santa Cruz
Mouse anti-14-3-3 $\eta$ antibody (10847-MM06)	1:50	Sino Biological
Mouse anti-14-3-3 $\gamma$ antibody (D-6) (sc-398423)	1:50	Santa Cruz
Mouse anti-14-3-3 $\sigma$ antibody (E-11) (sc-166473)	1:50	Santa Cruz
Mouse anti-14-3-3 $\tau/\theta$ antibody (1A1) (NBP1-21301)	1:50	Novus Biologicals
Mouse anti-14-3-3 $\theta$ antibody (5J20) (sc-69720)	1:50	Santa Cruz
Mouse anti-14-3-3 $\zeta$ antibody (1B3) (sc-293415)	1:50	Santa Cruz
Mouse anti-14-3-3 $\zeta$ antibody (G-2) (sc-518031)	1:50	Santa Cruz
Mouse anti- $\alpha$ -tubulin antibody	1:50	Abcam
Mouse anti-pan 14-3-3 antibody (H-8) (sc-1657)	1:50	Santa Cruz
Mouse anti-Rac1 antibody	1:50	Cytoskeleton, Inc
Rabbit anti-calnexin antibody	1:50	Santa Cruz
Rabbit anti-GFP antibody	1:50	Clontech
Rabbit anti-HSP60 antibody	1:50	Novus Biologicals
TRITC-conjugated donkey anti-rabbit IgG antibody	1:100	Jackson ImmunoRes

---

### **Chapter 3: Results I - Subcellular Localization of 14-3-3 Proteins**

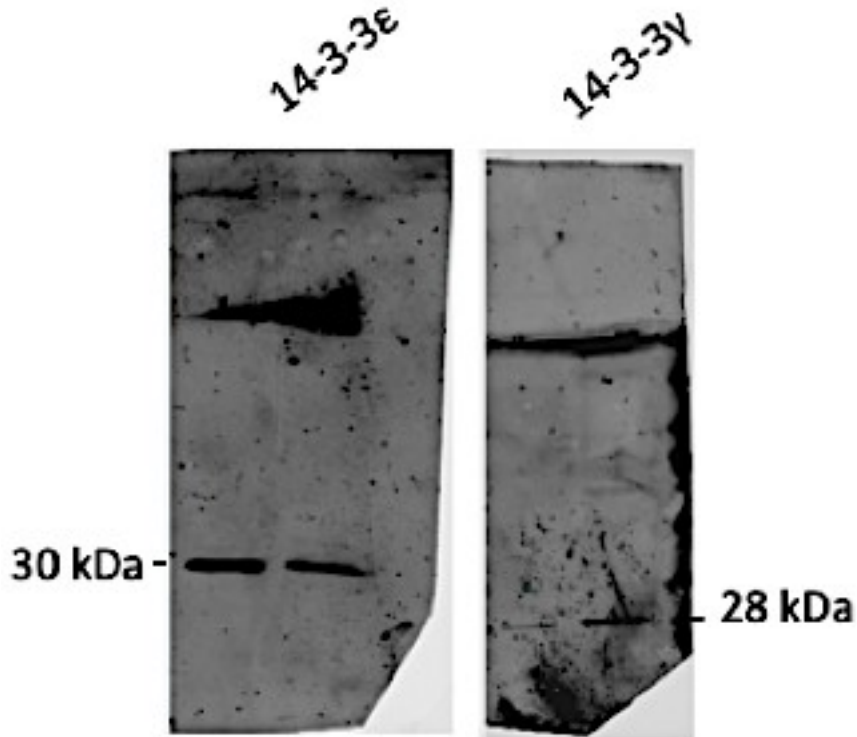
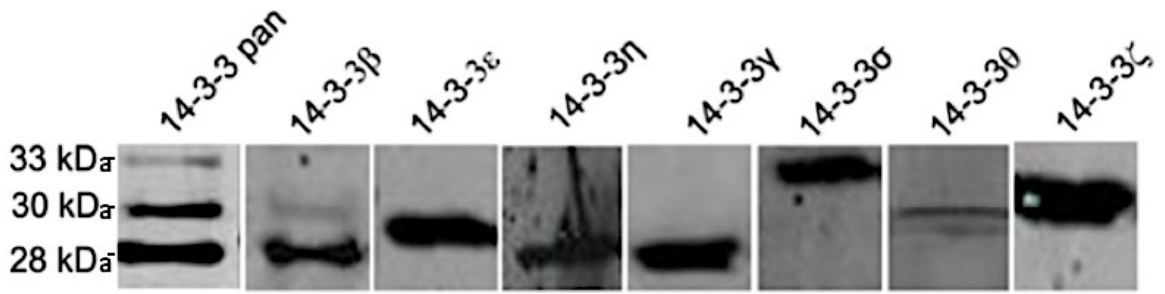
The information presented in this chapter has been submitted and is currently under revision in Scientific Reports with me as a co-first author: Abdrabou, A., Brandwein, D., Wang, Z. (2019). Different subcellular distribution and translocation of seven 14-3-3 isoforms in response to EGF and during cell cycle.

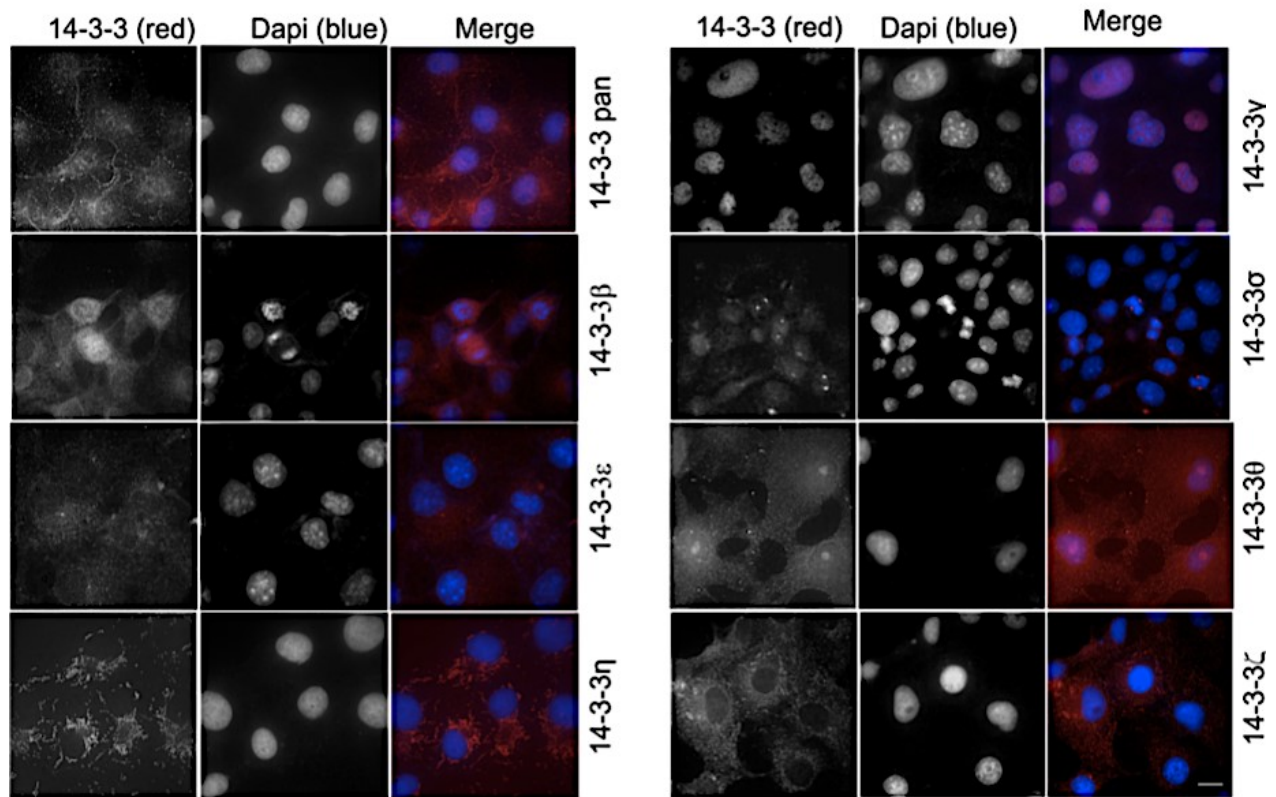
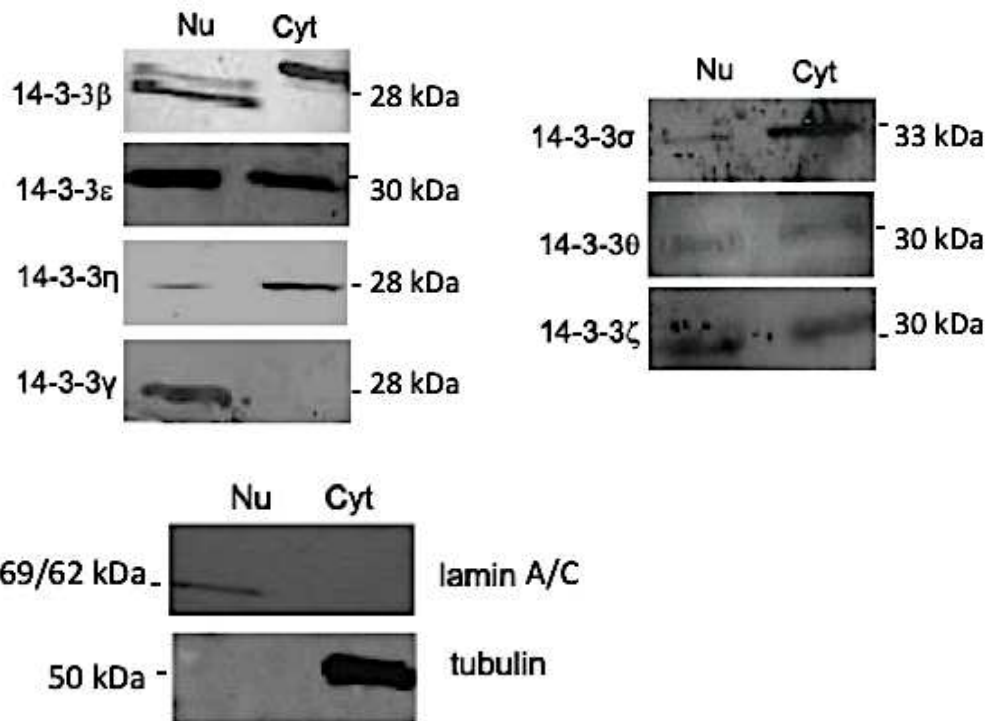
#### **3.1 Total 14-3-3 protein and 14-3-3 isoforms have different expressions and subcellular localizations in COS-7 cells**

I want to point out that every result I show in this thesis is representative and have been repeated at least three times. I first determined the expression of the total 14-3-3 protein (with a pan 14-3-3 mouse monoclonal antibody) and each of the seven 14-3-3 isoforms (with 14-3-3  $\beta$ ,  $\epsilon$ ,  $\eta$ ,  $\gamma$ ,  $\sigma$ ,  $\tau/\theta$ , and  $\zeta$  mouse monoclonal antibodies) by immunoblotting in COS-7 cells. As shown in Figure 3.1A, the partial immunoblots show that pan 14-3-3 antibody detected three bands with molecular weights at 28, 30, and 33 kDa. 14-3-3 $\beta$ ,  $\eta$ , and  $\gamma$  correspond to the lower band of pan 14-3-3 at 28 kDa. 14-3-3 $\epsilon$ ,  $\tau/\theta$ , and  $\zeta$  correspond to the middle band of pan 14-3-3 at 30 kDa. Finally, 14-3-3 $\sigma$  corresponds to the higher band of pan 14-3-3 at 33 kDa. In the whole immunoblots, 14-3-3 $\epsilon$  and  $\gamma$  both showed one specific band at 30 kDa and 28 kDa, respectively. There were no non-specific bands at the other molecular weights.

I next examined the subcellular localization of the total 14-3-3 protein and each 14-3-3 isoform by indirect immunofluorescence. In Figure 3.1B, the red colour represents pan 14-3-3 and the 14-3-3 isoforms and the blue colour represents DAPI. As shown in Figure 3.1B, pan 14-3-3 localized both to the nucleus and to the cytoplasm. The most noticeable cytoplasmic stain of pan 14-3-3 was a fiber-like pattern both near the PM and across the cell, which resembled the actin fibers. 14-3-3 $\beta$  localized mostly to the cytoplasm and showed weak microtubule-like

**A**



**B****C**

**Figure 3.1 The expression levels and subcellular localizations of pan 14-3-3 and 14-3-3 isoforms in COS-7 cells.** Total 14-3-3 protein was determined by a pan 14-3-3 antibody. Each 14-3-3 isoform was determined by antibodies to each specific isoform. Immunoblotting, immunofluorescence and subcellular fractionation were performed as described in Methods. (A) The expression level of total and seven isoforms of 14-3-3 proteins by immunoblotting in COS-7 cells (whole and partial immunoblots). The expression of tubulin was used as control. (B) Subcellular localization of pan 14-3-3 and seven 14-3-3 isoforms in COS-7 cells by immunofluorescence. 14-3-3 proteins were revealed by TRITC (red) and the chromatin was stained by DAPI (blue). Size bar = 10  $\mu$ m. (C) Nuclear and cytoplasmic localization of 14-3-3 proteins by subcellular fractionation followed by immunoblotting. A-tubulin was used as a marker for the cytoplasm and lamin A/C was used as a marker for the nucleus.

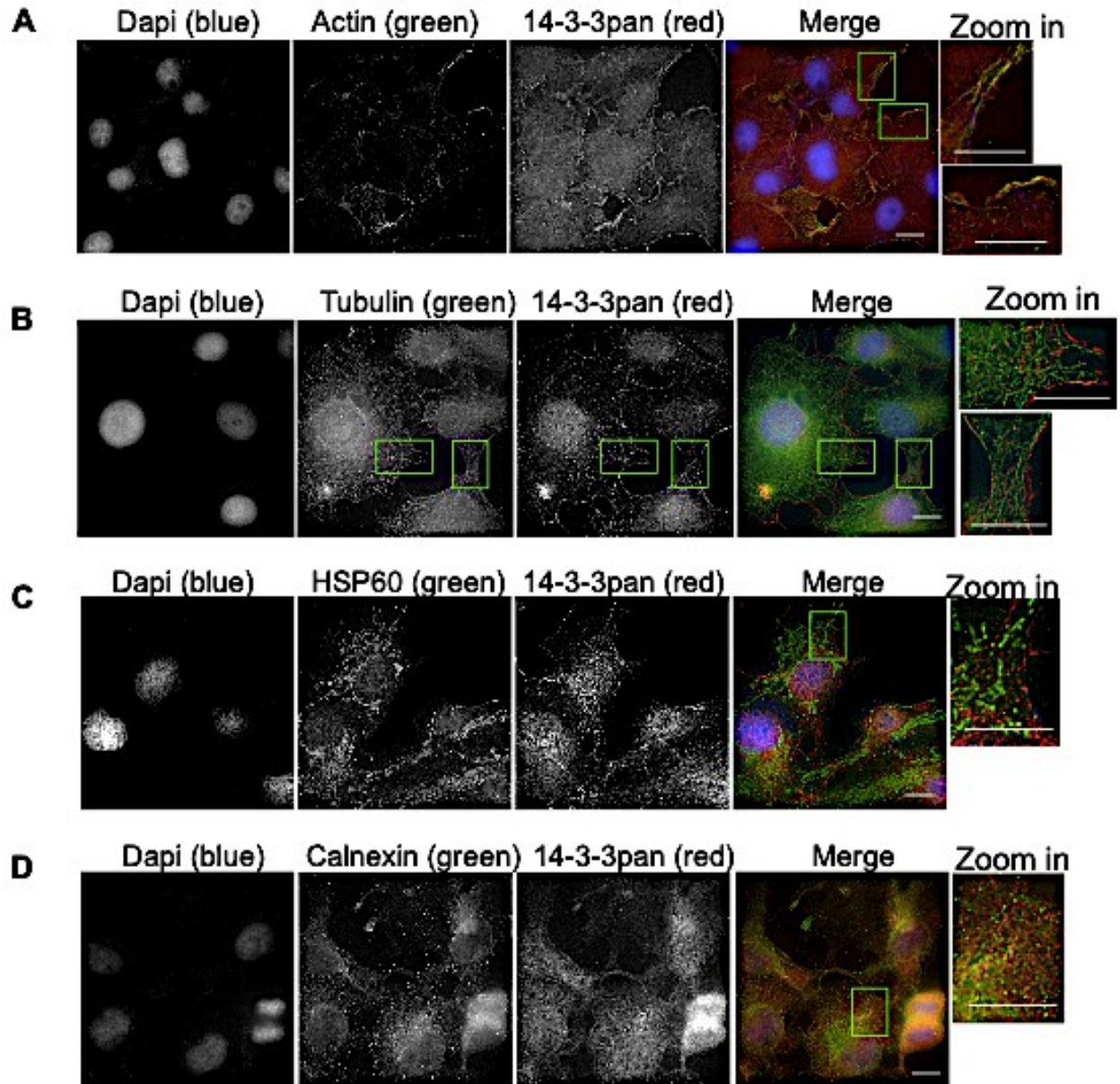
patterns. 14-3-3 $\beta$  showed less nuclear localization. 14-3-3 $\epsilon$  almost exclusively localized to the cytoplasm where it showed strong particles, mostly in the perinuclear region towards one side of the nucleus, likely in the ER-Golgi area. This would need to be confirmed with Golgi-specific markers. 14-3-3 $\eta$ ,  $\gamma$ ,  $\sigma$ , and  $\zeta$  all showed very specific subcellular localizations. 14-3-3 $\eta$  almost exclusively localized to the mitochondria, particularly in the mitochondrial matrix. 14-3-3 $\gamma$  completely localized to the nucleus. Furthermore, 14-3-3 $\gamma$  formed fine particles throughout the nucleus but was absent from nucleoli (data not shown). In interphase cells, 14-3-3 $\sigma$  localized both to the nucleus and to the cytoplasm. However, most strikingly, 14-3-3 $\sigma$  showed strong and specific centrosome localization during mitosis, particularly in metaphase at the tubulin spindle. Lastly, 14-3-3 $\zeta$  exclusively localized to the cytoplasm, without any clear nuclear staining. In the cytoplasm, 14-3-3 $\zeta$  showed both ER and microtubule localizations.

I further confirmed my indirect immunofluorescence results with other techniques such as subcellular fractionation and immunoblotting. I first isolated nuclear and cytoplasmic fractions from total cell homogenates. Nuclear and cytoplasmic fractions can be verified using characteristic protein fingerprints, which identify marker proteins specific for the nuclei and the cytoplasm, and their specific cellular activities. For instance, the nuclear fraction can be verified by testing the nuclear fraction for the presence of a nuclear marker protein, such as the nuclear structural protein lamin. By using lamin A/C as the marker for the nucleus and  $\alpha$ -tubulin as the marker for the cytoplasm, I showed that the fractionations were specific (Figure 3.1C). As shown in Figure 3.1C, 14-3-3 $\beta$ ,  $\epsilon$ ,  $\sigma$ ,  $\tau/\theta$ , and  $\zeta$  were detected in both the nuclear and the cytoplasmic fractions, while 14-3-3 $\gamma$  was only detectable in the nuclear fraction, and 14-3-3 $\eta$  was primarily detected in the cytoplasmic fraction.

### 3.2 Pan 14-3-3 localizes to the actin fibers in COS-7 cells

I next examined the subcellular localization and the translocation of pan 14-3-3 and each 14-3-3 isoform in response to EGF, and during the cell cycle, by indirect immunofluorescence. The mouse pan 14-3-3 antibody (H-8) (sc-1657) is specific for an epitope mapping between amino acids 1-30 at the N-terminus of 14-3-3 $\beta$  of human origin. I first studied the total 14-3-3 protein in COS-7 cells by using a pan 14-3-3 antibody to test its immunoreactivity. Pan 14-3-3 is not a specific isoform but rather shows the subcellular localization of the total amount of 14-3-3 protein in the cell. Based on the subcellular distribution pattern of pan 14-3-3, I examined if pan 14-3-3 colocalized with various subcellular markers. A-actin and  $\alpha$ -tubulin are markers for the cytoskeleton, HSP60 is a marker for the mitochondria, calnexin is a marker for the endoplasmic reticulum (ER), and phosphorylated EGFR (pEGFR) is a marker for the PM and the endosomes. As revealed by double indirect immunofluorescence, pan 14-3-3 strongly colocalized with actin fibers, especially in the regions close to the cell membrane (Figure 3.2A). Pan 14-3-3 also showed some colocalization with microtubules, but in the peripheral region, pan 14-3-3 frequently parallels with tubulin (Figure 3.2B). Limited colocalization between pan 14-3-3 and HSP60 (Figure 3.2C) and limited colocalization between pan 14-3-3 and calnexin (Figure 3.2D) were also observed. The localization of pan 14-3-3 in both the nucleus and the cytosol was also prominent.

I then examined if EGF stimulates the re-distribution of pan 14-3-3 and if the subcellular localization of pan 14-3-3 changes during mitosis. EGF stimulates the activation of many signaling pathways, which leads to the serine/threonine phosphorylation of many proteins within different subcellular compartments (Wee and Wang, 2018). These phosphorylated proteins could be potential 14-3-3 binding partners. Thus, EGF may regulate the subcellular localization of 14-



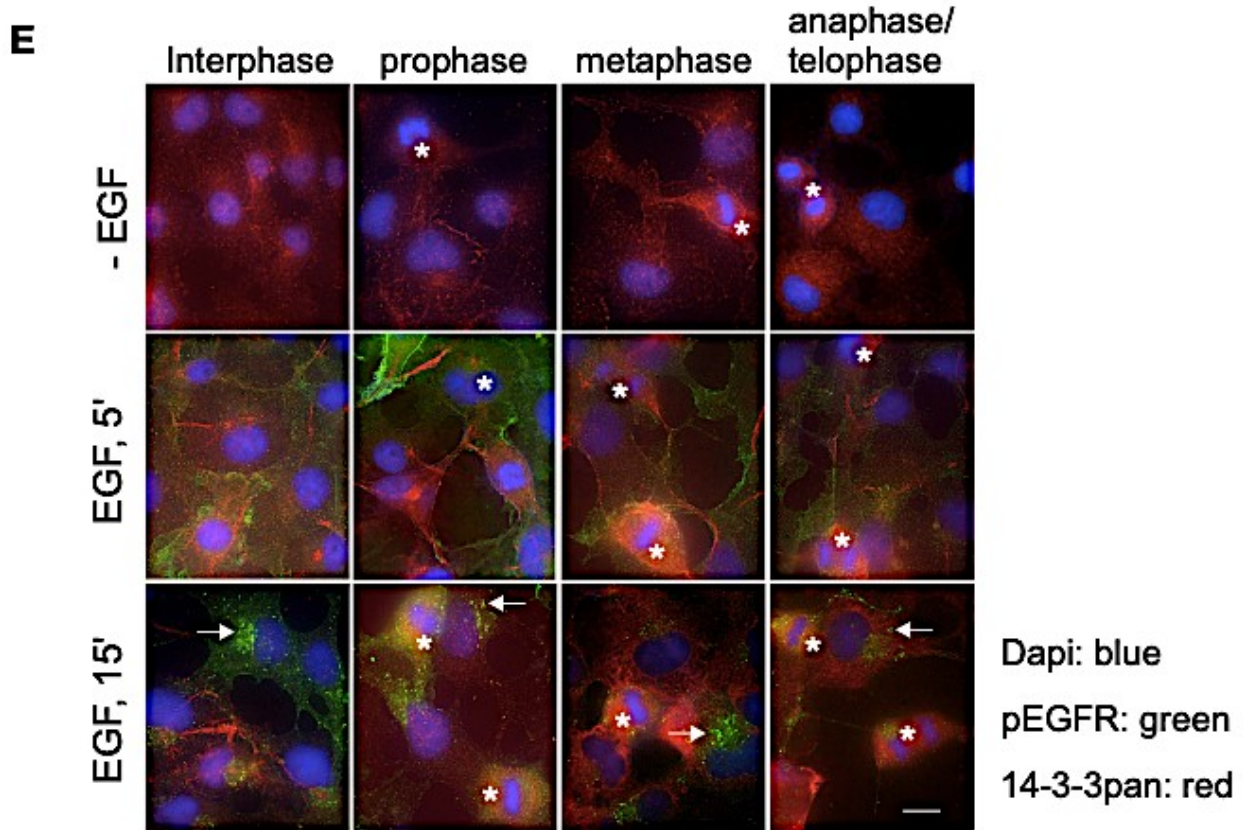
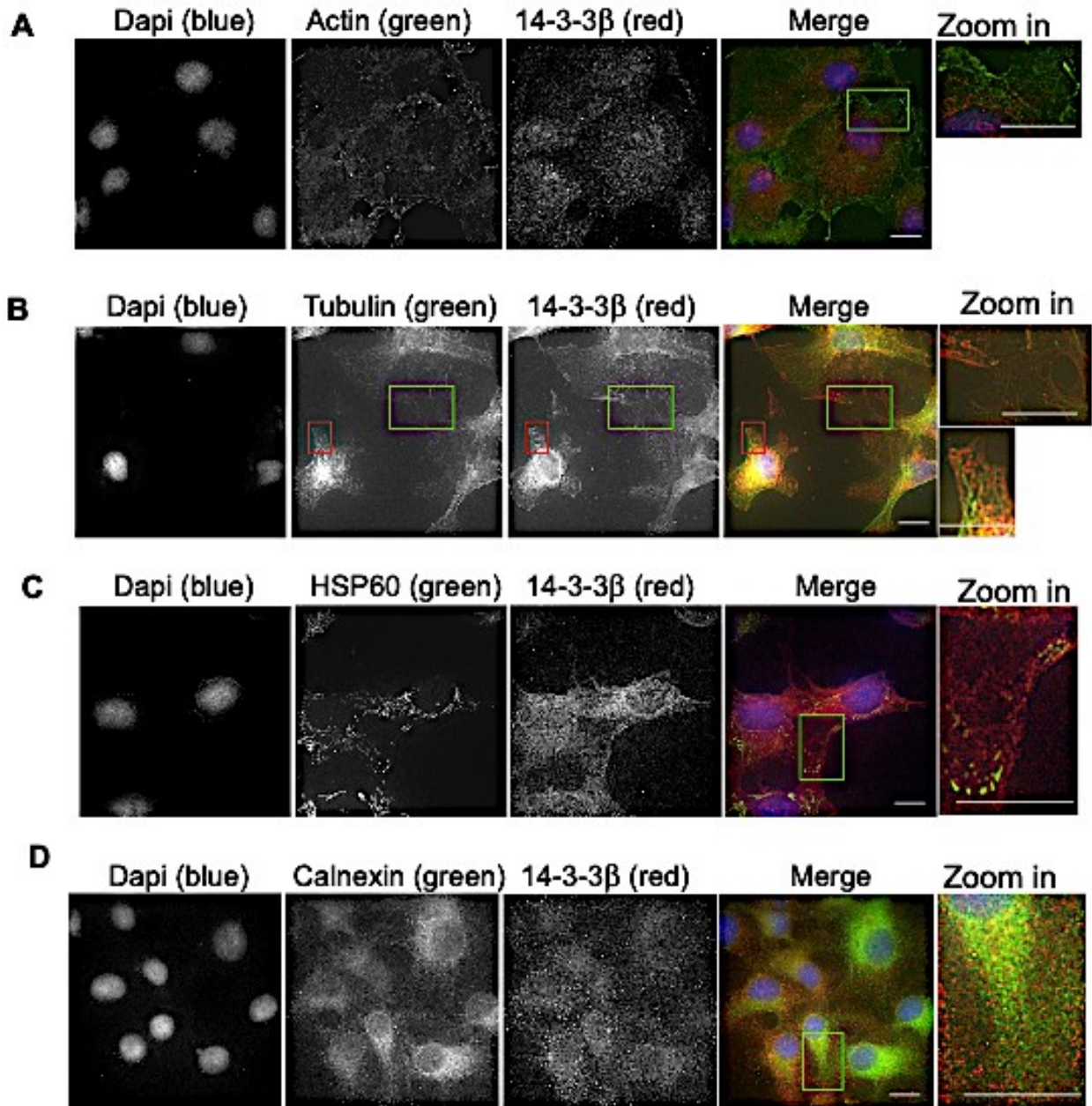


**Figure 3.2 Pan 14-3-3 localizes to the actin fibers in COS-7 cells.** (A) Colocalization of pan 14-3-3 (red) and actin (green). (B) Colocalization of pan 14-3-3 protein (red) and tubulin (green). (C) Colocalization of pan 14-3-3 protein (red) and HSP60 (green). (D) Colocalization of pan 14-3-3 protein (red) and calnexin (green). (E) Subcellular localization of pan 14-3-3 protein during the cell cycle and in response to EGF. With or without EGF stimulation, pan 14-3-3 proteins (red) and pEGFR (green) were revealed by double indirect immunofluorescence. Mitotic cells were labelled by \* and endosomes were marked by arrows. Size bar = 10  $\mu$ m.

3-3 proteins. As shown in Figure 3.2E, EGF showed some increase in the localization of pan 14-3-3 to the actin fibers similar to the ones shown in Figure 3.2A. For the cell cycle, I compared the localization between interphase and mitosis, and within the different stages of mitosis. I did not distinguish between the G1, S, and G2 phases. Thus, there is no need to synchronize the cells as I can readily identify the mitotic cells and interphase cells. Similarly, the actin fiber-like stain of pan 14-3-3 was also stronger in mitotic cells than in interphase cells. As pEGFR localized mostly in the PM following EGF stimulation for 5 min and localized in the endosome following longer EGF stimulation, pEGFR is a good maker for the endocytic pathway. As shown in Figure 3.2E, pan 14-3-3 had limited colocalization with pEGFR at the PM, and not much colocalization in the endosomes.

### **3.3 14-3-3 $\beta$ localizes to the microtubules in COS-7 cells**

I then examined the subcellular localization and the translocation of 14-3-3 $\beta$  in response to EGF and during the cell cycle in COS-7 cells. The mouse 14-3-3 $\beta$  antibody (A-6) (sc-25276) is specific for an epitope mapping between amino acids 225-244 at the C-terminus of 14-3-3 $\beta$  of human origin. Colocalization by double indirect immunofluorescence showed that 14-3-3 $\beta$  had some colocalization with the actin fibers (Figure 3.3A), but the antibody showed stronger intensity/colocalization with the  $\alpha$ -tubulin/microtubules (Figure 3.3B). I also observed some colocalization of 14-3-3 $\beta$  with HSP60 in the distal region of the cell (Figure 3.3C) and some colocalization with calnexin (Figure 3.3D). I also did not observe any noticeable changes in terms of the subcellular localization of 14-3-3 $\beta$  in response to EGF stimulation (Figure 3.3E). Mitotic cells showed stronger 14-3-3 $\beta$  staining than interphase cells, but this could be due to the round-up of the cells during mitosis or high expression of 14-3-3 $\beta$  during mitosis. I also did not observe any strong colocalization between 14-3-3 $\beta$  and pEGFR.



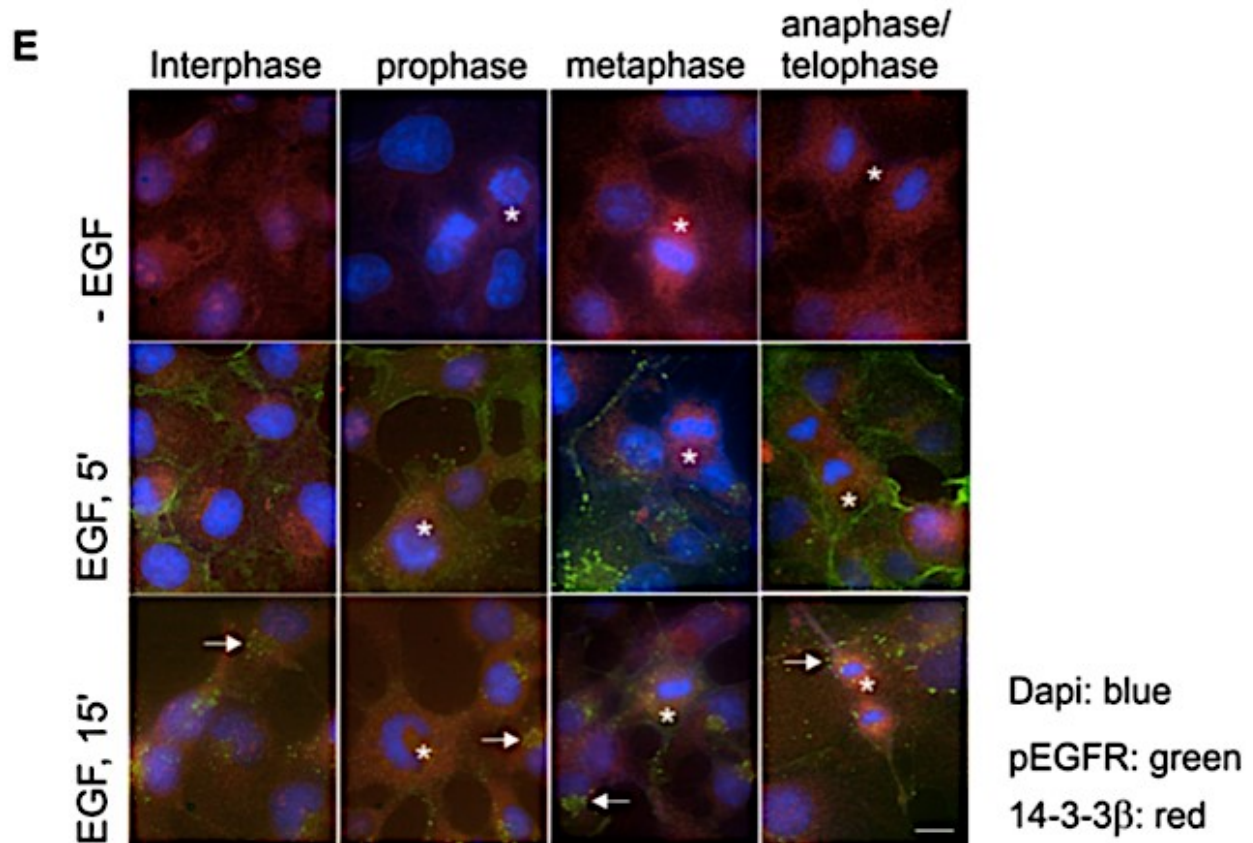


**Figure 3.3 14-3-3β localizes to the microtubules in COS-7 cells.** (A) Colocalization of 14-3-3β (red) and actin (green). (B) Colocalization of 14-3-3β (red) and tubulin (green). (C) Colocalization of 14-3-3β (red) and HSP60 (green). (D) Colocalization of 14-3-3β (red) and calnexin (green). (E) Subcellular localization of 14-3-3β during the cell cycle and in response to EGF. With or without EGF stimulation, 14-3-3β (red) and pEGFR (green) were revealed by double indirect immunofluorescence. Mitotic cells were labelled by \* and endosomes were marked by arrows. Size bar = 10 μm.

### **3.4 14-3-3 $\epsilon$ localizes to the microtubules in COS-7 cells**

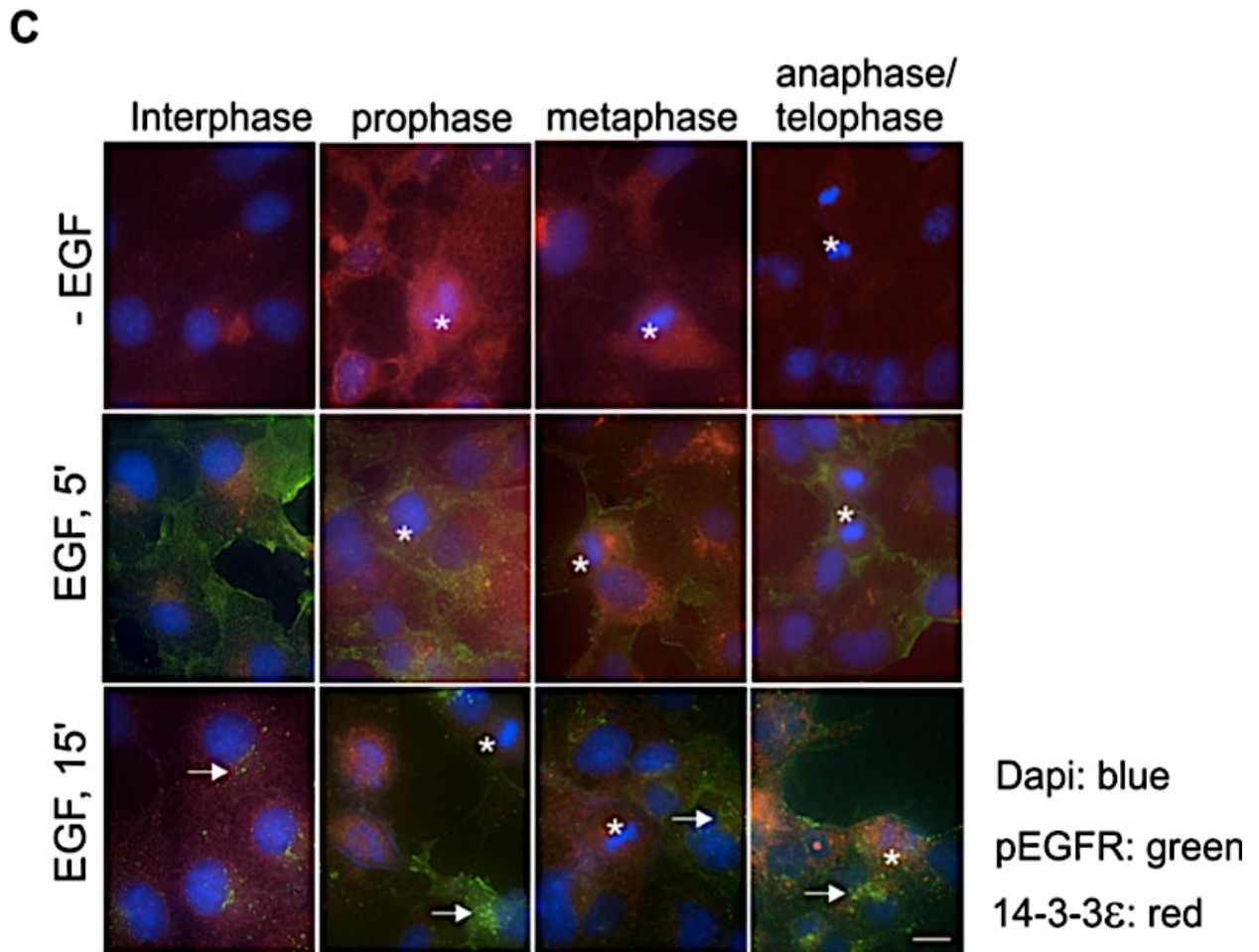
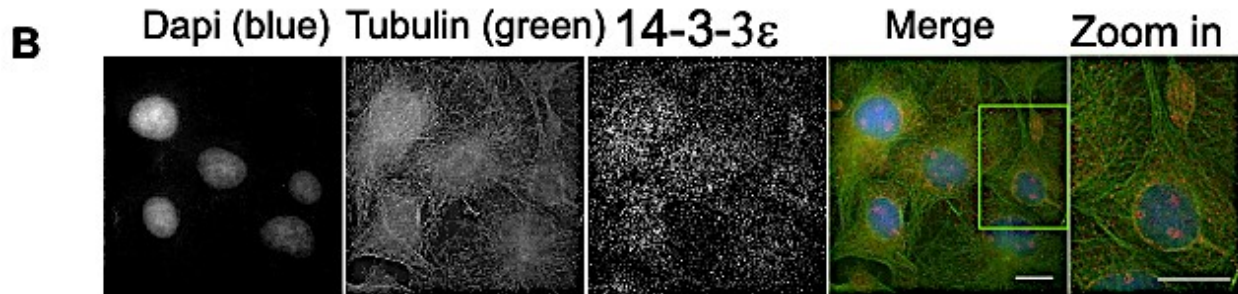
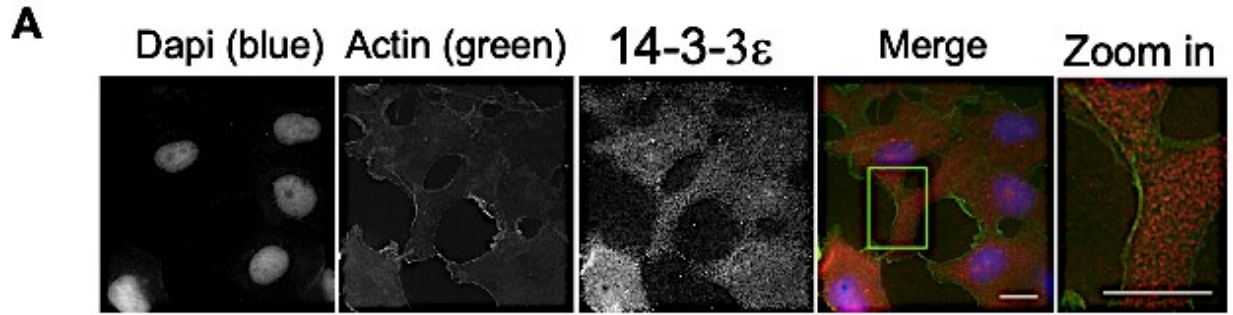
I next examined the subcellular localization and the translocation of 14-3-3 $\epsilon$  in response to EGF and during the cell cycle in COS-7 cells. The mouse 14-3-3 $\epsilon$  antibody (F-3) (sc-393177) is specific for an epitope mapping between amino acids 136-175 within an internal region of 14-3-3 $\epsilon$  of human origin. Colocalization by double indirect immunofluorescence showed that 14-3-3 $\epsilon$  had weak colocalization with actin fibers (Figure 3.4A), but noticeable colocalization with microtubules (Figure 3.4B). 14-3-3 $\epsilon$  showed diffuse distribution within the cytoplasm. EGF stimulation did not cause noticeable changes in the subcellular localization of 14-3-3 $\epsilon$  (Figure 3.4C). There were also very little changes in 14-3-3 $\epsilon$  subcellular distribution during mitosis. I also did not observe any colocalization between 14-3-3 $\epsilon$  and pEGFR.

### **3.5 14-3-3 $\eta$ localizes to the mitochondria in COS-7 cells**

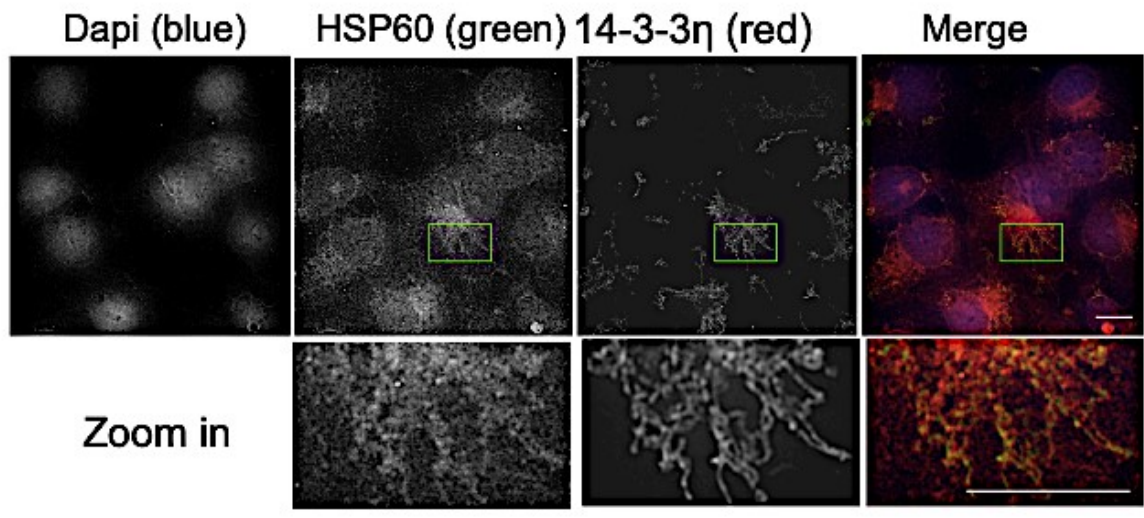
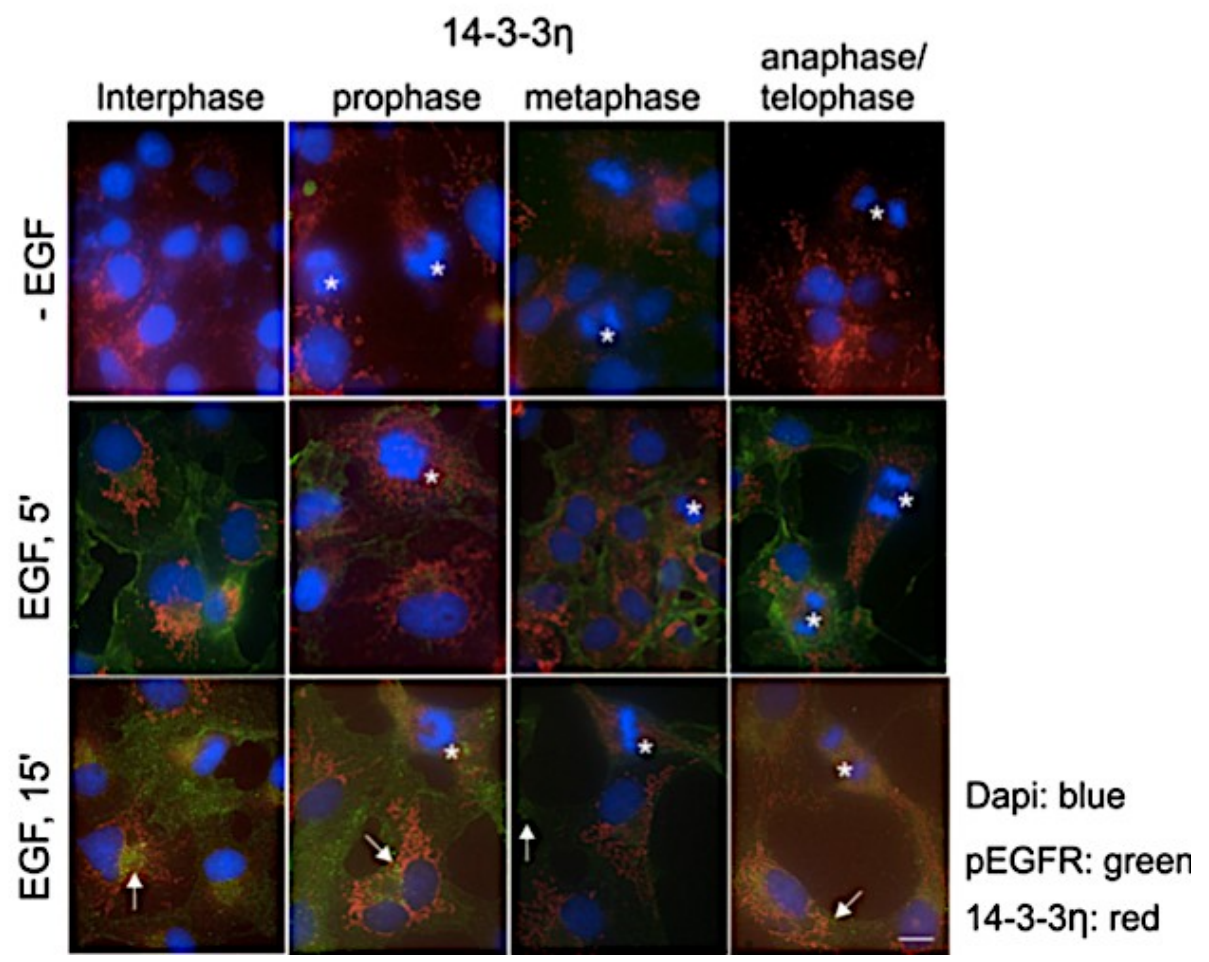
By using double indirect immunofluorescence, I first examined the colocalization of 14-3-3 $\eta$  with HSP60 as 14-3-3 $\eta$  showed clear and almost exclusive mitochondrial localization in Figure 3.1B. The mouse 14-3-3 $\eta$  antibody (6A12) (sc-293464) is raised against amino acids 71-170 representing the partial length of 14-3-3 $\eta$  of human origin. Indeed, as shown in Figure 3.5A, 14-3-3 $\eta$  strongly colocalized with HSP60. Moreover, EGF stimulation did not change the mitochondrial localization of 14-3-3 $\eta$  (Figure 3.5B). However, in most cases, the stain of 14-3-3 $\eta$  was weaker during mitosis.

### **3.6 14-3-3 $\gamma$ localizes to the nucleus and forms smaller particles in response to EGF in COS-7 cells**

I showed above that 14-3-3 $\gamma$  was exclusively localized to the nucleus (Figure 3.1B).

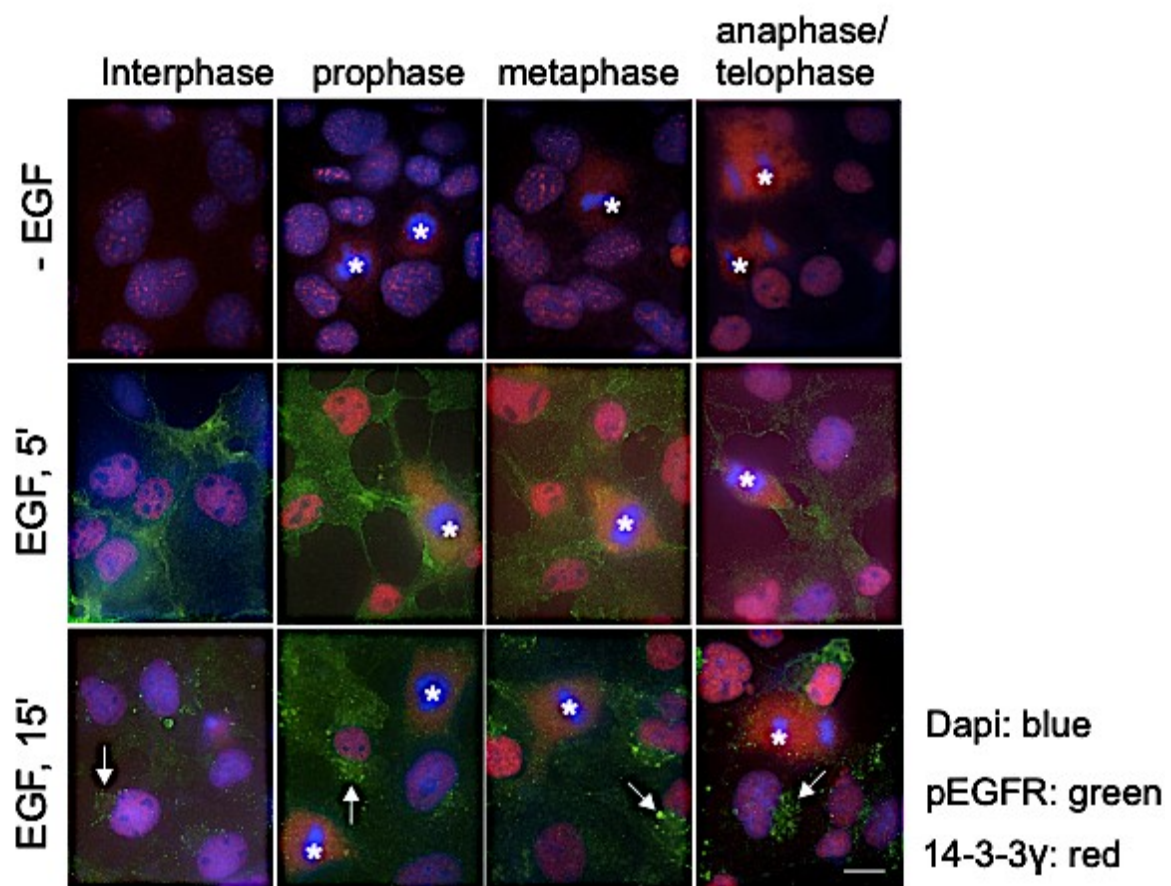


**Figure 3.4 14-3-3 $\epsilon$  localizes to the microtubules in COS-7 cells.** (A) Colocalization of 14-3-3 $\epsilon$  (red) and actin (green). (B) Colocalization of 14-3-3 $\epsilon$  (red) and tubulin (green). (C) Subcellular localization of 14-3-3 $\epsilon$  during the cell cycle and in response to EGF. With or without EGF stimulation, 14-3-3 $\epsilon$  (red) and pEGFR (green) were revealed by double indirect immunofluorescence. Mitotic cells were labelled by \* and endosomes were marked by arrows. Size bar = 10  $\mu$ m.

**A****B**

**Figure 3.5 14-3-3 $\eta$  localizes to the mitochondria in COS-7 cells.** (A) Colocalization of 14-3-3 $\eta$  (red) and HSP60 (green). (B) Subcellular localization of 14-3-3 $\eta$  during the cell cycle and in response to EGF. With or without EGF stimulation, 14-3-3 $\eta$  (red) and pEGFR (green) were revealed by double indirect immunofluorescence. Mitotic cells were labelled by \* and endosomes were marked by arrows. Size bar = 10  $\mu$ m.

**A**



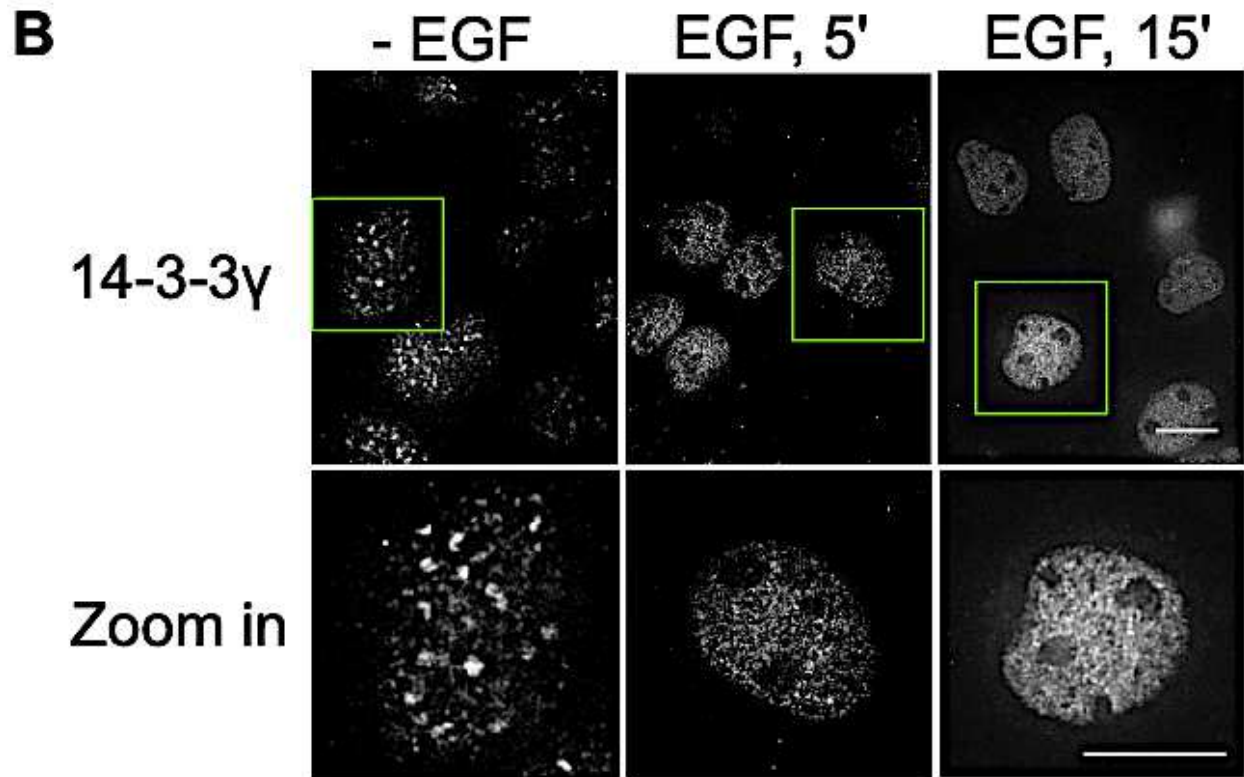


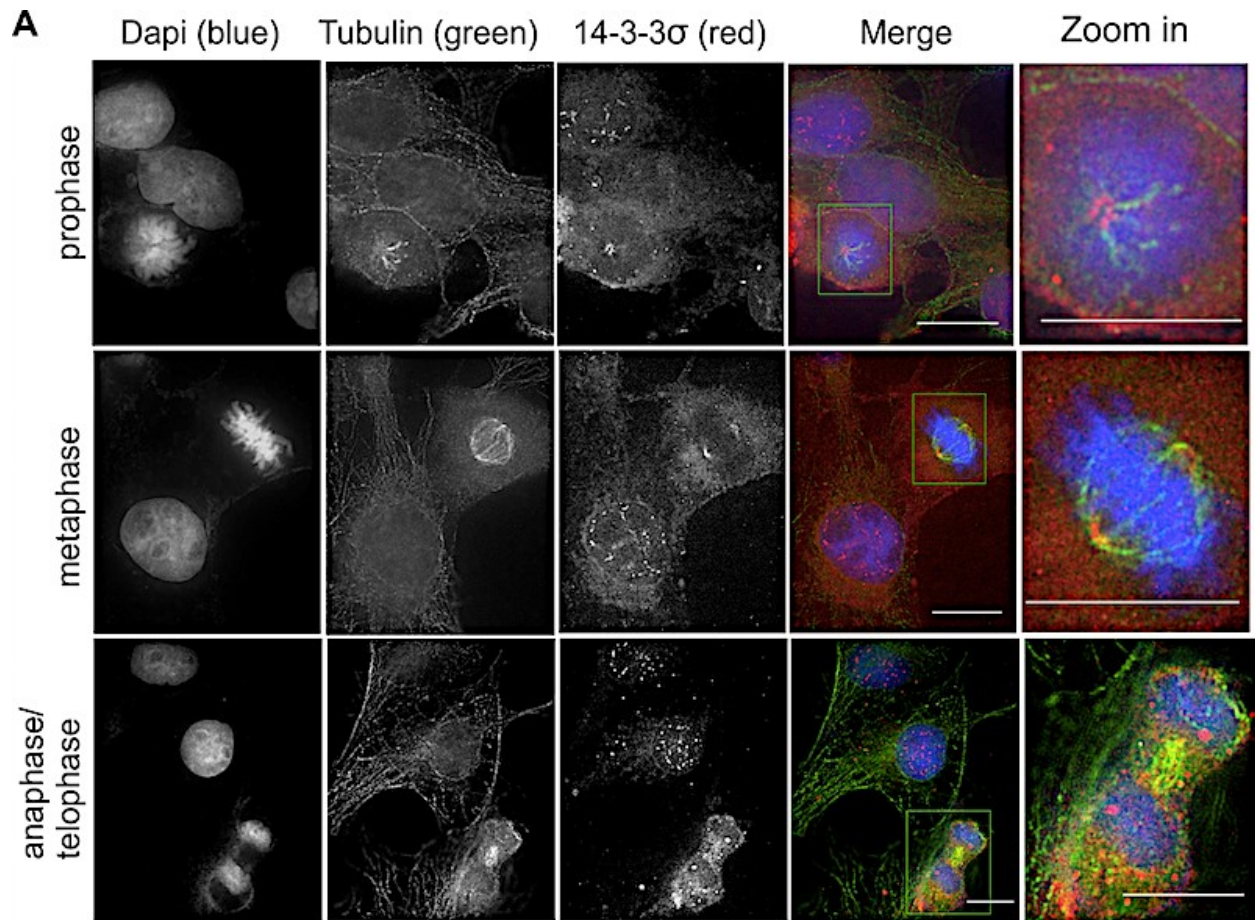
**Figure 3.6 14-3-3 $\gamma$  localizes to the nucleus and forms smaller particles in response to EGF in COS-7 cells.** (A) Subcellular localization of 14-3-3 $\gamma$  during the cell cycle and in response to EGF. With or without EGF stimulation, 14-3-3 $\gamma$  (red) and pEGFR (green) were revealed by double indirect immunofluorescence. Mitotic cells were labelled by \* and endosomes were marked by arrows. (B) The change of 14-3-3 $\gamma$  sub-nuclear localization in response to EGF during interphase. Size bar = 10  $\mu$ m.

### **3.7 14-3-3 $\sigma$ localizes to the centrosomes and to the microtubules during mitosis in COS-7 cells**

I next examined the subcellular localization and translocation of 14-3-3 $\sigma$  in response to EGF and during the cell cycle in COS-7 cells by double indirect immunofluorescence. The mouse 14-3-3 $\sigma$  antibody (E-11) (sc-166473) is specific for an epitope mapping between amino acids 25-38 at the N-terminus of 14-3-3 $\sigma$  of human origin. I showed above that 14-3-3 $\sigma$  localized both to the cytoplasm and to the nucleus in interphase, but strongly associated with the centrosome during mitosis (Figure 3.7A). Here, I first examined the colocalization of 14-3-3 $\sigma$  with microtubules during mitosis. As shown in Figure 3.7A, 14-3-3 $\sigma$  strongly colocalized with microtubules in the origin of the tubulin spindle. The subcellular localization of 14-3-3 $\sigma$  did not show any changes in response to EGF (Figure 3.7B).

### **3.8 14-3-3 $\tau/\theta$ localizes to the endoplasmic reticulum in COS-7 cells**

I also examined the colocalization of 14-3-3 $\tau/\theta$  with the various markers by double indirect immunofluorescence in COS-7 cells. The mouse 14-3-3 $\tau/\theta$  antibody is raised against amino acids 1-245 of human origin purified from *E. coli* (NP\_006817). There was only a weak colocalization between 14-3-3 $\tau/\theta$  and actin near the PM (Figure 3.8A). There was some colocalization between 14-3-3 $\tau/\theta$  and microtubules near the nuclear membrane (Figure 3.8B). However, there was a strong colocalization between 14-3-3 $\tau/\theta$  and calnexin (Figure 3.8C). I then examined the translocation of 14-3-3 $\tau/\theta$  in response to EGF and during the cell cycle. The addition of EGF did not change the subcellular localization of 14-3-3 $\tau/\theta$  (Figure 3.8D). During mitosis, in the absence of the nuclear membrane, 14-3-3 $\tau/\theta$  is distributed diffusely throughout the cell with no specific pattern changes.



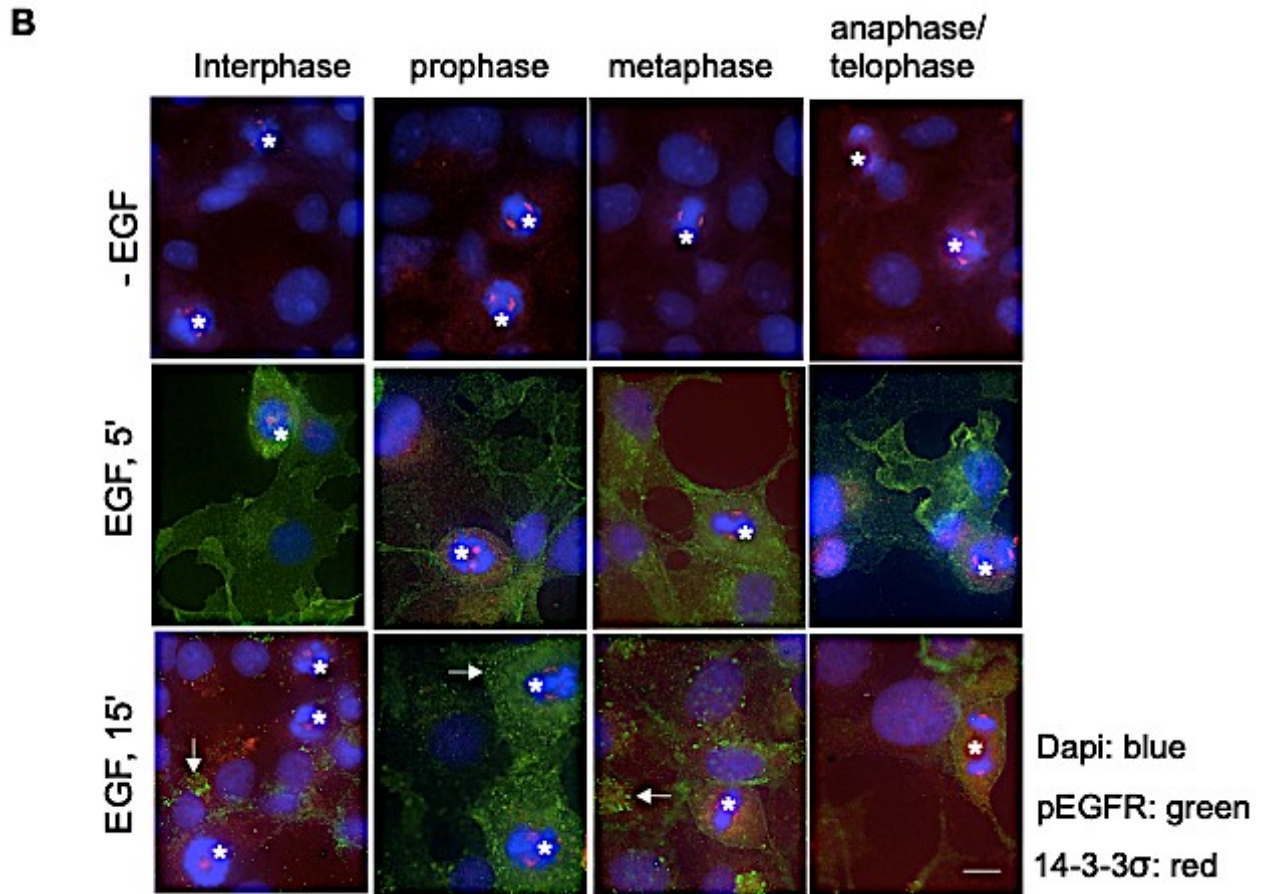
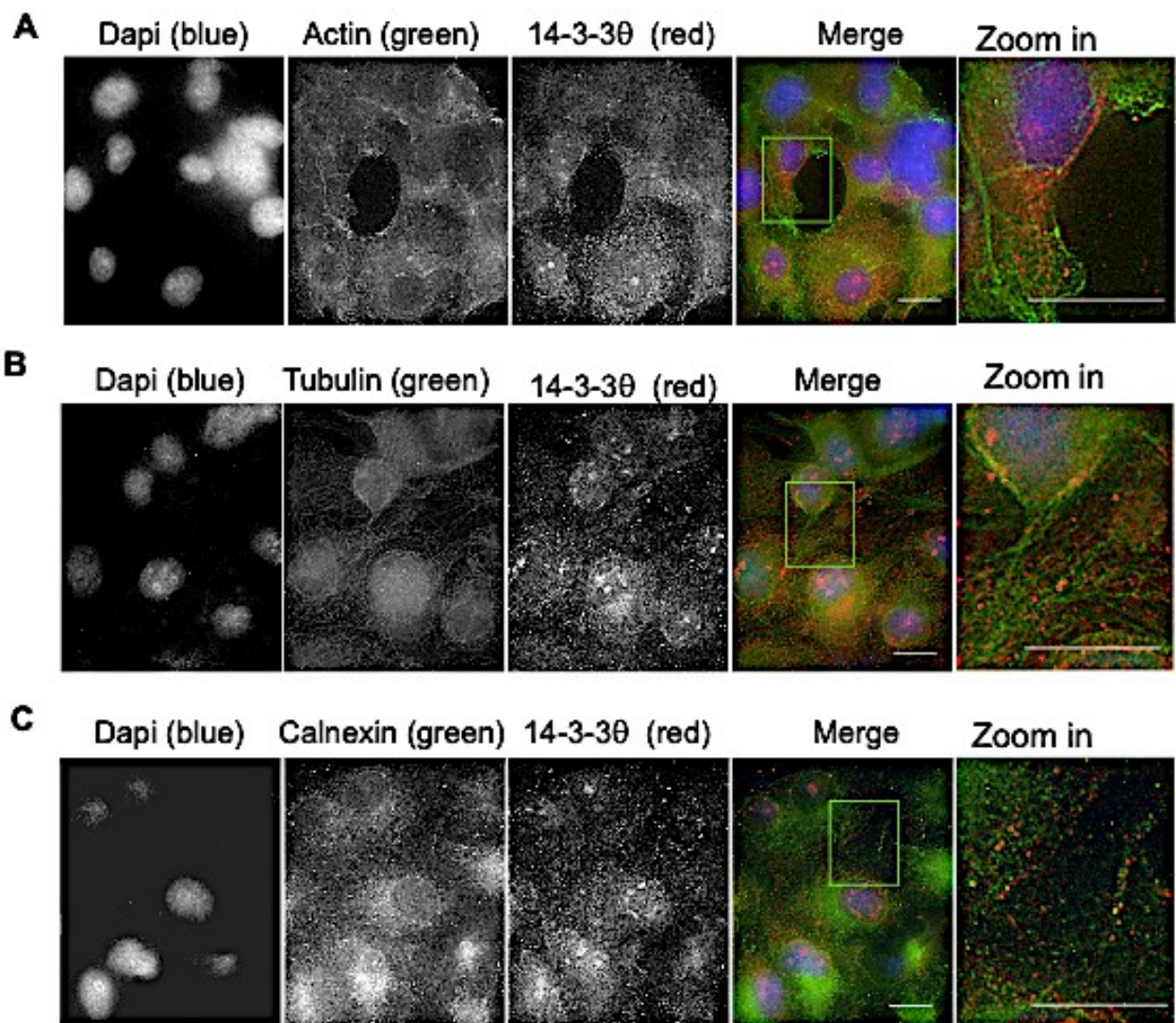


**Figure 3.7 14-3-3 $\sigma$  localizes to the centrosomes and to the microtubules during mitosis**

**in COS-7 cells.** (A) Colocalization of 14-3-3 $\sigma$  (red) and tubulin (green) during mitosis. (B)

Subcellular localization of 14-3-3 $\sigma$  during the cell cycle and in response to EGF. With or without EGF stimulation, 14-3-3 $\sigma$  (red) and pEGFR (green) were revealed by double indirect immunofluorescence. Mitotic cells were labelled by \* and endosomes were marked by arrows.

Size bar = 10  $\mu$ m.



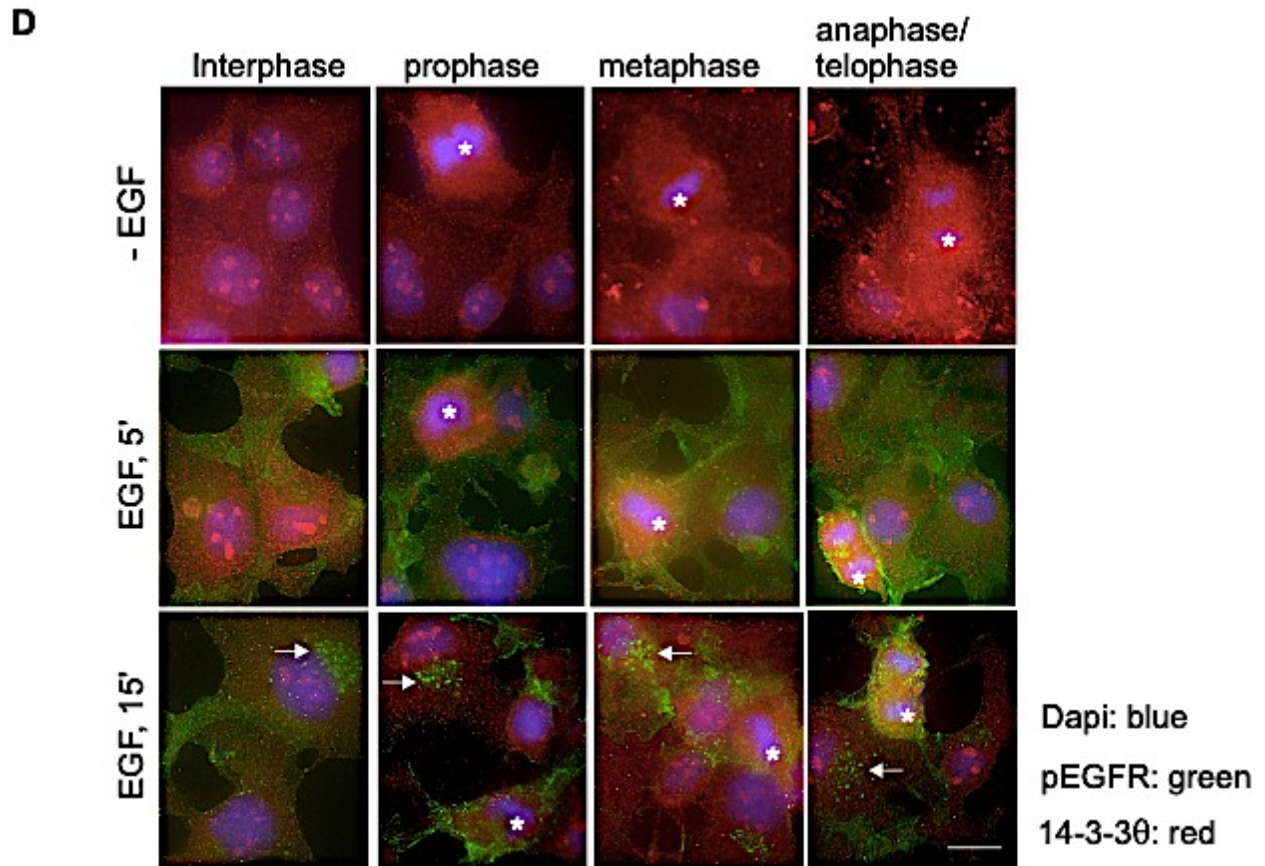


**Figure 3.8 14-3-3 $\tau/\theta$  localizes to the endoplasmic reticulum in COS-7 cells. (A)**

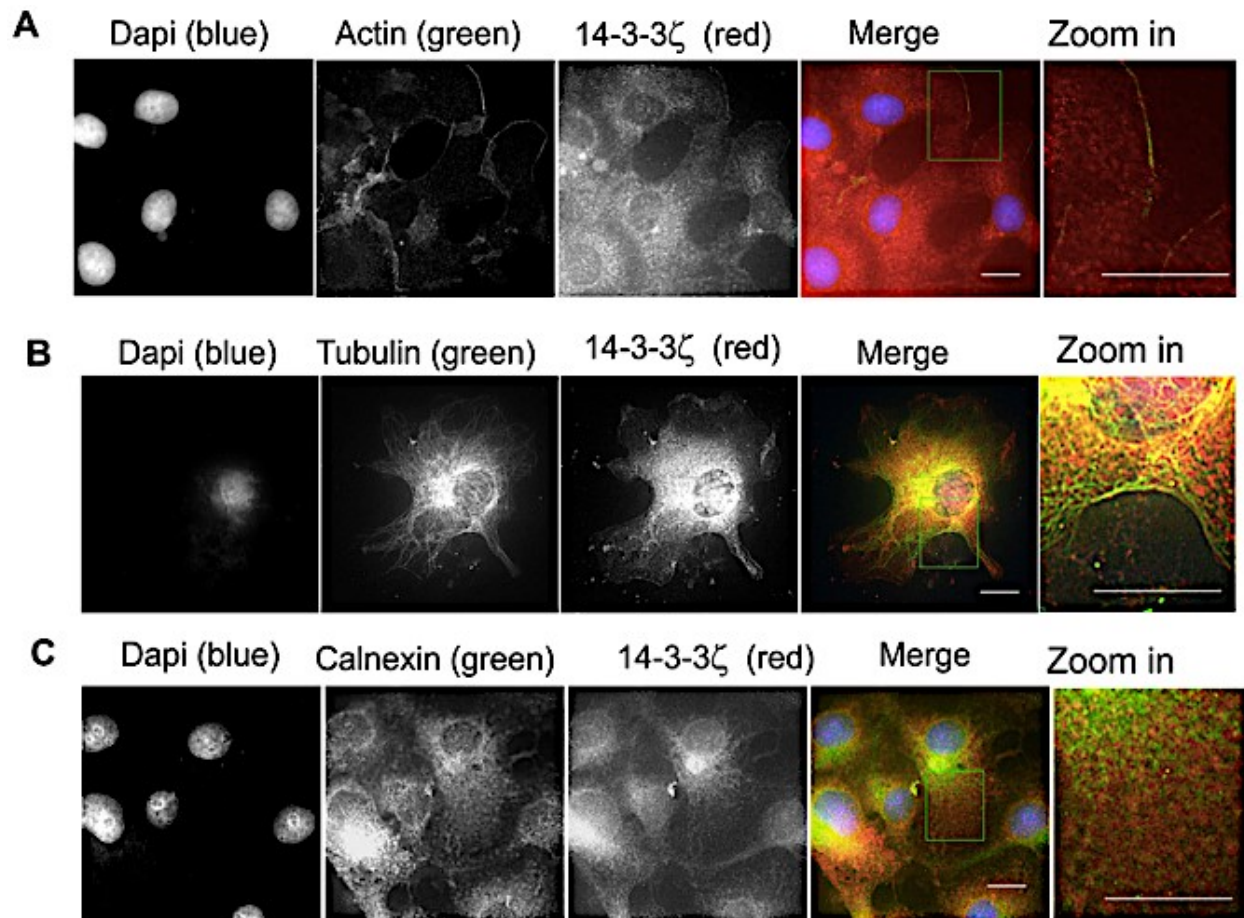
Colocalization of 14-3-3 $\tau/\theta$  (red) and actin (green). (B) Colocalization of 14-3-3 $\tau/\theta$  (red) and tubulin (green). (C) Colocalization of 14-3-3 $\tau/\theta$  (red) and calnexin (green). (D) Subcellular localization of 14-3-3 $\tau/\theta$  during the cell cycle and in response to EGF. With or without EGF stimulation, 14-3-3 $\tau/\theta$  (red) and pEGFR (green) were revealed by double indirect immunofluorescence. Mitotic cells were labelled by \* and endosomes were marked by arrows. Size bar = 10  $\mu\text{m}$ .

### **3.9 14-3-3 $\zeta$ localizes to the actin fibers, microtubules, endoplasmic reticulum, plasma membrane and endosomes in response to EGF in COS-7 cells**

Finally, I examined the colocalization of 14-3-3 $\zeta$  with actin, tubulin and calnexin. The mouse 14-3-3 $\zeta$  antibody (1B3) (sc-293415) is raised against amino acids 51-150, representing the partial length of 14-3-3 $\zeta$  of human origin. As shown in Figure 3.9A, 14-3-3 $\zeta$  showed strong colocalizations with the actin fibers near the PM. 14-3-3 $\zeta$  also showed colocalization with microtubules (Figure 3.9B). The colocalization between 14-3-3 $\zeta$  and the calnexin was also strong (Figure 3.9C). Stimulation with EGF did not induce the subcellular translocation of 14-3-3 $\zeta$ ; however, the fiber-like pattern of 14-3-3 $\zeta$  was stronger in response to EGF (Figure 3.9D). 14-3-3 $\zeta$ , in mitotic cells, generally had stronger PM localization. Interestingly, there was a strong colocalization between 14-3-3 $\zeta$  and pEGFR in the PM following EGF stimulation for 5 min (Figure 3.9E).

### **3.10 Summary of total 14-3-3 protein and 14-3-3 isoform subcellular localizations and colocalizations with different subcellular markers in COS-7 cells**

Pan 14-3-3 primarily localized to the actin fibers and a lesser extent to the microtubules, ER, mitochondria, PM and endosomes (Table 3.1). 14-3-3 $\beta$  primarily localized to the microtubules and with some actin fibers, ER and mitochondrial localizations. 14-3-3 $\epsilon$  primarily localized to the microtubules with some actin fiber localization. 14-3-3 $\eta$  primarily localized to the mitochondria. 14-3-3 $\gamma$  primarily localized to the nucleus. 14-3-3 $\sigma$  primarily localized to the nucleus, specifically to the centrosomes and to the microtubules, possibly at the mitotic spindle apparatus. 14-3-3 $\tau/\theta$  primarily localized to the ER with some localization to the actin fibers and the microtubules. 14-3-3 $\zeta$  primarily localized to the actin fibers, microtubules, ER, PM and



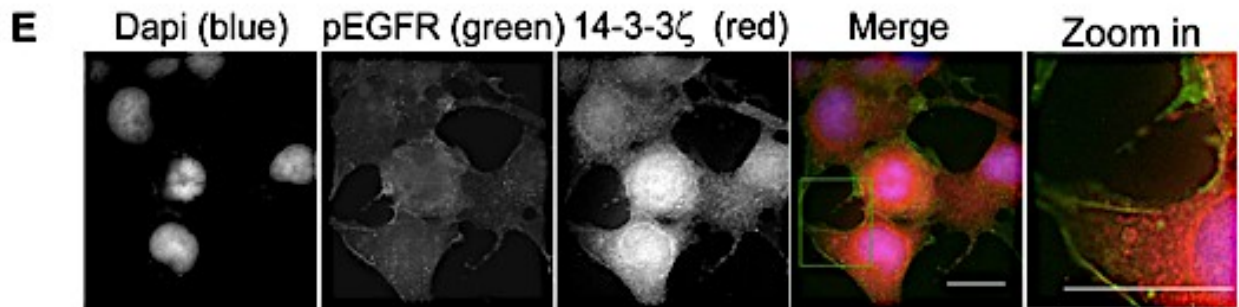
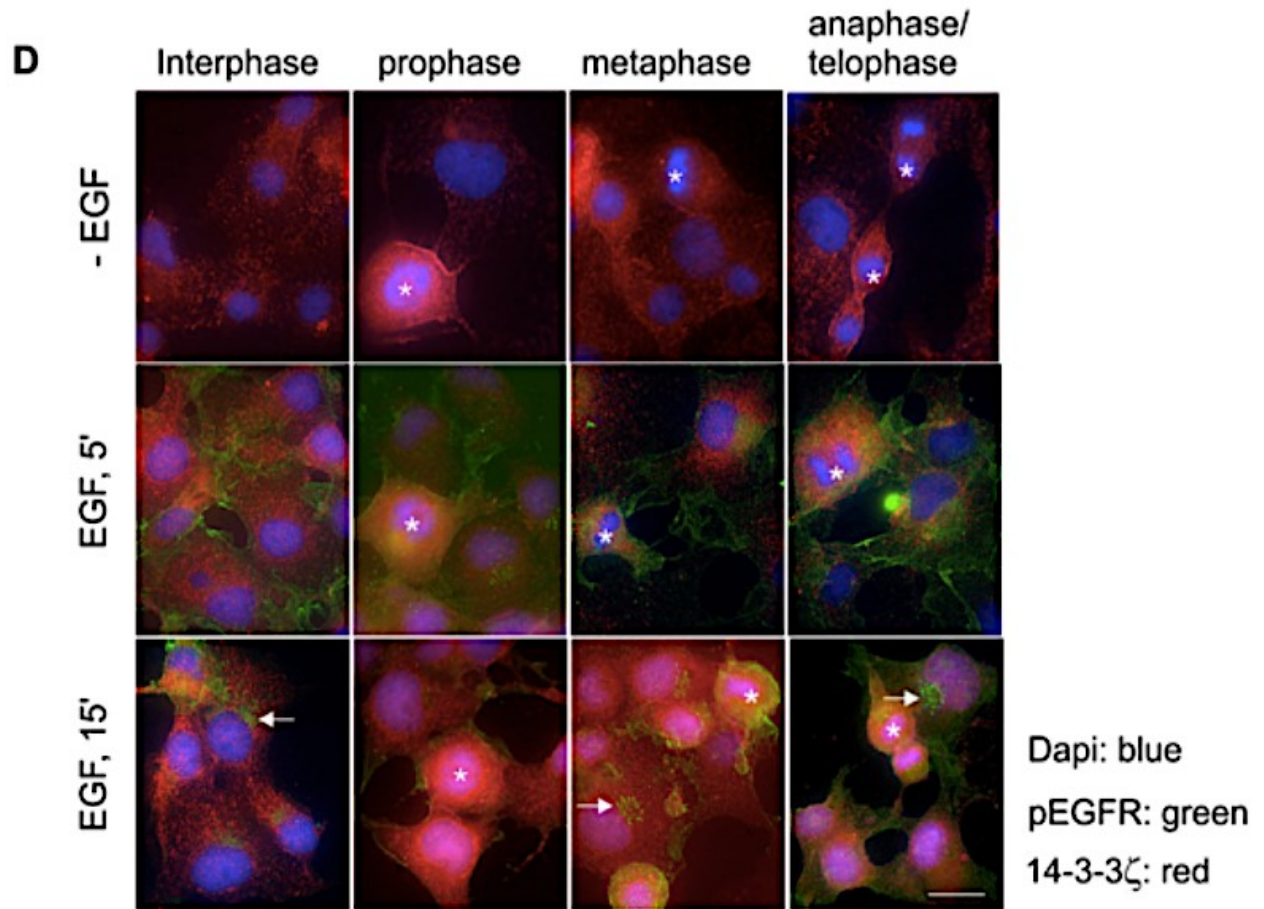


**Figure 3.9 14-3-3 $\zeta$  localizes to the actin fibers, microtubules, endoplasmic reticulum, plasma membrane and endosomes in response to EGF in COS-7 cells.** (A) Colocalization of 14-3-3 $\zeta$  (red) and actin (green). (B) Colocalization of 14-3-3 $\zeta$  (red) and tubulin (green). (C) Colocalization of 14-3-3 $\zeta$  (red) and calnexin (green). (D) Subcellular localization of 14-3-3 $\zeta$  during the cell cycle and in response to EGF. With or without EGF stimulation, 14-3-3 $\zeta$  (red) and pEGFR (green) were revealed by double indirect immunofluorescence. (E) Colocalization of 14-3-3 $\zeta$  (red) and pEGFR (green) following EGF stimulation for 5 min. Mitotic cells were labelled by \* and endosomes were marked by arrows. Size bar = 10  $\mu$ m.

**Table 3.1 Summary of total 14-3-3 protein and 14-3-3 isoform subcellular localizations**

	Nucleus	Mitochondria	Centrosome	Endoplasmic Reticulum	Actin	Microtubule	Plasma membrane /endosome
pan 14-3-3		✓		✓	✓	✓	✓
14-3-3 isoforms							
$\gamma$	✓						
$\eta$		✓					
$\sigma$	✓		✓			✓	
$\tau/\theta$				✓	✓	✓	
$\beta$		✓		✓	✓	✓	
$\varepsilon$					✓	✓	
$\zeta$				✓	✓	✓	✓

Bigger check marks denote the primary subcellular localization of the 14-3-3 isoform while the smaller check marks denote less subcellular localization. No check marks denote zero subcellular localization.

endosomes upon EGF stimulation for 5 min, compared to the other isoforms which did not colocalize with pEGFR at the PM.

### **3.11 Total 14-3-3 protein and 14-3-3 isoforms have similar subcellular localizations in HEK293T, MDA-MB-231 and MCF-7 cells**

All of the above experiments were performed in COS-7 cells derived from monkey kidney cells. To determine if my above observations are only limited to COS-7 cells, I examined the subcellular localization of total and each isoform of 14-3-3 proteins in HEK293T, MCF-7, and MDA-MB-231 cells derived from human embryonic kidney and human breast tumours, respectively. As shown in Figures 3.10, 3.11, and 3.12, for interphase cells, 14-3-3 proteins were localized throughout the cell with a pan 14-3-3 antibody. Similar to COS-7 cells, the most prominent cytoplasmic stain of pan 14-3-3 was an actin fiber-like pattern both near the plasma membrane and across the cell. One noticeable difference was the strong perinuclear stain, which could be related to the Golgi apparatus. For mitotic cells, pan 14-3-3 was evenly distributed throughout the cells. For interphase cells, 14-3-3 $\beta$  showed mostly cytoplasmic staining with certain fiber-like staining. The nuclear stain of 14-3-3 $\beta$  is much weaker than the cytoplasmic stain. In mitotic cells, 14-3-3 $\beta$  was evenly distributed throughout the cells except near the chromosomes. 14-3-3 $\epsilon$  is almost exclusively localized to the cytoplasm with very weak nuclear staining in interphase cells. In the cytoplasm, the 14-3-3 $\epsilon$  stains showed strong particulate patterns. During mitosis, 14-3-3 $\epsilon$  was evenly distributed throughout the cell except near the chromosomes. 14-3-3 $\eta$  showed strong fiber-like and mitochondrial patterns. 14-3-3 $\gamma$  was completely localized to the nucleus. In interphase cells, the 14-3-3 $\sigma$  stain was stronger in the nucleus than in the cytoplasm. However, most strikingly, 14-3-3 $\sigma$  showed strong and specific

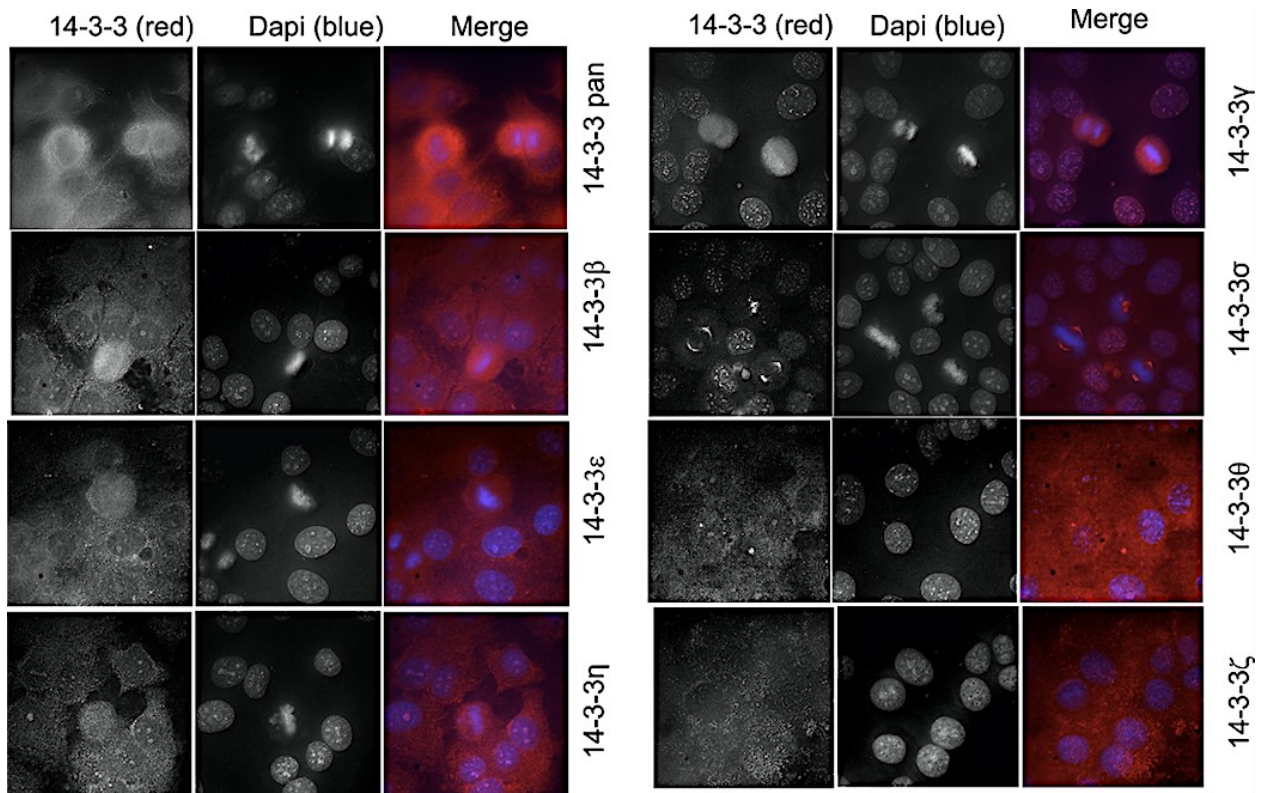


**Figure 3.10 Total 14-3-3 protein and 14-3-3 isoforms in HEK293T cells have similar subcellular localizations to COS-7 cells.** Total 14-3-3 protein was determined by assessing the immunoreactivity of the pan 14-3-3 antibody. Each 14-3-3 isoform was determined by immunoreactive antibodies to each specific isoform. Immunofluorescence were performed as described in Methods. Subcellular localization of pan 14-3-3 and seven 14-3-3 isoforms in HEK293T cells by immunofluorescence. 14-3-3 proteins were revealed by TRITC (red) and the chromatin was stained by DAPI (blue). Size bar = 10  $\mu$ m.

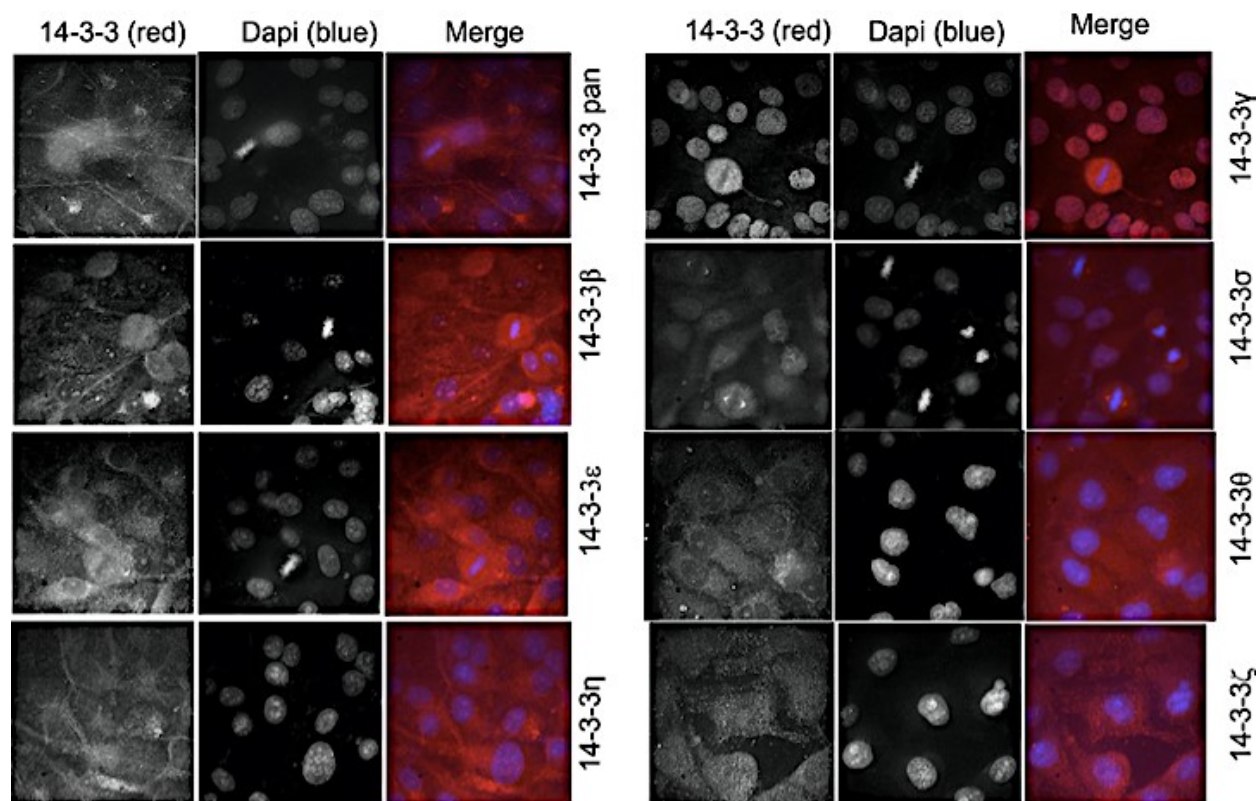


**Figure 3.11 Total 14-3-3 protein and 14-3-3 isoforms in MDA-MB-231 cells have similar subcellular localizations to COS-7 cells.** Total 14-3-3 protein was determined by a pan 14-3-3 antibody to assess its immunoreactivity. Each 14-3-3 isoform was determined by immunoreactive antibodies to each specific isoform. Immunofluorescence were performed as described in Methods. Subcellular localization of pan 14-3-3 and seven 14-3-3 isoforms in MDA-MB-231 cells by immunofluorescence. 14-3-3 proteins were revealed by TRITC (red) and the chromatin was stained by DAPI (blue). Size bar = 10  $\mu$ m

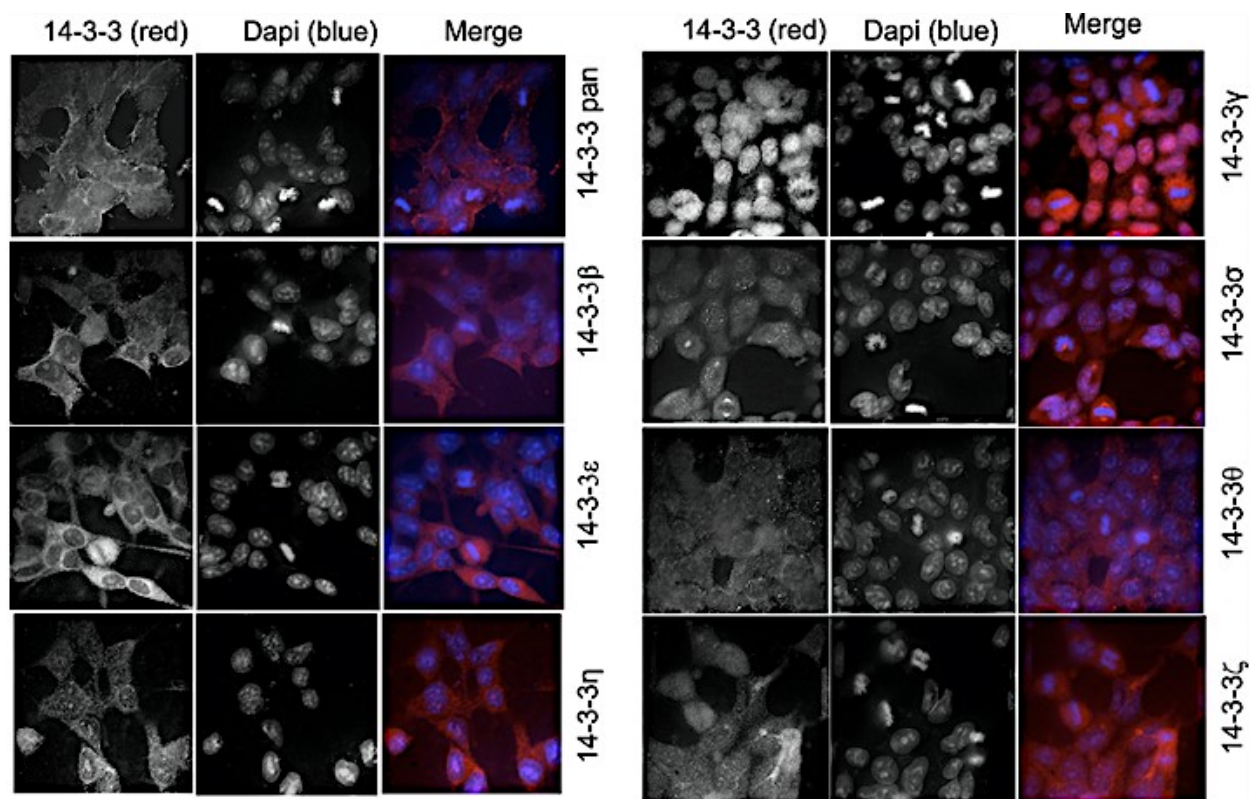


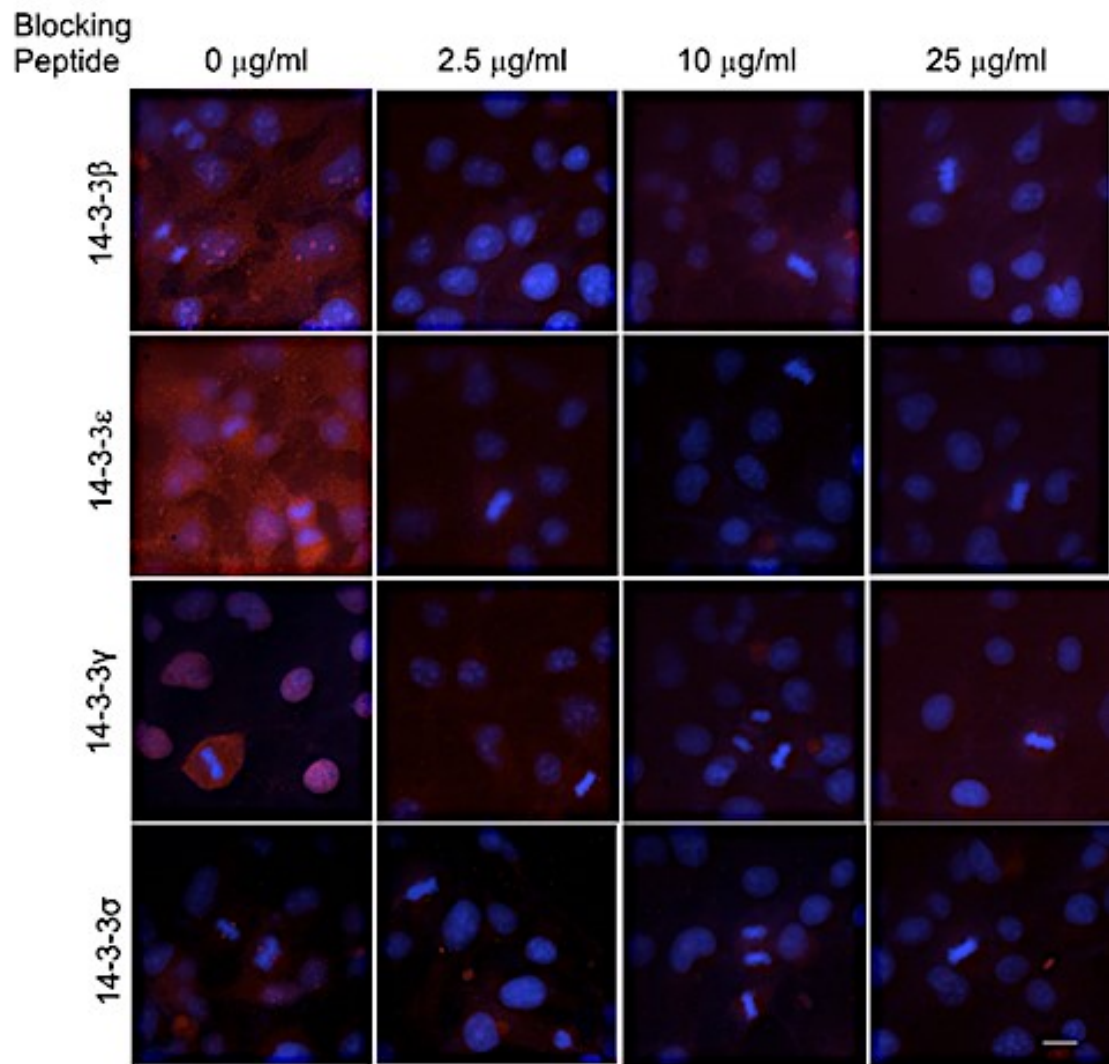
**Figure 3.12 Total 14-3-3 protein and 14-3-3 isoforms in MCF-7 cells have similar subcellular localizations to COS-7 cells.** Total 14-3-3 protein was determined by a pan 14-3-3 antibody to assess the antibody's immunoreactivity. Each 14-3-3 isoform was determined by antibodies to each specific isoform to assess the antibody's immunoreactivity. Immunofluorescence were performed as described in Methods. Subcellular localization of pan 14-3-3 and seven 14-3-3 isoforms in MCF-7 cells by immunofluorescence. 14-3-3 proteins were revealed by TRITC (red) and the chromatin was stained by DAPI (blue). Size bar = 10  $\mu$ m.

centrosome staining during mitosis. 14-3-3 $\tau/\theta$  is almost exclusively localized to the cytoplasm with only a few dots in some nuclei of the interphase cells. In the cytoplasm, the staining pattern of 14-3-3 $\tau/\theta$  was ER-like. The 14-3-3 $\zeta$  stain was strong throughout the cell including both the cytoplasm and the nucleus. In the cytoplasm, 14-3-3 $\zeta$  showed both ER-like patterns and dotted fiber-like patterns.

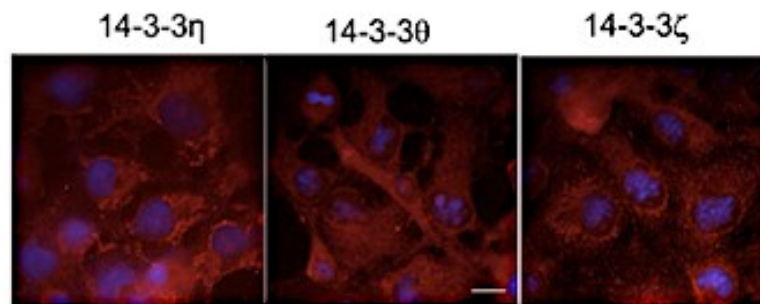
### **3.12 Antibody specificity was established using blocking peptides to several 14-3-3 isoforms in COS-7 cells**

It is important to test the specificity of the antibodies and validate the different antibodies' immunoreactivities. Among the antibodies that detected the seven 14-3-3 isoforms, four antibodies, including antibodies to 14-3-3 $\beta$ ,  $\epsilon$ ,  $\gamma$ , and  $\sigma$ , were raised against short peptides. I tested their specificity by using the peptides as blocking reagents. I showed that, in a dose-dependent manner, these peptides specifically and effectively blocked the immunoreactivity of the antibody, as the specific staining disappeared (Figure 3.13A). For the other three antibodies, including 14-3-3 $\eta$ ,  $\tau/\theta$ , and  $\zeta$ , there are no blocking peptides available. The mouse 14-3-3 $\eta$  antibody (10847-MM06) is produced from a hybridoma resulting from the fusion of mouse myeloma with B cells obtained from a mouse immunized with purified, recombinant human 14-3-3 *YWHAH*. The mouse 14-3-3 $\theta$  antibody (5J20) (sc-69720) is specific for the full length 14-3-3 $\theta$  of human origin. The mouse 14-3-3 $\zeta$  antibody is specific for an epitope between amino acids 122-140 within an internal region of 14-3-3 $\zeta$  of human origin. To validate my data, I performed localization experiments on these isoforms with different antibodies with different immunoreactivities and if they are similar to Figure 3.1B. As shown in Figure 3.13B, similar subcellular localizations of these 14-3-3 isoforms were revealed by these new antibodies.

**A**



**B**



14-3-3 (red) Dapi (blue)

**Figure 3.13 14-3-3 isoforms have different subcellular localizations after adding the blocking peptides in a dose-dependent manner in COS-7 cells.** (A) The effects of blocking peptide for 14-3-3 $\beta$ ,  $\epsilon$ ,  $\gamma$ , and  $\sigma$ . The indirect immunofluorescence experiments were performed as described for Figure 3.1B except that the antibodies were incubated with blocking peptides of the indicated concentration for 1 h prior to incubating the cells. The final concentration of each antibody is 2.5  $\mu\text{g/ml}$  and the concentrations of the blocking peptides as indicated. (B) The subcellular localization of 14-3-3 $\eta$ ,  $\tau/\theta$ , and  $\zeta$  were determined with different antibodies and different immunoreactivities than the ones used in Figure 3.1B since no blocking peptides were available. Size bar = 10  $\mu\text{m}$ .

## **Chapter 4: Results II - Interaction Between Rac1 and 14-3-3 proteins**

The information presented in this chapter has been published in *Cells* with me as a second author: Abdrabou, A. M., Brandwein, D., Liu, C., & Wang, Z. (2019). Rac1 S71 mediates the interaction between Rac1 and 14-3-3 proteins. *Cells*, 8(9), 1006. doi: 10.3390/cells8091006.

### **4.1 Rac1 and 14-3-3 proteins interact in response to EGF-induced Akt phosphorylation in COS-7 cells**

Here, I first determined whether endogenous 14-3-3 proteins bind to Rac1 in response to EGF by co-immunoprecipitation. COS-7 cells were treated with EGF, and Rac1 was immunoprecipitated with a mouse anti-Rac1 antibody. The co-immunoprecipitation of 14-3-3 was examined by immunoblotting with antibodies to pan 14-3-3. As shown in Figure 4.1A, 14-3-3 co-immunoprecipitated with Rac1 following EGF stimulation and the amount of co-immunoprecipitated 14-3-3 increased at 5-15 min following EGF stimulation. This data indicates that EGF stimulates the association between Rac1 and 14-3-3 proteins.

To understand this underlying interaction further, I analyzed the amino acid sequence of Rac1 to identify potential binding motifs for 14-3-3 protein. The mode I consensus 14-3-3 protein binding motif is RSXpSXP and the Rac1 sequence <sup>68</sup>RPLSYP<sup>73</sup> is likely a 14-3-3 protein binding motif following the phosphorylation of S71 (Figure 4.1B). Moreover, 14-3-3 Prediction software predicted the highest consensus between 14-3-3 and Rac1 to be within the S71 motif, which has a value of approximately 1 (Figure 4.1C). Thus, I propose that in response to EGF, Akt is phosphorylated by activated EGFR via PI3K, which results in Rac1 S71 phosphorylation, and Rac1 and 14-3-3 protein interaction.

To test this hypothesis, I treated the cells with EGF and showed that EGFR, Akt and Rac1 S71 are all phosphorylated in response to EGFR (Figure 4.1D). However, inhibition of

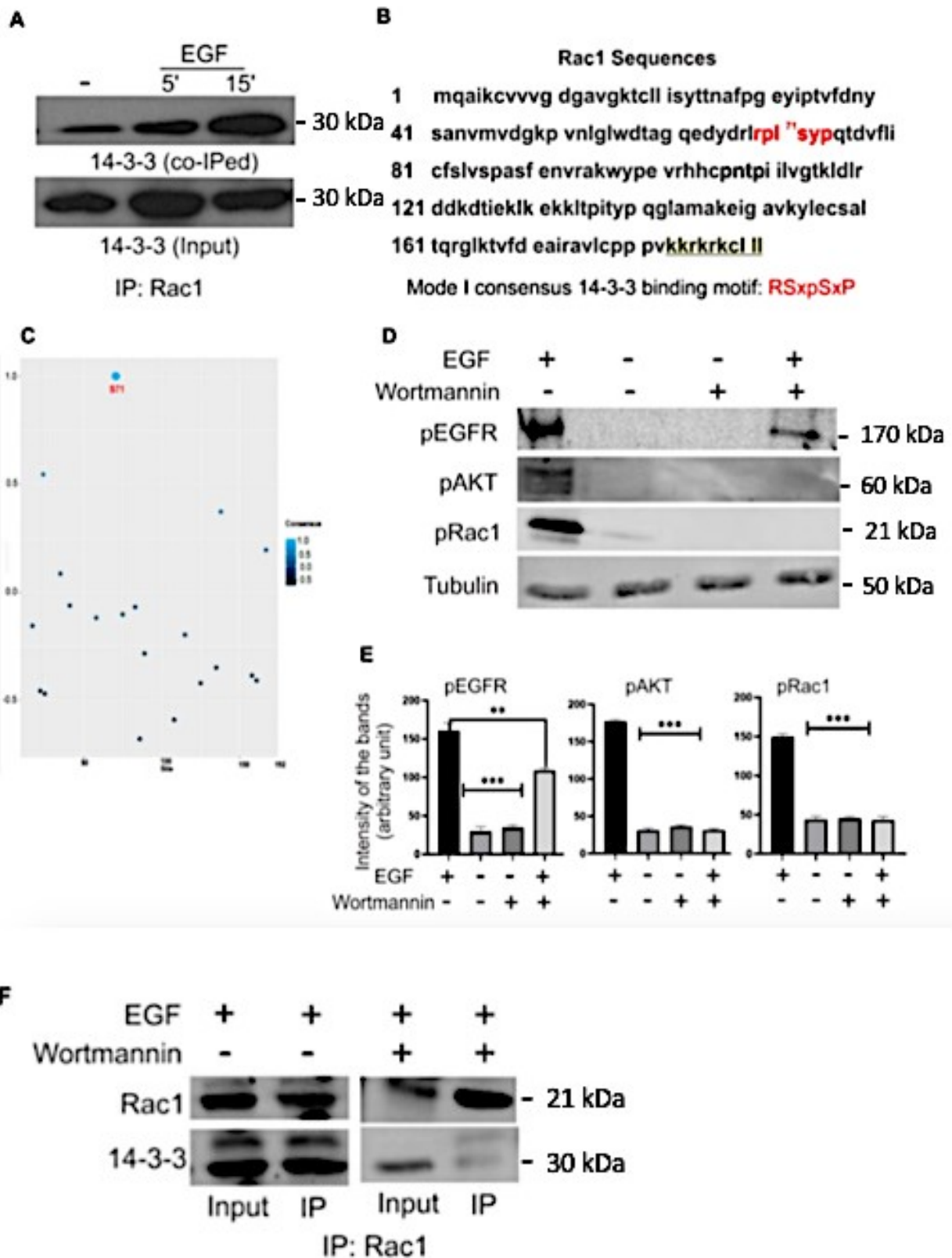


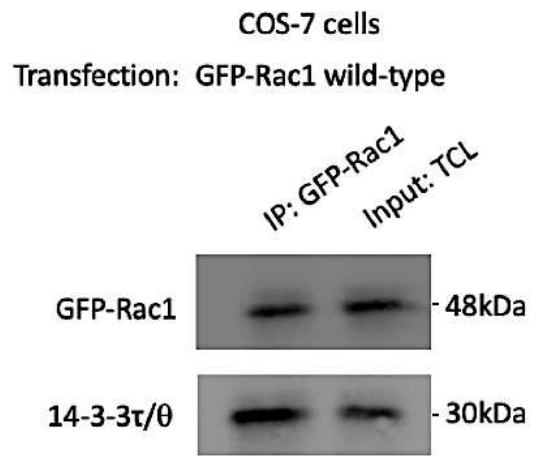
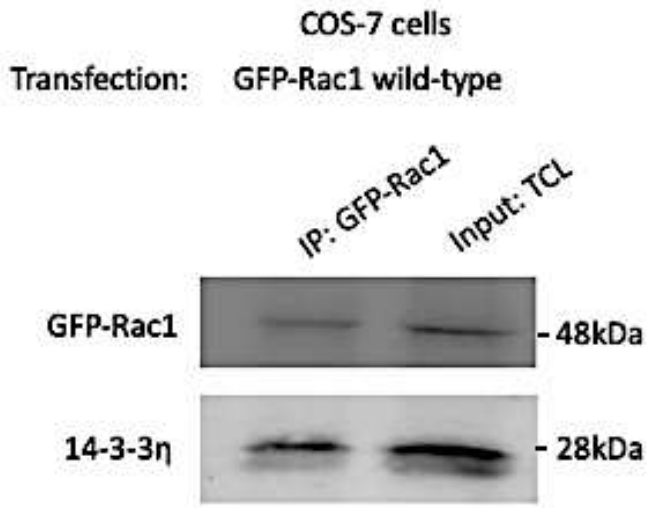
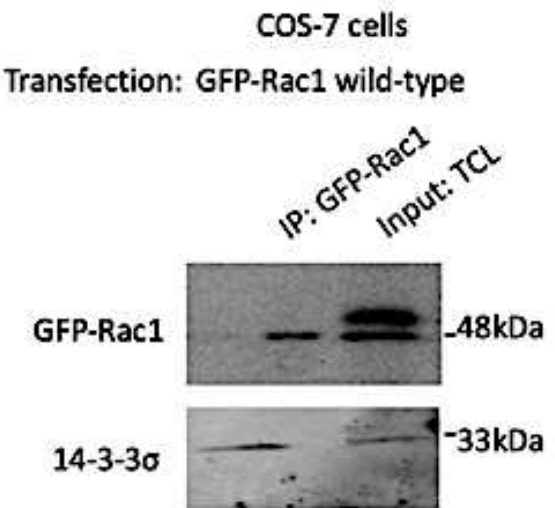
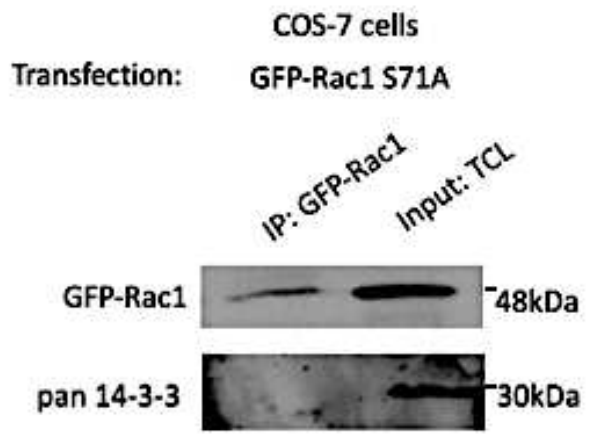
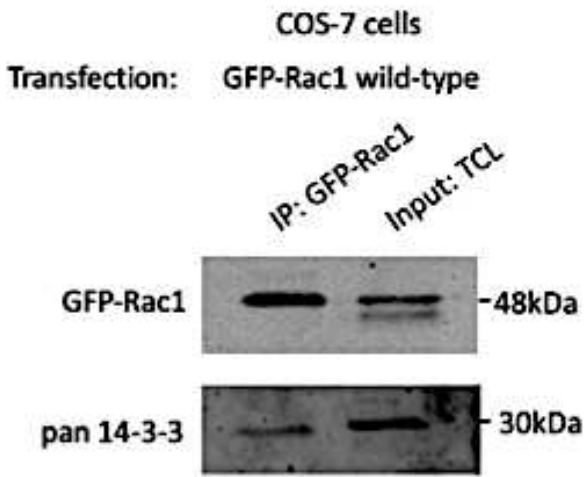
**Figure 4.1 Rac1 and 14-3-3 proteins interact in response to EGF-induced Akt**

**phosphorylation in COS-7 cells.** (A) 14-3-3 protein interacts with Rac1 in response to EGF in COS-7 cells. COS-7 cells were treated with EGF for the indicated time and the interaction between 14-3-3 and Rac1 was determined by co-IP. (B) Amino acid sequence analysis of Rac1 shows the presence of the mode I 14-3-3 binding motif<sup>68RPLSY<sup>73</sup></sup> if S71 is phosphorylated. (C) The highest consensus between 14-3-3 and Rac1 is within the S71 motif as predicted by 14-3-3 Prediction software. (D) The effects of EGF and wortmannin on the phosphorylation of EGFR, Akt and Rac1 S71. COS-7 cells were treated with EGF and/or wortmannin. The phosphorylation of EGFR, Akt and Rac1 S71 was revealed by immunoblotting with phospho-specific antibodies to Akt and Rac1. (E) Quantification of the data in (D). The level of protein phosphorylation was quantified by densitometry. Each value is the average of at least three experiments and the error bars depict standard error (SE). \*\*  $p < 0.01$ , \*\*\*  $p < 0.001$ . (F) The effects of EGF and wortmannin on the interaction between 14-3-3 and Rac1. COS-7 cells were treated with EGF and/or wortmannin as indicated. The interaction between 14-3-3 and Rac1 was determined by co-IP (Abdalla et al., 2019).

PI3K with wortmannin upstream blocks the downstream phosphorylation of both Akt and Rac1 S71. I then examined if wortmannin inhibits the Rac1 and 14-3-3 interaction. As shown in Figure 4.1E, wortmannin treatment inhibits the EGF-induced interaction between Rac1 and 14-3-3 proteins. These data suggest that EGF-induced Rac1 S71 phosphorylation, through Akt, leads to the Rac1 and 14-3-3 interaction.

#### **4.2 Total 14-3-3 protein and some 14-3-3 isoforms co-immunoprecipitate with Rac1 in GFP-Rac1 WT but not in GFP-Rac1 S71A COS-7 cells**

To confirm the role of S71 in mediating the interaction between Rac1 and 14-3-3 proteins, I transfected COS-7 cells with GFP-Rac1 S71A and GFP-Rac1 WT was used a control. As shown in Figure 4.2, GFP-Rac1 WT co-IPed with 14-3-3 proteins. Intriguingly, GFP-Rac1 S71A failed to co-IP with 14-3-3 proteins, which supports my hypothesis that S71 phosphorylation may mediate the interaction between Rac1 and 14-3-3 proteins. As mentioned above, the immunoprecipitated product is one-tenth the amount of the total cell lysate. I have shown above that the seven 14-3-3 isoforms have distinct subcellular localizations, so I examined which 14-3-3 isoforms interact with Rac1. I transfected COS-7 cells with GFP-Rac1 and IPed with an antibody to GFP and examined which 14-3-3 isoforms co-IPed with GFP-Rac1 by immunoblotting with antibodies to the seven 14-3-3 isoforms. As shown in Figure 4.2, 14-3-3 $\eta$ ,  $\sigma$  and  $\tau/\theta$  co-immunoprecipitated with Rac1; however, 14-3-3 $\beta$ ,  $\epsilon$ ,  $\gamma$  and  $\zeta$  did not co-immunoprecipitate with the Rac1 in GFP-Rac1 WT transfected COS-7 cells.



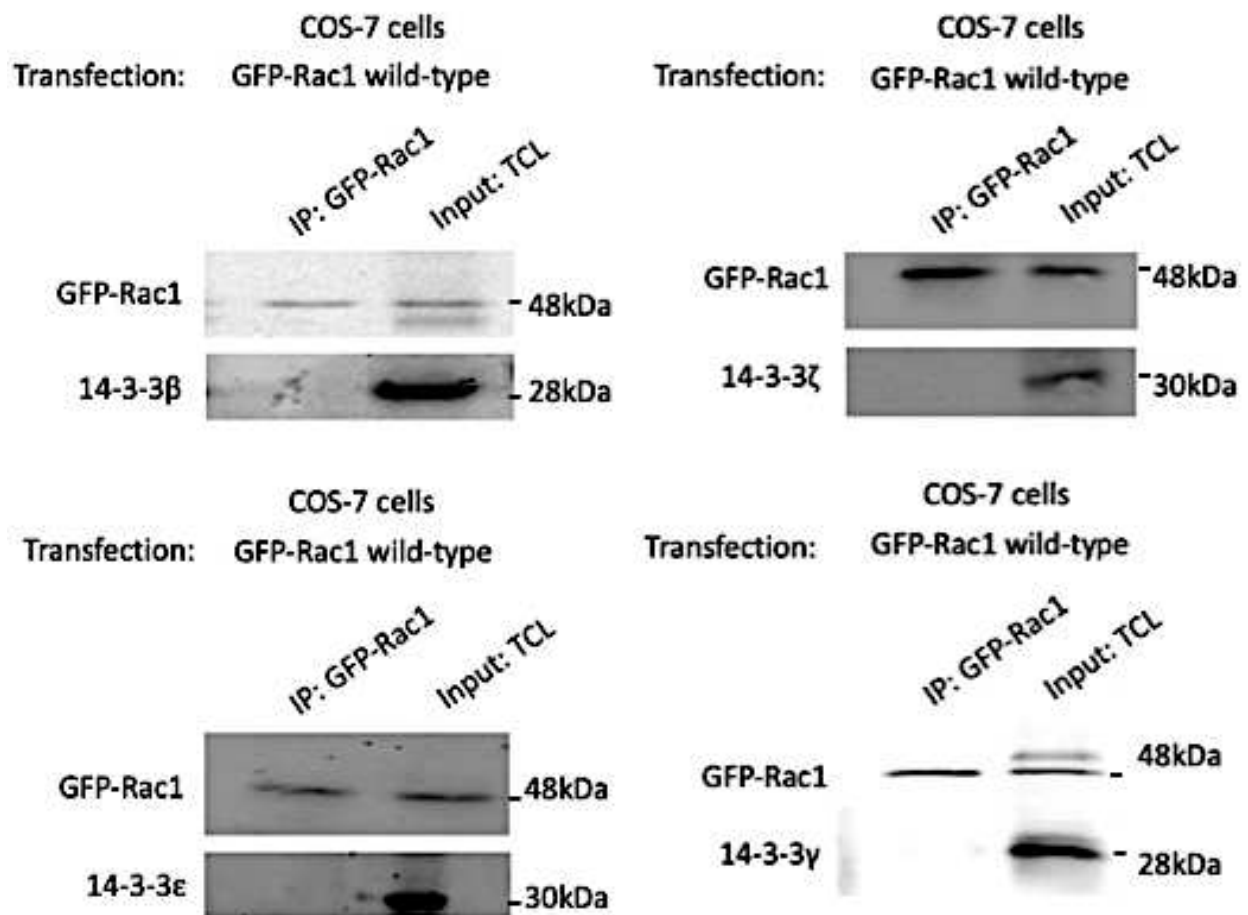


**Figure 4.2 Total 14-3-3 protein and some 14-3-3 isoforms co-immunoprecipitate with Rac1 in GFP-Rac1 WT but not in GFP-Rac1 S71A COS-7 cells.** Co-IP was used to determine if GFP-Rac1 S71A mutation affects the interaction between the total 14-3-3 protein and each 14-3-3 isoforms in COS-7 cells. COS-7 cells were transfected with GFP-Rac1 WT and GFP-Rac1 S71A. The expressed Rac1 was IPed with an antibody to GFP, and the co-IPed 14-3-3 was examined by immunoblotting. Total 14-3-3 protein was determined by a mouse pan 14-3-3 antibody. Each 14-3-3 isoform was determined by antibodies to each specific isoform. Co-immunoprecipitation followed by immunoblotting were performed as described in Methods. Lane 1: Co-immunoprecipitation Lane 2: Total cell lysate (TCL) (Abdalla et al., 2019).

## Chapter 5: Discussion

14-3-3 proteins are involved in many cellular processes as they are central regulators of many signaling pathways. There are seven 14-3-3 isoforms in mammals; however, it is not clear if these isoforms play redundant or distinct roles in cell signaling. Understanding the subcellular localization of 14-3-3 proteins expands upon what is known in the literature about 14-3-3 isoform-specific functions. The Rho family of GTPases is involved in regulating many cellular processes, and Rac1 specifically promotes the reorganization of actin filament polymerization in lamellipodia and membrane ruffles. Both 14-3-3 proteins and Rho GTPases regulate cytoskeleton remodeling and cell migration and understanding this interaction may uncover novel cell signaling networks and novel molecular mechanisms underlying certain diseases. In this thesis, I primarily studied 14-3-3 isoform subcellular localization and colocalization with various organelle/structural markers, redistribution throughout the cell cycle and translocation in response to EGF. I also have preliminary evidence suggesting 14-3-3 proteins binding and interacting with Rac1 through Rac1 S71.

Determining 14-3-3 isoform subcellular localization could inform 14-3-3 isoform-specific functions. Aberrant subcellular localization can potentially lead to abnormal phenotypes and altered cell functions which may result in cancer and disease. However, as mentioned above, studies of 14-3-3 protein subcellular localization have primarily been done in yeast, flies and plants with close to no studies being done in mammalian species. As demonstrated in this thesis, I first examined the subcellular localization of total 14-3-3 protein and each of the 14-3-3 isoforms in COS-7 cells. The subcellular localization of 14-3-3 proteins was mostly determined by indirect immunofluorescence by the staining pattern and by the colocalization with well-established markers for the various subcellular compartments. Subcellular fractionation and

immunoblotting were also employed to determine if an isoform was localized in the nucleus or cytoplasm. I showed that 14-3-3 proteins are broadly distributed throughout the cell and associated with many subcellular structures/organelles including the PM, mitochondria, ER, nucleus, microtubules and actin fibers. This broad subcellular distribution underlines the multiple functions identified for 14-3-3 proteins. Most notably, 14-3-3 $\eta$  is almost exclusively localized to the mitochondria, 14-3-3 $\gamma$  is only localized to the nucleus, and 14-3-3 $\sigma$  strongly and specifically associated with the centrosome during mitosis.

First, I looked at specific 14-3-3 isoform expression with antibodies specific to each isoform. I calculated the molecular weights with respect to the known protein ladders by visual inspection. Whole immunoblots of 14-3-3 $\epsilon$  and  $\gamma$  clearly show one band at 30 kDa and 28 kDa, respectively (Figure 1A). My results are mostly consistent with the antibody manufacturer's data, but there are slight differences in molecular weights in my 14-3-3 isoform expression data (data not shown). This may be due to the different cell lines or to the different antibodies the companies used. However, similar to the antibody manufacturers, I also do not have non-specific bands (data not shown) indicating 14-3-3 antibody specificity for each isoform. However, it would be beneficial to show the whole immunoblots for all of the isoforms in order to make conclusions about 14-3-3 isoform differences in subcellular localization and colocalization with various markers. Rather than visually determining the protein's molecular weight, I can measure the exact molecular weight of a protein by plotting the distance it travels in the gel against its molecular weight. Then, I can predict a protein's molecular weight simply by the distance it travels on the gel.

Phylogenetic analysis of these isoforms, using ClustalOmega software, shows that the 14-3-3 isoforms can be grouped into three pairs: 14-3-3 $\beta$  and  $\zeta$ , 14-3-3 $\sigma$  and  $\tau/\theta$ , 14-3-3 $\eta$  and  $\gamma$

(Figure 1.1). 14-3-3 $\epsilon$  does not belong with any of the three pairs since it differs the most in its primary structure. The two isoforms in each pair are the most similar to each other (Berg et al., 2003; Sluchanko and Gusev, 2010) (Figure 1.1). The pairs with high primary sequence homology also showed similar subcellular localizations. For example, 14-3-3 $\beta$  and  $\zeta$  both localized to the actin fibers, microtubules, and ER (Figures 3.3 and 3.9). In addition, both 14-3-3 $\sigma$  and  $\tau/\theta$  localized to the microtubules, with 14-3-3 $\sigma$  primarily being localized to the centrosomes (Figures 3.7 and 3.8). However, the subcellular colocalizations between 14-3-3 $\eta$  and  $\gamma$  are quite different. 14-3-3 $\gamma$  almost exclusively localized to the nucleus while 14-3-3 $\eta$  almost exclusively localized to the mitochondria (Figures 3.5 and 3.6). The fact that some of the isoforms showed similarities in their subcellular localization could be related to their high sequence similarity in the short variable stretches in their primary structure even though each isoform is encoded by a separate gene (Aitken, 2002; Sluchanko and Gusev, 2010).

In this thesis, I demonstrate that 14-3-3 proteins colocalized with different cytoskeletal markers such as actin fibers and microtubules. Both pan 14-3-3 and 14-3-3 $\zeta$  showed stronger actin fiber colocalizations (Figures 3.1, 3.2 and 3.9), while both 14-3-3 $\beta$  and  $\epsilon$  showed weaker actin fiber colocalizations (Figures 3.3 and 3.4). These results suggest that 14-3-3 proteins may regulate actin fiber formation. It would be interesting to study the entire endocytic pathway by using lysosomal specific markers. We only tested the colocalization with the plasma membrane and the endosome, but to be fully comprehensive, I would need to test other markers related to the endocytic pathway. This data also suggests that other control markers could be used to determine pan 14-3-3 colocalization with cytoskeletal markers since I did not see strong colocalization with this specific tubulin antibody.

As mentioned above, 14-3-3 protein has also been shown to regulate cytoskeleton remodeling and cell migration (Sluchanko and Gusev, 2010). Previous research showed that 14-3-3 $\gamma$  and  $\zeta$  directly interact and regulate F-actin (Kligys et al., 2009; Sluchanko and Gusev, 2010; Ye et al., 2016). However, later research showed 14-3-3 proteins regulate actin fiber formation through cofilin (Bamburg, 1999; Sluchanko and Gusev, 2010). Proteins involved in actin remodeling have been identified as 14-3-3 binding partners (Moores et al., 2000; Freeman and Morrison, 2011; Aghazadeh and Papadopoulos, 2016; Krtkova et al., 2017; Sluchanko and Gusev, 2017).

In this thesis, I demonstrate that 14-3-3 $\beta$ ,  $\epsilon$ ,  $\sigma$ , and  $\zeta$  all colocalized with microtubules, suggesting a possible role in regulating microtubule formation (Figures 3.3, 3.4, 3.7 and 3.9). My findings are mostly consistent with previous reports. Previous research showed that 14-3-3 $\epsilon$ ,  $\eta$ ,  $\sigma$ ,  $\gamma$ , and  $\zeta$  regulate microtubule formation (Qureshi et al., 2013; Park et al., 2014; Joo et al., 2015; Cornell et al., 2016; Jansen et al., 2017). 14-3-3 proteins regulate microtubules through tau proteins that stabilize microtubules and loss of this interaction leads to neurodegeneration (Chun et al., 2004; Sluchanko and Gusev, 2010). Many studies also implicated small GTPases, such as Rac and RhoA, in the regulation of microtubules by 14-3-3 proteins (Robinson, 2010; Zhou et al., 2010).

This thesis clearly demonstrates 14-3-3 $\eta$  localization in the mitochondria (Figure 3.5). There is also weak 14-3-3 $\beta$  localization in the mitochondria (Figure 3.3). 14-3-3 $\gamma$  has also been shown to be implicated in the mitochondria (He et al. 2018; Huang et al. 2018b), however, I did not observe any 14-3-3 $\gamma$  localization in the mitochondria (Figure 3.6). To further validate my data, I would have to test different cell lines, different antibodies and different markers to get a better picture of where 14-3-3 localize. 14-3-3 proteins have previously been reported to localize

to the mitochondria and to regulate various mitochondrial functions, including cell apoptosis and oxidation (Gardino and Yaffe, 2011; Sreedhar et al., 2015; Liu et al., 2018). 14-3-3 $\eta$  has been shown to protect against mitochondria-mediated apoptosis (Sreedhar et al., 2015). 14-3-3 $\eta$  has also been shown to be involved in the transportation and the anti-apoptotic function of Bcl-2 in the mitochondria (Zhang et al., 2018; Huang et al., 2018a).

This thesis clearly demonstrates the specific localization of 14-3-3 $\sigma$  to the centrosomes during mitosis (Figure 3.7A). Furthermore, this thesis shows 14-3-3 $\sigma$  to be localized to both the nucleus and the cytoplasm during interphase, but primarily localized to the centrosome during mitosis. 14-3-3 $\sigma$  centrosome localization suggests a potential role in regulating the microtubule spindle apparatus during mitosis. Centrosomes are the major microtubule nucleating and organizing centres and are critical for the proper formation and the dynamic nature of the microtubule spindle apparatus during mitosis. 14-3-3 proteins have been shown to interact with multiple proteins involved in mitotic regulation (Gardino and Yaffe, 2011). 14-3-3 proteins have also previously been implicated in the centrosome (Pietromonaco et al., 1996; Tollenaere et al., 2015; Mukhopadhyay et al., 2016). Previous research showed 14-3-3 $\epsilon$  and  $\gamma$  localization in the centrosome and the mitotic spindle apparatus in mouse leukemic FDCP cells (Pietromonaco et al., 1996). Recently, 14-3-3 protein was shown to regulate the formation of centriolar satellites by sequestering CEP131, a protein that regulates cilia/flagellum formation (Tollenaere et al., 2015). 14-3-3 $\gamma$  was also shown to localize to the centrosome and that loss of 14-3-3 $\gamma$  led to centrosome amplification (Mukhopadhyay et al., 2016). It is interesting to notice that 14-3-3 $\sigma$  is downregulated in many tumor types, suggesting its tumor suppressor activity (Robinson, 2010). Thus, 14-3-3 $\sigma$  could be a therapeutic target for cancer.

The mitotic centrosome localization of 14-3-3 $\sigma$  is the clearest subcellular change observed in this thesis. The other noticeable change observed in this thesis is the subcellular localization of 14-3-3 $\gamma$  to the nucleus in interphase cells, and the diffuse distribution throughout the cytoplasm during mitosis when the nuclear membrane breaks down (Figure 3.6A). Thus, mitosis may be the only time when 14-3-3 $\gamma$  is able to interact with the other isoforms. Although most 14-3-3 isoforms colocalized to the cytosol and the nucleus, 14-3-3 $\gamma$  is only localized to the nucleus and associated with none of the subcellular markers I tested.

I also studied the effects of EGF on the subcellular localization of 14-3-3 proteins. I identified two changes among the 14-3-3 isoforms in response to EGF. First, 14-3-3 $\gamma$  formed large particles in the nucleus in the absence of EGF (Figure 3.6B). However, in response to EGF stimulation for 5 and 15 min, 14-3-3 $\gamma$  formed smaller particles in the nucleus, while the larger particles disappeared. This could be due to the fact that 14-3-3 $\gamma$  may have re-associated with smaller nuclear structures after it dissociated from the initial larger nuclear structures. Many nuclear structures and subdomains have been discovered including nucleoli, nuclear speckles, paraspeckles, clastosomes, Cajal bodies, promyelocytic leukemia proteins (PMLs), Polycomb bodies, and histone locus bodies (HLBs) (Mao et al., 2011). To elucidate the nuclear function of 14-3-3 $\gamma$ , it would be interesting to determine which subnuclear structures 14-3-3 $\gamma$  associates with before and after EGF stimulation.

Second, this thesis clearly demonstrates the enhanced association with the actin fibers and the microtubules of some 14-3-3 isoforms including  $\beta$ ,  $\epsilon$ ,  $\sigma$ ,  $\tau/\theta$ , and  $\zeta$  (Figures 3.3, 3.4, 3.7, 3.8 and 3.9). This is not surprising because EGF has also been shown to regulate cytoskeleton remodelling and cell migration (Wang, 2017; A. Abdrabou and Wang, 2018). Binding to a client protein could significantly re-locate 14-3-3 proteins and is mostly dependent on the

phosphorylation of the client protein (Thomas et al., 2005). Protein phosphorylation is mostly regulated by growth factor stimulation. Thus, it is interesting to determine if the subcellular localization of 14-3-3 proteins is affected by growth factor stimulation. I could also stimulate the phosphorylation of proteins in an EGF-independent manner by using phosphatase inhibitors. This would further validate my results that phosphorylation mediates 14-3-3 protein subcellular localization and 14-3-3 protein interaction with Rac1.

In conclusion, this thesis demonstrates that the 14-3-3 isoforms have broad subcellular distributions and that the 14-3-3 isoforms colocalize with many subcellular structures/organelles including the PM, mitochondria, ER, nucleus, centrosome, microtubules, and actin fibers (Table 3.1). This broad subcellular distribution suggests distinctive 14-3-3 isoform-specific functions. For instance, 14-3-3 $\eta$  almost exclusively localized to the mitochondria (Figure 3.5), 14-3-3 $\gamma$  exclusively localized to the nucleus (Figure 3.6B), and 14-3-3 $\sigma$  localized to the centrosome during mitosis (Figure 3.7A).

Next, this thesis briefly examined other cell lines that natively express 14-3-3 proteins to detectable levels. I examined the subcellular localization of total 14-3-3 protein and each 14-3-3 isoform by indirect immunofluorescence (Figures 3.10, 3.11, and 3.12). The HEK293T, MDA-MB-231 and MCF-7 cell lines showed some similarities and differences to COS-7 subcellular localizations in the nucleus and in the cytosol. COS-7 cells and HEK293T cells are epithelial cells isolated from kidneys of African green monkeys and embryonic kidney cells of humans respectively. MDA-MB-231 cells and MCF-7 cells are epithelial cells isolated from mammary breast cancer tumours. These cell lines allow us to gain a broader perspective on how evolutionary mechanisms between tissues and species shape the subcellular localizations and functions of these highly conserved proteins. However, much more work needs to be done in

these cell lines to show specific localizations, colocalizations with different subcellular markers, their redistribution throughout the cell cycle and their translocation in response to EGF.

Next, I tested the specificity of some 14-3-3 isoform antibodies using short peptides as blocking reagents. This was meant to validate my 14-3-3 isoform subcellular localization data. I showed, in a dose-dependent manner, that these peptides specifically and effectively blocked the observed immunoreactivity of the 14-3-3 antibody, which showed the absence of isoform-specific subcellular localization patterns (Figure 3.13A). There are no blocking peptides available for the other three isoforms (14-3-3 $\eta$ ,  $\tau/\theta$ , and  $\zeta$ ). To validate my immunofluorescent data, I examined their subcellular localization with a different antibody and different immunoreactivities, and I showed that these new antibodies showed similar subcellular localizations as the antibodies I used in Figure 3.1B (Figure 3.13B). As these new antibodies were raised against different antigens with different immunoreactivities, these similar subcellular localization results validated my previous immunofluorescent observations and indicates the specificity of the staining pattern. However, I did not perform experiments with the blocking peptides to block the co-IP of 14-3-3 proteins with Rac1. In the future, it would be beneficial to see the expression of 14-3-3 proteins using Western blotting, and subsequent Rac1 expression as well, after addition of the blocking peptides.

As mentioned above, most 14-3-3 isoforms form homodimers and heterodimers *in vitro* and *in vivo* (Jones et al., 1995). My results suggest that 14-3-3 $\gamma$  and  $\sigma$  have very specific subcellular localizations in the nucleus and centrosomes, respectively (Figures 3.6 and 3.7). This may explain why these two isoforms tend to homodimerize and not interact with other isoforms *in vitro*. If two isoforms are not in the same subcellular compartment, then they will not dimerize. As mentioned above, 14-3-3 $\gamma$  can potentially interact with other isoforms once the

nuclear membrane breaks down during mitosis. Indeed, 14-3-3 $\gamma$  mostly prefers to form heterodimers with 14-3-3 $\epsilon$  *in vitro* in PC12 and COS-7 cells (Chaudhri et al., 2003).

Furthermore, 14-3-3 $\epsilon$  and  $\zeta$  were shown to form heterodimers *in vivo*. 14-3-3 $\epsilon$  heterodimerizes with 14-3-3 $\beta$ ,  $\eta$ ,  $\gamma$  and  $\zeta$  but no homodimers were detected. This may explain the 14-3-3 $\epsilon$  and  $\zeta$  cytoplasmic localizations and why they colocalize with many subcellular structures in the cytoplasm (Figures 3.4 and 3.9). More work is required to understand the effects of 14-3-3 isoform subcellular localizations and their ability to form homodimers and heterodimers *in vitro* and *in vivo*.

There are several limitations with my immunofluorescence data. First, the results would be more convincing if I looked at additional specific subcellular structures/organelles to get a more comprehensive picture of 14-3-3 isoform subcellular localization. Also, it might be beneficial show the different red and blue channels in separate images to avoid blurred images of overlapping channels in the merged insets. This can occur even when deconvolution is applied to the images which is a process that attempts to obtain high contrast/sharper images. I used visual analysis to examine colocalization, which may lead to random error and bias. If the compartments are not spatially distinct, the probes seen in overlapping compartments can be difficult to interpret. Superposition can give a spatial sense of where molecules colocalize, but visual images are not useful when comparing the degree of colocalization in different conditions nor determining whether this colocalization is due to chance. Therefore, it would be more beneficial to use quantitative and statistical measures to study colocalization. The most common methods that researchers use to analyze colocalization quantitatively and statistically are the Pearson's correlation coefficient (PCC) and Manders' Overlap Coefficient (MOC), each having their own strengths and weaknesses (Manders et al., 1993; Dunn et al., 2011). PCC can

separately determine to what extent the variation of signal intensity in one image can be explained by the corresponding variation of the other image. It may be useful to construct scatterplots by plotting the intensity of each pixel in one image along the x-axis and the intensity of the same pixel location in the second image on the y-axis, thereby forming a histogram that describes the relationship between the corresponding intensity values. Regions within the scatterplot does not always correspond to specific areas within the images, since it only gives intensity information. PCC is simple, quick and easy but one of the disadvantages is that it only works for simple, linear associations. MOC describes the total amount of fluorophores that overlap with each other. Therefore, it only takes into account the brightest pixels; however, this may overestimate the colocalization of two signals. MOC is a more intuitive approach, accounting for the concentrated weighted overlap between two image targets and is also relatively unaffected by noise. The main drawback is that background levels need to be established and MOC values can be inflated by unwanted signals by out-of-focus light or sample autofluorescence. Later research found a way to determine if the colocalization between two images can be randomly due to chance (Cortes et al., 2004). This research employed a test of statistical significance by subjecting one image to spatial scrambling, where pixels disperse randomly to different parts of the image. This can then be compared with another channel image that remained unscrambled and then a MOC value can be calculated. This value is compared to the true MOC value between the original images which can determine whether this colocalization is statistically significant or due to random chance. These quantitative measures can each provide their own unique perspective about colocalization and their usage depends on the type of biological question being asked (Aaron et al., 2018).

It is well-established that 14-3-3 protein signaling pathways and Rac1 signaling pathways regulate important cell functions including cytoskeleton remodeling and cell migration. The interaction is mostly through the interactions between 14-3-3 protein and Rac1 upstream regulators or downstream substrates (Brandwein and Wang, 2017). My thesis showed that some 14-3-3 isoforms are able to interact with Rac1, which provides an additional regulation of Rac1 signaling pathways by 14-3-3 protein. Interestingly, my co-IP experiments indicate that the interaction between 14-3-3 and Rac1 is dependent on EGF stimulation and subsequent Rac1 S71 phosphorylation (Figures 4.1 and 4.2). However, I only IPed with Rac1 and immunoblotted with 14-3-3 proteins. To be more comprehensive, I would also need to IP with 14-3-3 proteins and immunoblot with Rac1 to see if I get similar results. Also, I can use other specific PI3K inhibitors, such as LY294002, which is a reversible PI3K inhibitor. Wortmannin is an irreversible PI3K inhibitor, which, from a pharmacological standpoint, may not be useful when treating patients. If patients experience adverse side effects upon treatment with toxic doses of the inhibitor, it might take a long time for the body to recover and counteract the effects of the irreversible inhibitor. This because new PI3K enzymes need to be synthesized in order to recover PI3K activity.

The mutation of Rac1 S71 to A inhibited the interaction 14-3-3 protein and S71 phosphorylation facilitates the interaction. It is well established that 14-3-3 proteins function as scaffold proteins and regulate the activity of their binding partners. On the other hand, Rac1 is a Rho GTPase and functions as a molecular switch to directly/indirectly control many signaling pathways. Thus, 14-3-3 proteins may serve to regulate Rac1 activity and downstream functions.

I determined which 14-3-3 isoforms interact with Rac1 and showed that 14-3-3 $\eta$ ,  $\sigma$ , and  $\tau/\theta$  bind to Rac1 in COS-7 cells. As mentioned above, 14-3-3 $\eta$ ,  $\sigma$ , and  $\tau/\theta$  all associated with the

cytoskeleton and Rac1 has been shown to strongly associate with the cytoskeleton and regulate cytoskeleton remodeling and cell migration (Tong et al., 2013; Tong et al., 2016; A. Abdrabou and Wang, 2018; Payapilly and Malliri, 2018). This supports my findings that Rac1 interacts with 14-3-3 $\eta$ ,  $\sigma$ , and  $\tau/\theta$ .

This is preliminary data and definitely warrants future investigations to fully characterize if S71 phosphorylation affects Rac1 and 14-3-3 interactions. Much research has been done on 14-3-3 proteins and Rac1 separately and research has shown many indirect interactions between 14-3-3 proteins and various Rho effectors. However, there is no research to suggest a direct interaction and mutual regulation between these two groups of proteins. While, there may be an interaction, it could be due to several reasons. First, it may not be a direct interaction between 14-3-3 proteins and Rac1 since they may bind in a complex and indirectly interact with a third protein. Second, if in fact 14-3-3 proteins and Rac1 do interact *in vitro*, for example, using a yeast two-hybrid system, they may not be able to interact under true physiological conditions. As mentioned above, Rac1 is phosphorylated at multiple sites, including Y64 by FAK, and T108 by ERK. However, previous research has shown other 14-3-3 protein sites are involved in target protein binding. Furthermore, I also mentioned above that 14-3-3 proteins bind to proteins in phosphorylation-independent manners. Therefore, Rac1 and 14-3-3 may also interact without Rac1 S71 phosphorylation (Mils et al., 2000; Chun et al., 2004). Therefore, a long-term plan would be to mutate Rac1 at different sites that are not affected by Rac1 phosphorylation. Then, I can examine if these sites are important for 14-3-3 and Rac1 interactions.

There are many short-term and long-term future directions for this study. One important future research is to characterize the functional consequences of the 14-3-3 protein and Rac1 interaction. For this purpose, I will further determine if Rac1 phosphorylation on S71 mediates

the interaction between Rac1 and 14-3-3 proteins. This thesis shows that GFP-Rac1 WT, but not GFP-Rac1 S71A, is able to co-IP with pan 14-3-3 protein and GFP-Rac1 WT is also able to co-IP with 14-3-3  $\eta$ ,  $\sigma$ , and  $\tau/\theta$  (Figure 4.2). I will replicate these results at least more times in other cell lines such as HEK293T cells. I will then use GST-pull down assays to see if GST-Rac1 WT and GST-Rac1 S71A can directly interact with 14-3-3 proteins, similar to my co-IP experiments. Then, I will examine if Rac1 activity affects the Rac1 and 14-3-3 protein interaction using co-IP. Rac1 has several activity mutants, including a mutation of threonine 17 to asparagine (T17N), which is a dominant-negative, GDP-bound mutant. The other Rac1 activity mutant is a mutation of glutamine 61 to leucine (Q61L), which is a dominant active or constitutively active, GTP-hydrolysis deficient mutant. Then, I will determine if the interaction between Rac1 and 14-3-3 affects Rac1 activity and if the GFP-Rac1 S71A mutant is able to activate Rac1 using GST-PAK pull down assays.

Next, I will disrupt the interaction by inhibiting 14-3-3 docking sites with 2-(2,3-Dihydro-1,5-dimethyl-3-oxo-2-phenyl-1H-pyrazol-4-yl)-2,3-dihydro-1,3-dioxo-1H-isoindole-5-carboxylic acid (BV02) and see the effects on Rac1 activity. BV02 is a small, non-peptidic inhibitor of the 14-3-3 scaffolding protein docking sites such as mode I and mode II 14-3-3 binding motifs (Corradi et al., 2011; Mancini et al., 2011). BV02 was first discovered by computational-based virtual screening against the crystallographic structure of 14-3-3 $\sigma$  and BV02 was the top candidate compound since it showed bioactivity in cancer cells. (Corradi et al., 2010). More chemically stable derivatives of BV02 have been shown to bind and inhibit 14-3-3 $\sigma$  protein-protein interactions (PPIs), promote apoptosis and induce antiproliferative effects in CML cell lines (Corradi et al., 2011; Mancini et al., 2011; Mori et al., 2014; Iralde-Lorente et al., 2019). Then, I will determine if the interaction of 14-3-3 proteins and Rac1 affects the

subcellular localization of the two proteins. First, I will see where GFP-Rac1 WT and GFP-Rac1 S71A typically localize and then note any changes in Rac1 and 14-3-3 subcellular localizations after adding BV02.

For long-term future directions, I will see if other Rac1 mutants such as the mutation of serine 71 to glutamic acid (S71E), mutation of threonine 108 to alanine (T108A), and mutation of threonine 108 to glutamic acid (T108E) are also able to co-IP with 14-3-3 proteins. I will also use other assays to characterize the functional consequences of Rac1 and 14-3-3 protein interactions such as *in vitro* kinase assays, cell migration assays, cell proliferation assays, and wound healing assays. I may knockdown and knockout 14-3-3 isoforms using siRNA or shRNA and clustered regularly interspaced short palindromic repeats (CRISPR) and note any isoform-specific subcellular localization changes. Then, I will add back the 14-3-3 WT proteins and see if my antibodies are similarly immunoreactive, specific and can show the same isoform-specific subcellular localizations. CRISPR and guide RNA (gRNA) 14-3-3 $\sigma$  plasmids will first be created since 14-3-3 $\sigma$  shows specific involvement in the centrosome and in the mitotic spindle apparatus (Figure 3.7A). I can potentially extend this to the other 14-3-3 isoforms that also showed specific subcellular localizations and colocalizations with various subcellular markers. 14-3-3 proteins, as mentioned above, are central regulators of many signaling networks and are involved in many neurological diseases. Genetic studies and genetic expression studies have shown 14-3-3 isoforms to be candidate markers in schizophrenia, bipolar disorders, and major depressive disorder (MDD), and have also shown to have neuroprotective effects in these neuropsychiatric disorders (Vawter et al., 2001; Wong et al., 2003; Wong et al., 2005; Ikeda et al., 2008; Novak et al., 2009; Pers et al., 2011; Foote and Zhou, 2012; Shimada et al., 2013; Malki et al., 2014; Foote et al., 2015; Graham et al., 2019). 14-3-3 $\epsilon$ ,  $\gamma$  and  $\zeta$  are also involved in neurogenesis, neuronal

migration and neuromorphogenesis since knockout mice showed disruption to these critical processes and showed schizophrenic behaviours (Ikeda et al., 2008; Cornell et al., 2016). Therefore, targeting 14-3-3 proteins may have therapeutic value for patients with neuropsychiatric disorders. 14-3-3 $\zeta$  showed neonatal lethality in knockout mice because an endothelial-specific miRNA was downregulated in the lungs, causing respiratory distress (Yang et al., 2017). Rac1 is said to be “undruggable” since it does not have deep hydrophobic pockets to allow for pharmacological inhibition. Therefore, targeting Rac1 is not currently possible. Knocking out Rac1 may prove detrimental to the cell because removal of Rac1 in endothelial cells resulted in embryonic lethality in midgestation (around E9.5) (Sugihara et al., 1998; Tan et al., 2008).

The findings from this thesis provide novel and comprehensive data about 14-3-3 protein subcellular localization. My data suggest that 14-3-3 isoforms have different subcellular localizations, which could underline the distinctive functions of the isoforms. My thesis shows evidence of a potential interaction between 14-3-3 proteins and Rac1. These data will certainly help uncover novel molecular mechanisms of these proteins and how their signaling pathways contribute to cancer development and neurological disease.

## References

- Aaron, J. S., Taylor, A. B., & Chew, T. L. (2018). Image co-localization - co-occurrence versus correlation. *Journal of Cell Science*, *131*(3), 211847. doi: 10.1242/jcs.211847
- Abdrabou, A., & Wang, Z. (2018). Post-Translational Modification and Subcellular Distribution of Rac1: An Update. *Cells*, *7*(12), 263. doi: 10.3390/cells7120263
- Aghazadeh, Y., & Papadopoulos, V. (2016). The role of the 14-3-3 protein family in health, disease, and drug development. *Drug Discovery Today*, *21*(2), 278–287. doi: 10.1016/j.drudis.2015.09.012
- Aitken, A. (2002). Functional specificity in 14-3-3 isoform interactions through dimer formation and phosphorylation. Chromosome location of mammalian isoforms and variants. *Plant Molecular Biology*, *50*(6), 993-1010. doi: 10.1023/A:1021261931561
- Aitken, A. (2006). 14-3-3 proteins: a historic overview. *Seminars in Cancer Biology*, *16*(3), 162-172. doi: 10.1016/j.semcancer.2006.03.005
- Aitken, A., Ellis, C. A., Harris, A., Sellers, L. A., & Toker, A. (1990). Kinase and neurotransmitters. *Nature*, *344*(6267), 594. doi: 10.1038/344594a0
- Aznar, S., & Lacal, J. C. (2001). Rho signals to cell growth and apoptosis. *Cancer Letters*, *165*(1), 1–10. doi: 10.1016/S0304-3835(01)00412-8
- Bamburg, J. R. (1999). Proteins of the ADF/cofilin family: essential regulators of actin dynamics. *Annual Review of Cell and Developmental Biology*, *15*, 185-230. doi: 10.1146/annurev.cellbio.15.1.185
- Baxter, H. C., Liu, W. G., Forster, J. L., Aitken, A., & Fraser, J. R. (2002). Immunolocalisation of 14-3-3 isoforms in normal and scrapie infected murine brain. *Neuroscience*, *109*(1), 5-14. doi: 10.1016/S0306-4522(01)00492-4

- Benitah, S. A., Valeron, P. F., Van Aelst, L., Marshall, C. J., & Lacal, J. C. (2004). Rho GTPases in human cancer: An unresolved link to upstream and downstream transcriptional regulation. *Biochimica et Biophysica Acta*, 1705(2), 121–132. doi: 10.1016/j.bbcan.2004.10.002
- Berg, D., Holzmann, C., & Riess, O. (2003). 14-3-3 proteins in the nervous system. *Nature Reviews. Neuroscience*, 4(9), 752-762. doi: 10.1038/nrn1197
- Bialkowska, K., Zaffran, Y., Meyer, S. C., & Fox, J. E. (2003). 14-3-3 zeta mediates integrin-induced activation of Cdc42 and Rac. Platelet glycoprotein Ib-IX regulates integrin-induced signaling by sequestering 14-3-3 zeta. *The Journal of Biological Chemistry*, 278(35), 33342–33350. doi: 10.1074/jbc.M301217200
- Birkenfeld, J., Kartmann, B., Anliker, B., Ono, K., Schlötcke, B., Betz, H., & Roth, D. (2003). Characterization of zetin 1/rBSPRY, a novel binding partner of 14-3-3 proteins. *Biochemical and Biophysical Research Communications*, 302(3), 526-533. doi: 10.1016/S0006-291X(03)00182-7
- Bolis, A., Corbetta, S., Cioce, A., & de Curtis, I. (2003). Differential distribution of Rac1 and Rac3 GTPases in the developing mouse brain: Implications for a role of Rac3 in Purkinje cell differentiation. *European Journal of Neuroscience*, 18(9), 2417–2424. doi: 10.1046/j.1460-9568.2003.02938.x
- Bosco, E. E., Mulloy, J. C., & Zheng, Y. (2009). Rac1 GTPase: A “Rac” of all trades. *Cellular and Molecular Life Sciences : CMLS*, 66(3), 370–374. doi: 10.1007/s00018-008-8552-x
- Boston, P. F., Jackson, P., & Thompson, R. J. (1982a). Human 14-3-3 protein:

- radioimmunoassay, tissue distribution, and cerebrospinal fluid levels in patients with neurological disorders. *Journal of Neurochemistry*, 38(5), 1475-1482. doi: 10.1111/j.1471-4159.1982.tb07928.x
- Boston, P. F., Jackson, P., Kynoch, P. A., & Thompson, R. J. (1982b). Purification, Properties, and Immunohistochemical Localisation of Human Brain 14-3-3 Protein. *Journal of Neurochemistry*, 38(5), 1466-1474. doi: 10.1111/j.1471-4159.1982.tb07927.x
- Boureux, A., Vignal, E., Faure, S., & Fort, P. (2007). Evolution of the Rho family of Ras-like GTPases in eukaryotes. *Molecular Biology and Evolution*, 24(1), 203–216. doi: 10.1093/molbev/msl145
- Brandwein, D., & Wang, Z. (2017). Interaction between Rho GTPases and 14-3-3 proteins. *International Journal of Molecular Sciences*, 18(10), 2148. doi: 10.3390/ijms18102148
- Bridges, D., & Moorhead, G. B. (2004). 14-3-3 proteins: a number of functions for a numbered protein. *Science's STKE : Signal Transduction Knowledge Environment*, 2004(242), re10. doi: 10.1126/stke.2422004re10
- Brunet, A., Kanai, F., Stehn, J., Xu, J., Sarbassova, D., Frangioni, J. V.,... Yaffe, M. B. (2002). 14-3-3 transits to the nucleus and participates in dynamic nucleocytoplasmic transport. *The Journal of Cell Biology*, 157(3), 533. doi: 10.1083/jcb.200112059
- BurrIDGE, K., & Wennerberg, K. (2004). Rho and Rac take center stage. *Cell*, 116(2), 167–179. doi: 10.1016/S0092-8674(04)00003-0
- Cao, W. D., Zhang, X., Zhang, J. N., Yang, Z. J., Zhen, H. N., Cheng, G.,... Gao, D. (2006). Immunocytochemical detection of 14-3-3 in primary nervous system tumors. *Journal of Neuro-Oncology*, 77(2), 125–130. doi: 10.1007/s11060-005-9027-7

- Chahdi, A., & Sorokin, A. (2008). Protein kinase A-dependent phosphorylation modulates  $\beta$ 1Pix guanine nucleotide exchange factor activity through 14-3-3 $\beta$  binding. *Molecular and Cellular Biology*, 28(5), 1679–1687. doi: 10.1128/MCB.00898-07
- Chang, F., Lemmon, C., Lietha, D., Eck, M., & Romer, L. (2011). Tyrosine phosphorylation of Rac1: A role in regulation of cell spreading. *PLoS One*, 6(12), e28587. doi: 10.1371/journal.pone.0028587
- Chaudhri, M., Scarabel, M., & Aitken, A. (2003). Mammalian and yeast 14-3-3 isoforms form distinct patterns of dimers in vivo. *Biochemical and Biophysical Research Communications*, 300(3), 679-685. doi: 10.1016/S0006-291X(02)02902-9
- Chen, H. H., Fernandez-Funez, P., Acevedo, S. F., Lam, Y. C., Kaytor, M. D., Fernandez, M. H... Zoghbi, H. Y. (2003). Interaction of Akt-phosphorylated ataxin-1 with 14-3-3 mediates neurodegeneration in spinocerebellar ataxia type 1. *Cell*, 113(4), 457-468. doi: 10.1016/S0092-8674(03)00349-0
- Cheng, C. Y., Tseng, H. C., & Yang, C. M. (2012). Bradykinin-mediated cell proliferation depends on transactivation of EGF receptor in corneal fibroblasts. *Journal of Cellular Physiology*, 227(4), 1367–1381. doi: 10.1002/jcp.22849
- Cheng, L., Pan, C. X., Zhang, J. T., Zhang, S., Kinch, M. S., Li, L.,... Eble, J. N. (2004). Loss of 14-3-3sigma in prostate cancer and its precursors. *Clinical Cancer Research : An Official Journal of the American Association for Cancer Research*, 10(9), 3064–3068. doi: 10.1158/1078-0432.CCR-03-0652
- Chun, J., Kwon, T., Lee, E. J., Kim, C. H., Han, Y. S., Hong, S. K.,... Kang, S. S. (2004). 14-3-3 Protein mediates phosphorylation of microtubule-associated protein GSK3 b by serum- and glucocorticoid-induced protein kinase 1. *Molecules and Cells*, 18(3), 360-368.

Retrieved from

<http://www.molcells.org/journal/view.html?year=2004&volume=18&number=3&spage=360>

- Coblitz, B., Wu, M., Shikano, S., & Li, M. (2006). C-terminal binding: An expanded repertoire and function of 14-3-3 proteins. *FEBS Letters*, *580*(6), 1531–1535. doi: 10.1016/j.febslet.2006.02.014
- Corbetta, S., Gualdoni, S., Albertinazzi, C., Paris, S., Croci, L., Consalez, G. G., & de Curtis, I. (2005). Generation and characterization of Rac3 knockout mice. *Molecular and Cellular Biology*, *25*(13), 5763–5776. doi: 10.1128/MCB.25.13.5763-5776.2005
- Cornell, B., Wachi, T., Zhukarev, K., & Toyo-Oka, K. (2016). Regulation of neuronal morphogenesis by 14-3-3epsilon (Ywhae) via the microtubule binding protein, doublecortin. *Human Molecular Genetics*, *25*(20), 4405-4418. doi: 10.1093/hmg/ddw270
- Corradi, V., Mancini, M., Manetti, F., Petta, S., Santucci, M. A., & Botta, M. (2010). Identification of the first non-peptidic small molecule inhibitor of the c-Abl/14-3-3 protein-protein interactions able to drive sensitive and Imatinib-resistant leukemia cells to apoptosis. *Bioorganic & Medicinal Chemistry Letters*, *20*(20), 6133-6137. doi: 10.1016/j.bmcl.2010.08.019
- Corradi, V., Mancini, M., Santucci, M. A., Carlomagno, T., Sanfelice, D., Mori, M.,... Botta, M. (2011). Computational techniques are valuable tools for the discovery of protein-protein interaction inhibitors: the 14-3-3 $\sigma$  case. *Bioorganic & Medicinal Chemistry Letters*, *21*(22), 6867-6871. doi: 10.1016/j.bmcl.2011.09.011
- Costes, S. V., Daelemans, D., Cho, E. H., Dobbin, Z., Pavlakis, G., & Lockett, S. (2004).

- Automatic and Quantitative Measurement of Protein-Protein Colocalization in Live Cells. *Biophysical Journal*, 86(6), 3993-4003. doi: 10.1529/biophysj.103.038422
- Deakin, N. O., Bass, M. D., Warwood, S., Schoelermann, J., Mostafavi-Pour, Z., Knight, D.,... Humphries, M. J. (2009). An integrin- $\alpha$ 4- $\beta$ 1-3- $\zeta$ -paxillin ternary complex mediates localised Cdc42 activity and accelerates cell migration. *Journal of Cell Science*, 122(Pt 10), 1654-1664. doi: 10.1242/jcs.049130
- Didsbury, J., Weber, R. F., Bokoch, G. M., Evans, T., & Snyderman, R. (1989). Rac, a novel ras-related family of proteins that are botulinum toxin substrates. *The Journal of Biological Chemistry*, 264(28), 16378-16382. doi: 10.1002/(SICI)1097-0320(19970801)28:4<289::AID-CYTO3>3.0.CO;2-7
- Donovan, N., Becker, E. B., Konishi, Y., & Bonni, A. (2002). JNK phosphorylation and activation of BAD couples the stress-activated signaling pathway to the cell machinery. *The Journal of Biological Chemistry*, 277(43), 40944-40949. doi: 10.1074/jbc.M206113200
- Dunn, K. W., Kamocka, M. M., & McDonald, J. H. (2011). A practical guide to evaluating colocalization in biological microscopy. *American Journal of Physiology. Cell Physiology*, 300(4), 723-742. doi: 10.1151/ajpcell.00462.2010
- Dvorsky, R., & Ahmadian, M. R. (2004). Always look on the bright site of Rho: structural implications for a conserved intermolecular interface. *EMBO Reports*, 5(12), 1130-1136. doi: 10.1038/sj.embor.7400293
- Ellerbroek, S. M., Wennerberg, K., & Burridge, K. (2003). Serine phosphorylation negatively regulates RhoA in vivo. *The Journal of Biological Chemistry*, 278(21), 19023-19031. doi: 10.1074/jbc.M213066200

- Fantl, W. J., Muslin, A. J., Kikuchi, A., Martin, J. A., MacNicol, A. M., Gross, R. W..., Williams, L. T. (1994). Activation of Raf-1 by 14-3-3 proteins. *Nature*, 371(6498), 612-614. doi: 10.1038/371612a0
- Foote, M., & Zhou, Y. (2012). 14-3-3 proteins in neurological disorders. *International Journal of Biochemistry and Molecular Biology*, 3(2), 152-164.
- Foote, M., Qiao, H., Graham, K., Wu, Y., & Zhou, Y. (2015). Inhibition of 14-3-3 Proteins Leads to Schizophrenia-Related Behavioral Phenotypes and Synaptic Defects in Mice. *Biological Psychiatry*, 78(6), 386-395. doi: 10.1016/j.biopsych.2015.02.015
- Forget, M., Desrosiers, R., Gingras, D., & Beliveau, R. (2002). Phosphorylation states of Cdc42 and RhoA regulate their interactions with Rho GDP dissociation inhibitor and their extraction from biological membranes. *Biochemical Journal*, 361(Pt 2), 243–254. doi: 10.1042/bj3610243
- Franger, G. R., Widmann, C., Porter, A. C., Sather, S., Johnson, G. L., & Vaillancourt, R. R. (1998). 14-3-3 proteins interact with specific MEK kinases. *The Journal of Biological Chemistry*, 273(6), 3476-3483. doi: 10.1074/jbc.273.6.3476
- Freed, E., Symons, M., Macdonald, S. G., McCormick, F., & Ruggieri, R. (1994). Binding of 14-3-3 proteins to the protein kinase Raf and effects on its activation. *Science*, 265(5179), 1713-1716. doi: 10.1126/science.8085158
- Freeman, A. K., & Morrison, D. K. (2011). 14-3-3 Proteins: Diverse functions in cell proliferation and cancer progression. *Seminars in Cell & Developmental Biology*, 22(7), 681–687. doi: 10.1016/j.semcdb.2011.08.009
- Fu, H., Xia, K., Pallas, D. C., Cui, C., Conroy, K., Narsimhan, R. P.,... Roberts, T. M. (1994).

- Interaction of the protein kinase Raf-1 with 14-3-3 proteins. *Science*, 266(5182), 126-129. doi: 10.1126/science.7939632
- Gao, K., Tang, W., Li, Y., Zhang, P., Wang, D., Yu, L.,... Wu, D. (2015). Front-signal-dependent accumulation of the RHOA inhibitor FAM65B at leading edges polarizes neutrophils. *Journal of Cell Science*, 128(5), 992–1000. doi: 10.1242/jcs.161497
- Gardino, A. K., & Yaffe, M. B. (2011). 14-3-3 proteins as signaling integration points for cell cycle control and apoptosis. *Seminars in Cell & Developmental Biology*, 22(7), 688–695. doi: 10.1016/j.semcdb.2011.09.008
- Gerber, K. J., Squires, K. E., & Hepler, J. R. (2018). 14-3-3 $\gamma$  binds regulator of G protein signaling 14 (RGS14) at distinct sites to inhibit the RGS14:G $\alpha_i$ -AlF $_4^-$  signaling complex and RGS14 nuclear localization. *The Journal of Biological Chemistry*, 293(38), 14616-14631. doi: 10.1074/jbc.RA118.002816
- Goc, A., Abdalla, M., Al-Azayzih, A., & Somanath, P. R. (2012). Rac1 activation driven by 14-3-3zeta dimerization promotes prostate cancer cell-matrix interactions, motility and transendothelial migration. *PLoS One*, 7(7), e40594. doi: 10.1371/journal.pone.0040594
- Gohla, A., & Bokoch, G. M. (2002). 14-3-3 regulates actin dynamics by stabilizing phosphorylated cofilin. *Current Biology : CB*, 12(19), 1704–1710. doi: 10.1016/S0960-9822(02)01184-3
- Graham, K., Zhang, J., Qiao, H., Wu, Y., & Zhou, Y. (2019). Region-specific inhibition of 14-3-3 proteins induces psychomotor behaviors in mice. *NPJ Schizophrenia*, 5(1), 1. doi: 10.1038/s41537-018-0069-1
- Green, A. J., Thompson, E. J., Stewart, G. E., Zeidler, M., McKenzie, J. M., MacLeod, M. A., &

- Knight, R. S. (2001). Use of 14-3-3 and other brain-specific proteins in CSF in the diagnosis of variant Creutzfeldt-Jakob disease. *Journal of Neurology, Neurosurgery and Psychiatry*, 70(6), 744-748. doi: 10.1136/jnnp.70.6.744
- Gronholm, M., Jahan, F., Marchesan, S., Karvonen, U., Aatonen, M., Narumanchi, S., & Gahmberg, C. G. (2011). TCR-induced activation of LFA-1 involves signaling through Tiam1. *Journal of Immunology : Official Journal of the American Association of Immunologists*, 187(7), 3613–3619. doi: 10.4049/jimmunol.1100704
- Gu, Y. M., Jin, Y. H., Choi, J. K., Baek, K. H., Yeo, C. Y., & Lee, K. Y. (2006). Protein kinase A phosphorylates and regulates dimerization of 14-3-3 epsilon. *FEBS Letters*, 580(1), 305-310. doi: 10.1016/j.febslet.2005.12.024
- Haataja, L., Groffen, J., & Heisterkamp, N. (1997). Characterization of RAC3, a novel member of the Rho family. *The Journal of Biological Chemistry*, 272(33), 20384–20388. doi: 10.1074/jbc.272.33.20384
- He, H., Luo, Y., Qiao, Y., Zhang, Z., Yin, D., Yao, J... He, M. (2018). Curcumin attenuates doxorubicin-induced cardiotoxicity via suppressing oxidative stress and preventing mitochondrial dysfunction mediated by 14-3-3gamma. *Food & Function*, 9(8), 4404-4418. doi: 10.1039/c8fo00466h
- Hermeking, H., Lengauer, C., Polyak, K., He, T. C., Zhang, L., Thiagalingam, S,... Vogelstein, B. (1997). 14-3-3sigma is a p53-regulated inhibitor of G2/M progression. *Molecular Cell*, 1(1), 3–11. doi: 10.1016/S1097-2765(00)80002-7
- Honda, R., Ohba, Y., & Yasuda, H. (1997). 14-3-3 zeta protein binds to the carboxyl half of mouse wee1 kinase. *Biochemical and Biophysical Research Communications*, 230(2), 262-265. doi: 10.1006/bbrc.1996.5933

- Hong, H. Y., Jeon, W. K., Bae, E. J., Kim, S. T., Lee, H. J.,... Kim, B. C. (2010). 14-3-3 sigma and 14-3-3 zeta plays an opposite role in cell growth inhibition mediated by transforming growth factor- $\beta$  1. *Molecular and Cells*, 29(3), 305–309. doi: 10.1007/s10059-010-0037-8
- Huang, B., You, J., Qiao, Y., Wu, Z., Liu, D., Yin, D.,... He, M. (2018). Tetramethylpyrazine attenuates lipopolysaccharide-induced cardiomyocyte injury via improving mitochondrial function mediated by 14-3-3gamma. *European Journal of Pharmacology*, 832, 67-74. doi: 10.1016/j.ejphar.2018.05.019
- Huang, J., Liu, Z., Xu, P., Zhang, Z., Yin, D., Liu, J.,... He, M. (2018). Capsaicin prevents mitochondrial damage, protects cardiomyocytes subjected to anoxia/reoxygenation injury mediated by 14-3-3eta/Bcl-2. *European Journal of Pharmacology*, 819, 43-50. doi: 10.1016/j.ejphar.2017.11.028
- Ichimura, T., Isobe, T., Okuyama, T., Takahashi, N., Araki, K., Kuwano, R., & Takahashi, Y. (1988). Molecular cloning of cDNA coding for brain-specific 14-3-3 protein, a protein kinase-dependent activator of tyrosine and tryptophan hydroxylases. *Proceedings of the National Academy of Sciences of the United States of America*, 85(19), 7084–7088. doi: 10.1073/pnas.85.19.7084
- Ikeda, M., Hikita, T., Taya, S., Uraguchi-Asaki, J., Toyono-Oka, K., Wynshaw-Boris, A.,... Iwata, N. (2008). Identification of YWHAE, a gene encoding 14-3-3epsilon, as a possible susceptibility gene for schizophrenia. *Human Molecular Genetics*, 17(20), 3212–3222. doi: 10.1093/hmg/ddn217
- Inamdar, S. M., Lankford, C. K., Laird, J. G., Novbatova, G., Tatro, N., Whitmore, S. S.,...

- Baker, S. A. (2018). Analysis of 14-3-3 isoforms expressed in photoreceptors. *Experimental Eye Research*, 170, 108-116. doi: 10.1016/j.exer.2018.02.022
- Iralde-Lorente, L., Cau, Y., Clementi, L., Franci, L., Tassone, G., Valensin, D.,... Botta, M. (2019). Chemically stable inhibitors of 14-3-3 protein-protein interactions derived from BV02. *Journal of Enzyme Inhibition and Medicinal Chemistry*, 34(1), 657-664. doi: 10.1080/14756366.2019.1574779
- Ito, T., Nakata, M., Fukazawa, J., Ishida, S., & Takahashi, Y. (2014). Phosphorylation-independent binding of 14-3-3 to NtCDPK1 by a new mode. *Plant Signaling and Behavior*, 9(12), e977721. doi: 10.4161/15592324.2014.977721
- Jansen, S., Melkova, K., Trosanova, Z., Hanakova, K., Zachrdla, M., Novacek, ... Zidek, L. (2017). Quantitative mapping of microtubule-associated protein 2c (MAP2c) phosphorylation and regulatory protein 14-3-3zeta-binding sites reveals key differences between MAP2c and its homolog Tau. *The Journal of Biological Chemistry*, 292(16), 6715-6727. doi: 10.1074/jbc.M116.771097
- Jerome, M., & Paudel, H. K. (2014). 14-3-3zeta regulates nuclear trafficking of protein phosphatase 1alpha (PP1alpha) in HEK-293 cells. *Archives of Biochemistry and Biophysics*, 558, 28-35. doi: 10.1016/j.abb.2014.06.012
- Jia, Y., Yu, X., Zhang, B., Yuan, Y., Xu, Q., Shen, Y., & Shen, Y. (2004) An association study between polymorphisms in three genes of 14-3-3 (tyrosine 3-monooxygenase/tryptophan 5-monooxygenase activation protein) family and paranoid schizophrenia in northern Chinese population. *European Psychiatry : The Journal of the Association of European Psychiatrists*, 19(6), 377-379. doi: 10.1016/j.eurpsy.2004.07.006
- Jin, J., Smith, F. D., Stark, C., Wells, C. D., Fawcett, J. P., Kulkarni, S.,... Pawson, T. (2004).

- Proteomic, functional, and domain-based analysis of in vivo 14-3-3 binding proteins involved in cytoskeletal regulation and cellular organization. *Current Biology : CB*, *14*(16), 1436–1450. doi: 10.1016/j.cub.2004.07.051
- Jones, D. H., Ley, S., & Aitken, A. (1995). Isoforms of 14-3-3 protein can form homo- and heterodimers in vivo and in vitro: Implications for function as adapter proteins. *FEBS Letters*, *368*(1), 55–58. doi: 10.1016/0014-5793(95)00598-4
- Joo, Y., Schumacher, B., Landrieu, I., Bartel, M., Smet-Nocca, C., Jang, A.,... Suh, Y. H. (2015). Involvement of 14-3-3 in tubulin instability and impaired axon development is mediated by Tau. *FASEB Journal : Official Publication of the Federation of American Societies for Experimental Biology*, *29*(10), 4133-4144. doi: 10.1096/fj.14-265009
- Kakinuma, N., Roy, B. C., Zhu, Y., Wang, Y., & Kiyama, R. (2008). Kank regulates RhoA-dependent formation of actin stress fibers and cell migration via 14-3-3 in PI3K-Akt signaling. *Journal of Cell Biology*, *181*(3), 537-549. doi: 10.1083/jcb.200707022
- Kawashima, T., Bao, Y. C., Nomura, Y., Moon, Y., Tonozuka, Y., Minoshima, Y.,... Kitamura, T. (2006). Rac1 and a GTPase-activating protein, MgcRacGAP, are required for nuclear translocation of STAT transcription factors. *Journal of Cell Biology*, *175*(6), 937–946. doi: 10.1083/jcb.200604073
- Kligys, K., Yao, J., Yu, D., & Jones, J. C. (2009). 14-3-3zeta/tau heterodimers regulate Slingshot activity in migrating keratinocytes. *Biochemical and Biophysical Research Communications*, *383*(4), 450-454. doi: 10.1016/j.bbrc.2009.04.031
- Kobayashi, H., Ogura, Y., Sawada, M., Nakayama, R., Takano, K., Minato, Y.,... Imoto, M.

- (2011). Involvement of 14-3-3 proteins in the second epidermal growth factor-induced wave of Rac1 activation in the process of cell migration. *The Journal of Biological Chemistry*, 286(45), 39259–39268. doi: 10.1074/jbc.M111.255489
- Kraynov, V. S., Chamberlain, C., Bokoch, G. M., Schwartz, M. A., Slabaugh, S., & Hahn, K. M. (2000). Localized Rac activation dynamics visualized in living cells. *Science*, 290(5490), 333-337. doi: 10.1126/science.290.5490.333
- Krtkova, J., Xu, J., Lalle, M., Steele-Ogus, M., Alas, G. C. M., Sept, D., & Paredez, A. R. (2017). 14-3-3 Regulates Actin Filament Formation in the Deep-Branching Eukaryote *Giardia lamblia*. *mSphere*, 2(5), e00248-17. doi: 10.1128/mSphere.00248-17
- Kwon, T., Kwon, D., Chun, J., Kim, J., & Kang, S. (2000). Akt protein kinase inhibits Rac1-GTP binding through phosphorylation at serine 71 of Rac1. *The Journal of Biological Chemistry*, 275(1), 423–428. doi: 10.1074/jbc.275.1.423
- Lamba, S., Ravichandran, V., & Major, E. O. (2009). Glial cell type-specific subcellular localization of 14-3-3 zeta: an implication for JCV tropism. *Glia*, 57(9), 971-977. doi: 10.1002/glia.20821
- Lang, P., Gesbert, F., Delespine-Carmagnat, M., Stancou, R., Pouchelet, M., & Bertoglio, J. (1996). Protein kinase A phosphorylation of RhoA mediates the morphological and functional effects of cyclic AMP in cytotoxic lymphocytes. *The EMBO Journal*, 15(3), 510–519. doi: 10.1002/j.1460-2075.1996.tb00383.x
- Lanning, C., Ruiz-Velasco, R., & Williams, C. (2003). Novel mechanism of the co-regulation of nuclear transport of SmgGDS and Rac1. *The Journal of Biological Chemistry*, 278(14), 12495–12506. doi: 10.1074/jbc.M211286200
- Layfield, R., Fergusson, J., Aitken, A., Lowe, J., Landon, M., & Mayer, J. (1996).

- Neurofibrillary tangles of Alzheimer's disease brains contain 14-3-3 proteins.  
*Neuroscience Letters*, 209(1), 57-60. doi: 10.1016/0304-3940(96)12598-2
- Lee, C. H., Marino-Enriquez, A., Ou, W., Zhu, M., Ali, R. H., Chiang, S.,... Nucci, M. R. (2012). The clinicopathologic features of YWHAE-FAM22 endometrial stromal sarcomas: A histologically high-grade and clinically aggressive tumor. *American Journal of Surgical Pathology*, 36(5), 641–653. doi: 10.1097/PAS.0b013e31824a7b1a
- Liu, D., Bienkowska, J., Petosa, C., Collier, R. J., Fu, H., & Liddington, R. (1995). Crystal structure of the zeta isoform of the 14-3-3 protein. *Nature*, 376(6536), 191-194. doi: 10.1038/376191a0
- Liu, M., Bi, F., Zhou, X., & Zheng, Y. (2012). Rho GTPase regulation by miRNAs and covalent modifications. *Trends in Cell Biology*, 22(7), 365–373. doi: 10.1016/j.tcb.2012.04.004
- Liu, Y. C., Elly, C., Yoshida, H., Bonnefoy-Berard, N., & Altman, A. (1996). Activation-modulated association of 14-3-3 proteins with Cbl in T cells. *The Journal of Biological Chemistry*, 271(24), 14591-14595. doi: 10.1074/jbc.271.24.14591
- Liu, Z., Yang, L., Huang, J., Xu, P., Zhang, Z., Yin, D.,... He, M. (2018). Luteoloside attenuates anoxia/reoxygenation-induced cardiomyocytes injury via mitochondrial pathway mediated by 14-3-3eta protein. *Phytotherapy Research : PTR*, 32(6), 1126-1134. doi: 10.1002/ptr.6053
- Loirand, G., Guilluy, C., & Pacaud, P. (2006). Regulation of Rho proteins by phosphorylation in the cardiovascular system. *Trends in Cardiovascular Medicine*, 16(6), 199–204. doi: 10.1016/j.tcm.2006.03.010
- Lopez-Girona, A., Furnari, B., Mondesert, O., Russell, P. (1999). Nuclear localization of Cdc25

- is regulated by DNA damage and a 14-3-3 protein. *Nature*, 397(6715), 172-175. doi: 10.1038/16488
- Lu, Y., Ding, S., Zhou, R., & Wu, J. (2017). Structure of the complex of phosphorylated liver kinase B1 and 14-3-3 $\zeta$ . *Acta Crystallographica. Section F, Structural Biology Communications*, 73(Pt 4), 196-201. doi: 10.1107/S2053230X17003521
- Mackie, S., & Aitken, A. (2005). Novel brain 14-3-3 interacting proteins involved in neurodegenerative disease. *FEBS Journal*, 272(16), 4202-4210. doi: 10.1111/j.1742-4658.2005.04832.x
- Maderia, F., Tinti, M., Murugesan, G., Berrett, E., Stafford, M., Toth, R.,...Barton, G. J. (2015). 14-3-3-Pred: improved methods to predict 14-3-3-binding phosphopeptides. *Bioinformatics*, 31(14), 2276-2283. doi: 10.1093/bioinformatics/btv133
- Malki, K., Keers, R., Tosto, M. G., Lourdasamy, A., Carboni, L, Domenici, E.,... Schalkwyk, L. C. (2014). The endogenous and reactive depression subtypes revisited: integrative animal and human studies implicate multiple distinct molecular mechanisms underlying major depressive disorder. *BMC Medicine*, 12(1), 73. doi: 10.1186/1741-7015-12-73
- Mancini, M., Corradi, V., Petta, S., Barbieri, E., Manetti, F., Botta, M., & Santucci, M. A. (2011). A new nonpeptidic inhibitor of 14-3-3 induces apoptotic cell death in chronic myeloid leukemia sensitive or resistant to imatinib. *The Journal of Pharmacology and Experimental Therapeutics*, 336(3), 596-604. doi: 10.1124/jpet.110.172536
- Manders, E. M. M., Verbeek, F. J., & Aten, J. A. (1993). Measurement of co-localization of objects in dual-colour confocal images. *Journal of Microscopy*, 169(Pt 3), 375-382. doi: 10.1111/j.1365-2818.1993.tb03313.x
- Manser, E., Leung, T., Salihuddin, H., Zhao, Z. S., & Lim, L. (1994). A brain serine/threonine

- protein kinase activated by Cdc42 and Rac1. *Nature*, 367(6458), 40–46. doi:  
10.1038/367040a0
- Mao, Y. S., Zhang, B., & Spector, D. L. (2011). Biogenesis and function of nuclear bodies. *Trends in Genetics : TIG*, 27(8), 295-306. doi: 10.1016/j.tig.2011.05.006
- Masters, S. C., Subramanian, R. R., Truong, A., Yang, H., Fujii, K., Zhang, H., & Fu, H. (2002). Survival-promoting functions of 14-3-3 proteins. *Biochemical Society Transactions*, 30(4), 360–365. doi: 10.1042/
- Meiri, D., Greeve, M. A., Brunet, A., Finan, D., Wells, C. D., LaRose, J., & Rottapel, R. (2009). Modulation of Rho guanine exchange factor Lfc activity by protein kinase A-mediated phosphorylation. *Molecular and Cellular Biology*, 29(21), 5963–5973. doi:  
10.1128/MCB.01268-08
- Mettouchi, A., & Lemichez, E. (2012). Ubiquitylation of active Rac1 by the E3 ubiquitin-ligase HACE1. *Small GTPases*, 3(2), 102–106. doi: 10.4161/sgtp.19221
- Mhaweck, P. (2005). 14-3-3 proteins—An update. *Cell Research*, 15(4), 228–236. doi:  
10.1038/sj.cr.7290291
- Miki, H., Suetsugu, S., Takenawa, T. (1998). WAVE, a novel WASP-family protein involved in actin reorganization induced by Rac. *The EMBO Journal*, 17(23), 6932-6941.  
doi: 10.1093/emboj/17.23.6932
- Milburn, M. P., & Jeffrey, K. R. (1990). Dynamics of the phosphate group in phospholipid bilayers. A <sup>31</sup>P-1H transient Overhauser effect study. *Biophysical Journal*, 58(1), 187-194. doi: 10.1016/S0006-3495(90)82364-X
- Mils, V., Baldin, V., Goubin, F., Pinta, I., Papin, C., Waye, M., ... Ducommun, B.

- (2000). Specific interaction between 14-3-3 isoforms and the human CDC25B phosphatase. *Oncogene*, *19*(10), 1257-1265. doi: 10.1038/sj.onc.1203419
- Moon, S., & Zheng, Y. (2003). Rho GTPase-activating proteins in cell regulation. *Trends in Cell Biology*, *13*(1), 13–22. doi: 10.1016/S0962-8924(02)00004-1
- Moore, B. W., & Perez, V. J. (1967). Physiological and Biochemical Aspects of Nervous Integration. In F. D. Carlson (Ed.), (pp. 343–359). Prentice-Hall: New Jersey.
- Moores, S. L., Selfors, L. M., Fredericks, J., Breit, T., Fujikawa, K., Alt, F. W.,... Swat, W. (2000). Vav family proteins couple to diverse cell surface receptors. *Molecular and Cellular Biology*, *20*(17), 6364–6373. doi: 10.1128/MCB.20.17.6364-6373.2000
- Moreira, J. M., Gromov, P., & Celis, J. E. (2004). Expression of the tumor suppressor protein 14-3-3 sigma is down-regulated in invasive transitional cell carcinomas of the urinary bladder undergoing epithelial-to-mesenchymal transition. *Molecular and Cellular Proteomics : MCP*, *3*, 410–419. doi: 10.1074/mcp.M300134-MCP200
- Mori, M., Vignaroli, G., Cau, Y., Dinic, J., Hill, R., Rossi, M.,... Botta, M. (2014). Discovery of 14-3-3 protein-protein interaction inhibitors that sensitize multidrug-resistant cancer cells to doxorubicin and the Akt inhibitor GSK690693. *ChemMedChem*, *9*(5), 973-983. doi: 10.1002/cmdc.201400044
- Mukhopadhyay, A., Sehgal, L., Bose, A., Gulvady, A., Senapati, P., Thorat, R.,... Dalal, S. N. (2016). 14-3-3gamma Prevents Centrosome Amplification and Neoplastic Progression. *Scientific Reports*, *6*, 26580. doi: 10.1038/srep26580
- Nakanishi, K., Hashizume, S., Kato, M., Honjoh, T., Setoguchi, Y., & Yasumoto, K. (1997). Elevated expression levels of the 14-3-3 family of proteins in lung cancer tissues. *Human Antibodies*, *8*(4), 189–194. doi: 10.3233/HAB-1997-8404

- Navarro-Lerida, I., Sanchez-Perales, S., Calvo, M., Rentero, C., Zheng, Y., Enrich, C., & Del Pozo, M. A. (2012). A palmitoylation switch mechanism regulates Rac1 function and membrane organization. *The EMBO Journal*, *31*(3), 534–551. doi: 10.1038/emboj.2011.446
- Neal, C. L., & Yu, D. (2010). 14-3-3zeta as a prognostic marker and therapeutic target for cancer. *Expert Opinion on Therapeutic Targets*, *14*(12), 1343–1354. doi: 10.1517/14728222.2010.531011
- Nobes, C. D., & Hall, A. (1995). Rho, Rac and Cdc42 GTPases: regulators of actin structures, cell adhesion and motility. *Biochemical Society Transactions*, *23*(3), 456–459. doi: 10.1042/bst0230456
- Nobes, C. D., & Hall, A. (1999). Rho GTPases control polarity, protrusion, and adhesion during cell movement. *Journal of Cell Biology*, *144*(6), 1235–1244. doi: 10.1083/jcb.144.6.1235
- Novak, G., Boukhadra, J., Shaikh, S. A., Kennedy, J. L., & Le Foll, B. (2009). Association of a polymorphism in the NRXN3 gene with the degree of smoking in schizophrenia: a preliminary study. *The World Journal of Biological Psychiatry : The Official Journal of the World Federation of Societies of Biological Psychiatry*, *10*(4 Pt 3), 929–935. doi: 10.1080/15622970903079499
- O'Toole, T. E., Bialkowska, K., Li, X., & Fox, J. E. (2011). Tiam1 is recruited to  $\beta$ 1-integrin complexes by 14-3-3zeta where it mediates integrin-induced Rac1 activation and motility. *Journal of Cellular Physiology*, *226*(11), 2965–2978. doi: 10.1002/jcp.22644
- Obsilova, V., Kopecka, M., Kosek, D., Kacirova, M., Kylarova, S., Rezabkova, L., & Obsil, T. (2014). Mechanisms of the 14-3-3 protein function: Regulation of protein function through conformational modulation. *Physiological Research*, *63*(Suppl. 1), S155–

- S164. Retrieved from  
[http://www.biomed.cas.cz/physiolres/pdf/63%20Suppl%201/63\\_S155.pdf](http://www.biomed.cas.cz/physiolres/pdf/63%20Suppl%201/63_S155.pdf)
- Ostrerova, N., Petrucelli, L., Farrer, M., Mehta, N., Choi, P., Hardy, J.,... Wolozin, B. (1999). Alpha-synuclein shares physical and functional homology with 14-3-3 proteins. *The Journal of Neuroscience : The Official Journal of the Society for Neuroscience*, 19(14), 5782-5791. doi: 10.1523/JNEUROSCI.19-14-05782.1999
- Ottmann, C., Yasmin, L., Weyand, M., Veessenmeyer, J. L., Diaz, M. H., Palmer, R. H.,... Hallberg, B. (2007). Phosphorylation-independent interaction between 14-3-3 and exoenzyme S: from structure to pathogenesis. *The EMBO Journal*, 26(3), 902-913. doi: 10.1038/sj.emboj.7601530
- Park, G. Y., Han, J. Y., Han, Y. K., Kim, S. D., Kim, J. S., Jo, W. S.,... Lee, C. G. (2014). 14-3-3 eta depletion sensitizes glioblastoma cells to irradiation due to enhanced mitotic cell death. *Cancer Gene Therapy*, 21(4), 158-163. doi: 10.1038/cgt.2014.11
- Patel, A., Cummings, N., Batchelor, M., Hill, P. J., Dubois, T., Mellits, K. H.,... Connerton, I. (2006). Host protein interactions with enteropathogenic Escherichia coli (EPEC): 14-3-3tau binds Tir and has a role in EPEC-induced actin polymerization. *Cellular Microbiology*, 8(1), 55-71. doi: 10.1111/j.1462-5822.2005.00600.x
- Paul, A. L., Sehnke, P. C. & Ferl, R. J. (2005). Isoform-specific subcellular localization among 14-3-3 proteins in Arabidopsis seems to be driven by client interactions. *Molecular Biology of the Cell*, 16(4), 1735-1743. doi: 10.1091/mbc.E04-09-0839
- Payapilly, A., & Malliri, A. (2018). Compartmentalisation of RAC1 signaling. *Current Opinion in Cell Biology*, 54, 50-56. doi: 10.1016/j.ceb.2018.04.009
- Pennington, C., Chohan, G., Mackenzie, J., Andrews, M., Will, R., Knight, R., & Green, A.

- (2009). The role of cerebrospinal fluid proteins as early diagnostic markers for sporadic Creutzfeldt-Jakob disease. *Neuroscience Letters*, 455(1), 56-59. doi: 10.1016/j.neulet.2009.02.067
- Perego, L., & Berruti, G. (1997). Molecular cloning and tissue-specific expression of the mouse homologue of the rat brain 14-3-3 theta protein: characterization of its cellular and developmental pattern of expression in the male germ line. *Molecular Reproduction and Development*, 47(4), 370-379. doi: 10.1002/(SICI)1098-2795(199708)47:4<370::AID-MRD3>3.0.CO;2-H
- Pers, T. H., Hansen, N. T., Lage, K., Koefoed, P., Sworzynski, P., Miller, M. L.,... Brunak, S. (2011). Meta-analysis of heterogeneous data sources for genome-scale identification of risk genes in complex phenotypes. *Genetic Epidemiology*, 35(5), 318-332. doi: 10.1002/gepi.20580
- Pietromonaco, S. F., Seluja, G. A., Aitken, A., & Elias, L. (1996). Association of 14-3-3 proteins with centrosomes. *Blood Cells, Molecules & Diseases*, 22(3), 225-237. doi: 10.1006/bcmd.1996.0103
- Pollard, T. D., & Borisy, G. G. (2003). Cellular motility driven by assembly and disassembly of actin filaments. *Cell*, 113(4), 549. doi: 10.1016/S0092-8674(03)00120-X
- Qi, W., & Martinez, J. D. (2003). Reduction of 14-3-3 proteins correlates with increased sensitivity to killing of human lung cancer cells by ionizing radiation. *Radiation Research*, 160(2), 217-223. doi: 10.1667/RR3038
- Qureshi, H. Y., Han, D., MacDonald, R., & Paudel, H. K. (2013). Overexpression of 14-3-3z

- promotes tau phosphorylation at Ser262 and accelerates proteosomal degradation of synaptophysin in rat primary hippocampal neurons. *PLoS One*, 8(12), e84615. doi: 10.1371/journal.pone.0084615
- Radhakrishnan, V. M., & Martinez, J. D. (2010). 14-3-3gamma induces oncogenic transformation by stimulating MAP kinase and PI3K signaling. *PLoS One*, 5(7), e11433. doi: 10.1371/journal.pone.0011433
- Ravi, D., Chen, Y., Karia, B., Brown, A., Gu, T. T., Li, J., & Bishop, A. J. (2011). 14-3-3 sigma expression effects G2/M response to oxygen and correlates with ovarian cancer metastasis. *PLoS One*, 6(1), e15864. doi: 10.1371/journal.pone.0015864
- Reuther, G. W., Fu, H., Cripe, L. D., Collier, R. J., & Pendergast, A. M. (1994). Association of the protein kinases c-Bcr and Bcr-Abl with proteins of the 14-3-3 family. *Science*, 266(5182), 129-133. doi: 10.1126/science.7939633
- Ridley, A. J. (2001a). Rho GTPases and cell migration. *Journal of Cell Science*, 114(Pt 15), 2713-2722.
- Ridley, A. J. (2001b). Rho proteins: linking signaling with membrane trafficking. *Traffic*, 2(5), 303-310. doi: 10.1034/j.1600-0854.2001.002005303.x
- Ridley, A. J. (2006). Rho GTPases and actin dynamics in membrane protrusions and vesicle trafficking. *Trends in Cell Biology*, 16(10), 522-529. doi: 10.1016/j.tcb.2006.08.006
- Ridley, A. J., & Hall, A. (1992). The small GTP-binding protein rho regulates the assembly of focal adhesions and actin stress fibers in response to growth factors. *Cell*, 70(3), 389-399. doi: [https://doi.org/10.1016/0092-8674\(92\)90163-7](https://doi.org/10.1016/0092-8674(92)90163-7)
- Ridley, A. J., Paterson, H. F., Johnston, C. L., Diekmann, D., & Hall, A. (1992). The small GTP-

- binding protein rac regulates growth factor-induced membrane ruffling. *Cell*, 70(3), 401-410. [https://doi.org/10.1016/0092-8674\(92\)90164-8](https://doi.org/10.1016/0092-8674(92)90164-8)
- Riento, K., Guasch, R. M., Garg, R., Jin, B., & Ridley, A. J. (2003). RhoE binds to ROCK I and inhibits downstream signaling. *Molecular and Cellular Biology*, 23(12), 4219–4229. doi: 10.1128/MCB.23.12.4219-4229.2003
- Riou, P., Kjaer, S., Garg, R., Purkiss, A., George, R., Cain, R. J.,... Ridley, A. J. (2013). 14-3-3 proteins interact with a hybrid prenyl-phosphorylation motif to inhibit G proteins. *Cell*, 153(3), 640–653. doi: 10.1016/j.cell.2013.03.044
- Rittinger, K., Budman, J., Xu, J., Volinia, S., Cantley, L. C., Smerdon, S. J.,... Yaffe, M. B. (1999). Structural analysis of 14-3-3 phosphopeptide complexes identifies a dual role for the nuclear export signal of 14-3-3 in ligand binding. *Molecular Cell*, 4(2), 153–166. doi: 10.1016/S1097-2765(00)80363-9
- Robinson, D. N. (2010). 14-3-3, an integrator of cell mechanics and cytokinesis. *Small GTPases*, 1(3), 165-169. doi: 10.4161/sgtp.1.3.14432
- Rosenquist, M., Alsterfjord, M., Larsson, C., & Sommarin, M. (2001). Data mining the Arabidopsis genome reveals fifteen 14-3-3 genes. Expression is demonstrated for two out of five novel genes. *Plant Physiology*, 127(1), 142-149. doi: 10.1104/pp.127.1.142
- Rosenquist, M., Sehnke, P., Ferl, R. J., Sommarin, M., & Larsson, C. (2000). Evolution of the 14-3-3 protein family: does the large number of isoforms in multicellular organisms reflect functional specificity? *Journal of Molecular Evolution*, 51(5), 446-458. doi: 10.1007/s002390010107
- Samuel, F., & Hynds, D. L. (2010). RHO GTPase signaling for axon extension: Is prenylation important? *Molecular Neurobiology*, 42(2), 133–142. doi: 10.1007/s12035-010-8144-2

- Satoh, J., Onoue, H., Arima, K., & Yamamura, T. (2005). The 14-3-3 protein forms a molecular complex with heat shock protein Hsp60 and cellular prion protein. *Journal of Neuropathology and Experimental Neurology*, *64*(10), 858-868. doi: 10.1097/01.jnen.0000182979.56612.08
- Sauzeau, V., Le Jeune, H., Cario-Toumaniantz, C., Smolenski, A., Lohmann, S., Bertoglio, J.,... Loirand, G. (2000). Cyclic GMP-dependent protein kinase signaling pathway inhibits RhoA-induced Ca<sup>2+</sup> sensitization of contraction in vascular smooth muscle. *The Journal of Biological Chemistry*, *275*(28), 21722–21729. doi: 10.1074/jbc.M000753200
- Schindler, C. K., Heverin, M., & Henshall, D. C. (2006). Isoform- and subcellular fraction-specific differences in hippocampal 14-3-3 levels following experimentally evoked seizures and in human temporal lobe epilepsy. *Journal of Neurochemistry*, *99*(2), 561-569. doi: 10.1111/j.1471-4159.2006.04153.x
- Schoentaube, J., Olling, A., Tatge, H., Just, I., & Gerhard, R. (2009). Serine-71 phosphorylation of Rac1/Cdc42 diminishes the pathogenic effect of Clostridium difficile toxin A. *Cellular Microbiology*, *11*(12), 1816-1826. doi: 10.1111/j.1462-5822.2009.01373.x
- Scholz, R. P., Regner, J., Theil, A., Erlmann, P., Holeiter, G., Jahne, R.,... Olayioye, M. A. (2009). DLC1 interacts with 14-3-3 proteins to inhibit RhoGAP activity and block nucleocytoplasmic shuttling. *Journal of Cell Science*, *122*(Pt 1), 92–102. doi: 10.1242/jcs.036251
- Schwarz, J., Proff, J., Havemeier, A., Ladwein, M., Rottner, K., Barlag, B.,... Gerhard, R. (2012). Serine-71 phosphorylation of Rac1 modulates downstream signaling. *PLoS One*, *7*(9), e44358. doi: 10.1371/journal.pone.0044358
- Seimiya, H., Sawada, H., Muramatsu, Y., Shimizu, M., Ohko, K., Yamane, K., & Tsuruo, T.

- (2000). Involvement of 14-3-3 proteins in nuclear localization of telomerase. *The EMBO Journal*, 19(11), 2652-2661. doi: 10.1093/emboj/19.11.2652
- Shen, Y. H., Godlewski, J., Bronisz, A., Zhu, J., Comb, M. J., Avruch, J., & Tzivion, G. (2003). Significance of 14-3-3 Self-Dimerization for Phosphorylation-dependent Target Binding. *Molecular Biology of the Cell*, 14(11), 4721-4733. doi: 10.1091/mbc.E02-12-0821
- Shikano, S., Coblitz, B., Sun, H., & Li, M. (2005). Genetic isolation of transport signals directing cell surface expression. *Nature Cell Biology*, 7(10), 985–992. doi: 10.1038/ncb1297
- Shimada, T., Fournier, A. E., & Yamagata, K. (2013). Neuroprotective function of 14-3-3 proteins in neurodegeneration. *BioMed Research International*, 2013(5), 564534. doi: 10.1155/2013/564534
- Shirsat, N. V., Pignolo, R. J., Kreider, B. L., & Rovera, G. (1990). A member of the ras gene superfamily is expressed specifically in T, B and myeloid hemopoietic cells. *Oncogene*, 5(5), 769–772. Retrieved from <https://www.ncbi.nlm.nih.gov/pubmed/2189110>
- Simon, A. R., Vikis, H. G., Stewart, S., Fanburg, B. L., Cochran, B. H., & Guan, K. L. (2000). Regulation of STAT3 by direct binding to the Rac1 GTPase. *Science*, 290(5489), 144–147. doi: 10.1126/science.290.5489.144
- Sluchanko, N. N., & Gusev, N. B. (2010). 14-3-3 proteins and regulation of cytoskeleton. *Biochemistry Biokhimiia*, 75(13), 1528-1546. doi: 10.1134/S0006297910130031
- Sluchanko, N. N., & Gusev, N. B. (2017). Moonlighting chaperone-like activity of the universal regulatory 14-3-3 proteins. *FEBS Journal*, 284(9), 1279–1295. doi: 10.1111/febs.13986
- Small, J. V., Stradal, T., Vignal, E., & Rottner, K. (2002). The lamellipodium: where motility begins. *Trends in Cell Biology*, 12(3), 112-120. doi: 10.1016/S0962-8924(01)02237-1
- Somanath, P. R., & Byzova, T. V. (2009). 14-3-3 $\beta$ -Rac1-p21 activated kinase signaling regulates

- Akt1-mediated cytoskeletal organization, lamellipodia formation and fibronectin matrix assembly. *Journal of Cellular Physiology*, 218(2), 394–404. doi: 10.1002/jcp.21612
- Sreedhar, R., Arumugam, S., Thandavarayan, R. A., Giridharan, V. V., Karuppagounder, V., Pitchaimani, V.,... Watanabe, K. (2015). Myocardial 14-3-3eta protein protects against mitochondria mediated apoptosis. *Cellular Signalling*, 27(4), 770-776. doi: 10.1016/j.cellsig.2014.12.021
- Su, T. T., Parry, D. H., Donahoe, B., Chien, C. T., O'Farrell, P. H., & Purdy, A. (2001). Cell cycle roles for two 14-3-3 proteins during Drosophila development. *Journal of Cell Science*, 114(Pt 19), 3445-3454. Retrieved from <http://jcs.biologists.org/content/114/19/3445>
- Sugihara, K., Nakatsuji, N., Nakamura, K., Nakao, K., Hashimoto, R., Otani, H.,... Karsuki, M. (1998). Rac1 is required for the formation of three germ layers during gastrulation. *Oncogene*, 17(26), 3427-3433. doi: 10.1038/sj.onc.1202595
- Sumioka, A., Nagaishi, S., Yoshida, T., Lin, A., Miura, M., & Suzuki, T. (2005). Role of 14-3-3gamma in FE65-dependent gene transactivation mediated by the amyloid beta-protein precursor cytoplasmic fragment. *The Journal of Biological Chemistry*, 280(51), 42364-42374. doi: 10.1074/jbc.M504278200
- Symons, M., & Settleman, J. (2000). Rho family GTPases: More than simple switches. *Trends in Cell Biology*, 10(10), 415–419. doi: 10.1016/S0962-8924(00)01832-8
- Takahara, Y., Matsuda, Y., & Hara, J. (2000). Role of the  $\beta$  isoform of 14-3-3 proteins in cellular proliferation and oncogenic transformation. *Carcinogenesis*, 21(11), 2073–2077. doi: 10.1093/carcin/21.11.2073
- Tan, W., Palmby, T. R., Gavard, J., Amornphimoltham, P., Zheng, Y., & Gutkind, J. S. (2008).

- An essential role for Rac1 in endothelial cell function and vascular development. *FASEB Journal : Official Publication of the Federation of American Societies for Experimental Biology*, 22(6), 1829-1838. doi: 10.1096/fj.07-096438
- Thomas, D., Guthridge, M., Woodcock, J., & Lopez, A. (2005). 14-3-3 protein signaling in development and growth factor responses. *Current Topics in Developmental Biology*, 67, 285-303. doi: 10.1016/S0070-2153(05)67009-3
- Toker, A., Ellis, C. A., Sellers, L. A., & Aitken, A. (1990). Protein kinase C inhibitor proteins: purification from sheep brain and sequence similarity to lipocortins and 14-3-3 protein. *European Journal of Biochemistry*, 191(2), 421-429. doi: 10.1111/j.1432-1033.1990.tb19138.x
- Toker, A., Sellers, L. A., Amess, B., Patel, Y., Harris, A., & Aitken, A. (1992). Multiple isoforms of a protein kinase C inhibitor (KCIP-1/14-3-3) from sheep brain. Amino acid sequence of phosphorylated forms. *European Journal of Biochemistry*, 206(2), 453-461. doi: 10.1111/j.1432-1033.1992.tb16946.x
- Tollenaere, M. A. X., Villumsen, B. H., Blasius, M., Nielsen, J. C., Wagner, S. A., Bartek, J.,... Bekker-Jensen, S. (2015). p38- and MK2-dependent signalling promotes stress-induced centriolar satellite remodelling via 14-3-3-dependent sequestration of CEP131/AZI1. *Nature Communications*, 6, 10075. doi: 10.1038/ncomms10075
- Tong, J., Li, L., Ballermann, B., & Wang, Z. (2013). Phosphorylation of Rac1 T108 by extracellular signal-regulated kinase in response to epidermal growth factor: A novel mechanism to regulate Rac1 function. *Molecular and Cellular Biology*, 33(22), 4538-4551. doi: 10.1128/MCB.00822-13
- Tong, J., Li, L., Ballermann, B., & Wang, Z. (2016). Phosphorylation and activation of RhoA by

- ERK in response to epidermal growth factor stimulation. *PLoS One*, *11*(1), e0147103.  
doi: 10.1371/journal.pone.0147103
- Toyo-Oka, K., Muratake, T., Tanaka, T., Igarashi, S., Watanabe, H., Takeuchi, H.,... Takahashi, Y. (1999). 14-3-3 protein eta chain gene (YWHAH) polymorphism and its genetic association with schizophrenia. *American Journal of Medical Genetics*, *88*(2), 164–167.  
doi: 10.1002/(SIC)1096-8628(19990416)88:2<164::AID-AJMG13>3.3.CO;2-V
- Tu, S., Wu, W., Wang, J., & Cerione, R. (2003). Epidermal growth factor-dependent regulation of Cdc42 is mediated by the Src tyrosine kinase. *The Journal of Biological Chemistry*, *278*(49), 49293–49300. doi: 10.1074/jbc.M307021200
- Umahara, T., Uchihara, T., & Iwamoto, T. (2012). Structure-oriented review of 14-3-3 protein isoforms in geriatric neuroscience. *Geriatrics & Gerontology International*, *12*(4), 586–599. doi: 10.1111/j.1447-0594.2012.00860.x
- Van Aelst, L., & D'Souza-Schorey, C. (1997). Rho GTPases and signaling networks. *Genes & Development*, *11*(18), 2295–2322. doi: 10.1101/gad.11.18.2295
- Vawter, M. P., Barrett, T., Cheadle, C., Sokolov, B. P., Wood, W. H. 3rd, Donovan, D. M.,... Becker, K. G. (2001). Application of cDNA microarrays to examine gene expression differences in schizophrenia. *Brain Research Bulletin*, *55*(5), 641–650. doi: 10.1016/S0361-9230(01)00522-6
- Vetter, J. R., & Wittinghofer, A. (2001). The guanine nucleotide-binding switch in three dimensions. *Science*, *294*(5545), 1299-1304. doi: 10.1126/science.1062023
- Waelter, A., Boeddrich, A., Lurz, R., Scherzinger, E., Lueder, G., Lehrach, H., & Wanker, E. E.

- (2001). Accumulation of mutant huntingtin fragments in aggresome-like inclusion bodies as a result of insufficient protein degradation. *Molecular Biology of the Cell*, 12(5), 1393-1407. doi: 10.1091/mbc.12.5.1393
- Wang, B., Liu, K., Lin, H. Y., Bellam, N., Ling, S., & Lin, W. C. (2010). 14-3-3Tau regulates ubiquitin-independent proteasomal degradation of p21, a novel mechanism of p21 downregulation in breast cancer. *Molecular and Cellular Biology*, 30(6), 1508–1527. doi: 10.1128/MCB.01335-09
- Wang, B., Yang, H., Liu, Y. C., Jelinek, T., Zhang, L., Ruoslahti, E., & Fu, H. (1999). Isolation of high-affinity peptide antagonists of 14-3-3 proteins by phage display. *Biochemistry*, 38(38), 12499–12504. doi: 10.1021/bi991353h
- Wang, W., & Shakes, D. C. (1996). Molecular evolution of the 14-3-3 protein family. *Journal of Molecular Evolution*, 43(4), 384-398. doi: 10.1007/PL00006097
- Wang, Z. (2017). ErbB Receptors and Cancer. In *Methods in Molecular Biology* (Eds.), *ErbB Receptor Signaling* (pp. 3-35). doi: 10.1007/978-1-4939-7219-7\_1
- Wang, Z., Nesland, J. M., Suo, Z., Trope, C. G., & Holm, R. (2011). The prognostic value of 14-3-3 isoforms in vulvar squamous cell carcinoma cases: 14-3-3 $\beta$  and epsilon are independent prognostic factors for these tumors. *PLoS One*, 6(9), e24843. doi: 10.1371/journal.pone.0024843
- Wee, P., & Wang, Z. (2018). Regulation of EGFR Endocytosis by CBL During Mitosis. *Cells*, 7(12), E257. doi: 10.3390/cells7120257
- Welch, M. D., & Mullins, R. D. (2002). Cellular control of actin nucleation. *Annual Review of Cell and Developmental Biology*, 18, 247-288. doi: 10.1146/annurev.cellbio.18.040202.112133

- West-Foyle, H., Kothari, P., Osborne, J., & Robinson, D. N. (2018). 14-3-3 proteins tune non-muscle myosin II assembly. *The Journal of Biological Chemistry*, 293(18), 6751-6761. doi: 10.1074/jbc.M117.819391
- Wiltfang, J., Otto, M., Baxter, H. C., Bodemer, M., Steinacker, P., Bahn, E.,... Aitken, A. (1999). Isoform pattern of 14-3-3 proteins in the cerebrospinal fluid of patients with Creutzfeldt-Jakob disease. *Journal of Neurochemistry*, 73(6), 2485-2490. doi: 10.1046/j.1471-4159.1999.0732485.x
- Wong, A. H., Lihodi, O., Trakalo, J., Yusuf, M., Sinha, A., Pato, C. N.,... Kennedy, J. L. (2005). Genetic and post-mortem mRNA analysis of the 14-3-3 genes that encode phosphoserine/threonine-binding regulatory proteins in schizophrenia and bipolar disorder. *Schizophrenia Research*, 78(2-3), 137-146. doi: 10.1016/j.schres.2005.06.009
- Wong, A. H., Macciardi, F., Klempan, T., Kawczynski, W., Barr, C. L., Lakatoo, S.,... Van Tol, H. H. (2003). Identification of candidate genes for psychosis in rat models, and possible association between schizophrenia and the 14-3-3eta gene. *Molecular Psychiatry*, 8(2), 156-166. doi: 10.1038/sj.mp.4001237
- Xiao, B., Smerdon, S. J., Jones, D. H., Dodson, G. G., Soneji, Y., Aitken, A., & Gamblin, S. J. (1995). Structure of a 14-3-3 protein and implications for coordination of multiple signalling pathways. *Nature*, 376(6536), 188-191. doi: 10.1038/376188a0
- Xiao, T., Ying, W., Li, L., Hu, Z., Ma, Y., Jiao, L.,... Cheng, S. (2005). An approach to studying lung cancer-related proteins in human blood. *Molecular and Cellular Proteomics*, 4(10), 1480-1486. doi: 10.1074/mcp.M500055-MCP200
- Xiao, Y., Lin, V. Y., Ke, S., Lin, G. E., Lin, F. T., & Lin, W. C. (2014). 14-3-3Tau promotes

- breast cancer invasion and metastasis by inhibiting RhoGDIalpha. *Molecular and Cellular Biology*, 34(14), 2635–2649. doi: 10.1128/MCB.00076-14
- Yaffe, M. B., Rittinger, K., Volinia, S., Caron, P. R., Aitken, A., Leffers, H.,... Cantley, L. C. (1997). The structural basis for 14-3-3: Phosphopeptide binding specificity. *Cell*, 91(7), 961–971. doi: 10.1016/S0092-8674(00)80487-0
- Yamazaki, D., Suetsugu, S., Miki, H., Kataoka, Y., Nishikawa, S., Fujiwara, T.,... Takenawa, T. (2003). WAVE2 is required for directed cell migration and cardiovascular development. *Nature*, 424(6947), 452-456. doi: 10.1038/nature01770
- Yang, J., Joshi, S., Wang, Q., Li, P., Wang, H., Xiong, Y.,... Yu, D. (2017). 14-3-3ζ loss leads to neonatal lethality by microRNA-126 downregulation-mediated developmental defects in lung vasculature. *Cell and Bioscience*, 7, 58. doi: 10.1186/s13578-017-0186-y
- Ye, Y., Yang, Y., Cai, X., Liu, L., Wu, K., & Yu, M. (2016). Down-regulation of 14-3-3 Zeta Inhibits TGF-beta1-Induced Actomyosin Contraction in Human Trabecular Meshwork Cells Through RhoA Signaling Pathway. *Investigative Ophthalmology & Visual Science*, 57(2), 719-730. doi: 10.1167/iovs.15-17438
- Yoshida, K., Yamaguchi, T., Natsume, T., Kufe, D., & Miki, Y. (2005). JNK phosphorylation of 14-3-3 proteins regulates nuclear targeting of c-Abl in the apoptotic response to DNA damage. *Nature Cell Biology*, 7(3), 278-285. doi: 10.1038/ncb1228
- Yu, J., Chen, L., Chen, Y., Hasan, M. K., Ghia, E. M., Zhang, L.,... Kipps, T. J. (2017). Wnt5a induces ROR1 to associate with 14-3-3zeta for enhanced chemotaxis and proliferation of chronic lymphocytic leukemia cells. *Leukemia*, 31(12), 2608-2614. doi: 10.1038/leu.2017.132
- Zenke, F. T., Krendel, M., DerMardirossian, C., King, C. C., Bohl, B. P., & Bokoch, G. M.

- (2004). P21-activated kinase 1 phosphorylates and regulates 14-3-3 binding to GEF-H1, a microtubule-localized Rho exchange factor. *The Journal of Biological Chemistry*, 279(18), 18392–18400. doi: 10.1074/jbc.M400084200
- Zhai, J., Lin, H., Shamim, M., Schlaepfer, W. W., & Canete-Soler, R. (2001). Identification of a novel interaction of 14-3-3 with p190RhoGEF. *The Journal of Biological Chemistry*, 276(44), 41318–41324. doi: 10.1074/jbc.M107709200
- Zhang, Z., He, H., Qiao, Y., Huang, J., Wu, Z., Xu, P.,... He, M. (2018). Tanshinone IIA Pretreatment Protects H9c2 Cells against Anoxia/Reoxygenation Injury: Involvement of the Translocation of Bcl-2 to Mitochondria Mediated by 14-3-3eta. *Oxidative Medicine and Cellular Longevity*, 2018, 3583921. doi: 10.1155/2018/3583921
- Zhou, Q., Kee, Y. S., Poirier, C. C., Jelinek, C., Osborne, J., Divi, S.,... Robinson, D. N. (2010). 14-3-3 coordinates microtubules, Rac, and myosin II to control cell mechanics and cytokinesis. *Current Biology : CB*, 20(21), 1881–1889. doi: 10.1016/j.cub.2010.09.048
- Zhu, G., Fan, Z., Ding, M., Zhang, H., Mu, L., Ding, Y.,... Wu, W. (2015). An EGFR/PI3K/AKT axis promotes accumulation of the Rac1-GEF Tiam1 that is critical in EGFR-driven tumorigenesis. *Oncogene*, 34(49), 5971–5982. doi: 10.1038/onc.2015.45